

QCD cusp anomalous dimension: Current status

Andrey Grozin

*Budker Institute of Nuclear Physics,
 Russian Academy of Sciences, Siberian Branch
 Akademika Lavrentiev Avenue 11,
 630090 Novosibirsk, Russia
 A.G.Grozin@inp.nsk.su*

Received 16 December 2022

Revised 11 February 2023

Accepted 14 February 2023

Published 13 April 2023

Calculation results for the HQET field anomalous dimension and the QCD cusp anomalous dimension, as well as their properties, are reviewed. The HQET field anomalous dimension γ_h is known up to four loops. The cusp anomalous dimension $\Gamma(\varphi)$ is known up to three loops, and its small-angle and large-angle asymptotics up to four loops. Some (but not all) color structures at four loops are known with the full φ -dependence. Some simple contributions are known at higher loops. For the $\varphi \rightarrow \infty$ asymptotics of $\Gamma(\varphi)$ (the light-like cusp anomalous dimension) and the φ^2 -term of the small- φ expansion (the Bremsstrahlung function), the $\mathcal{N} = 4$ SYM results are equal to the highest-weight parts of the QCD results. There is an interesting conjecture about the structure of $\Gamma(\varphi)$ which holds up to three loops; at four loops it holds for some color structures and breaks down for other ones. In the cases when it holds, it related highly nontrivial functions of φ , and it cannot be accidental; however, the reasons of this conjecture and its failures are not understood. The cusp anomalous dimension at the Euclidean angle $\phi \rightarrow \pi$ is related to the static quark–antiquark potential due to conformal symmetry; in QCD, this relation is broken by an anomalous term proportional to the β -function.

Some new results are also presented. Using the recent four-loop result for γ_h , here we obtain analytical expressions for some terms in the four-loop on-shell renormalization constant of the massive quark field Z_Q^{os} which were previously known only numerically. We also present two new contributions to γ_h , $\Gamma(\varphi)$ at five loops and to the quark–antiquark potential at four loops.

Keywords: Wilson lines; multiloop calculations; HQET.

PACS numbers: 11.15.-q, 12.38.-t, 12.38.Bx

1. Introduction

A Wilson line in a gauge theory is the phase factor for a classical pointlike charged particle (in some representation R of the gauge group) moving along a

A. Grozin

worldline C ,

$$W_0 = \left\langle P \exp \left[i g_0 \int_C dx_\mu A_0^{a\mu}(x) t_R^a \right] \right\rangle = Z_W(\alpha_s(\mu), a(\mu)) W(\mu), \quad (1.1)$$

where g_0 and A_0 are the bare coupling and gauge field, t_R^a are the generators of the representation R , $W(\mu)$ is the renormalized Wilson line (we use the $\overline{\text{MS}}$ scheme, $d = 4 - 2\varepsilon$) and $a(\mu)$ is the renormalized gauge parameter. We use the covariant gauge,

$$\overset{a}{\underset{\mu}{\text{wavy line}}} \overset{k}{\rightarrow} \overset{b}{\underset{\nu}{\text{wavy line}}} = i \delta^{ab} D_0^{\mu\nu}(k), \quad D_0^{\mu\nu}(k) = \frac{1}{-k^2} \left[g^{\mu\nu} + (1 - a_0) \frac{k^\mu k^\nu}{-k^2} \right].$$

The renormalized gauge parameter $a(\mu)$ is related to the bare one a_0 by the gluon field renormalization constant: $a_0 = Z_A(\alpha_s(\mu), a(\mu))a(\mu)$. Wilson lines are widely used in gauge theories, see e.g. the textbook.¹ Renormalization of Wilson lines is considered in Refs. 2–4, see Ref. 5 for review and more references. The $\overline{\text{MS}}$ renormalization constant Z_W accumulates ultraviolet (UV) divergences of the bare Wilson line, and is determined only by singular points of the line — its ends and cusps (we consider only lines without self-intersections); smooth segments don't contribute.

Infrared (IR) properties of scattering amplitudes in gauge theories are closely related to Wilson lines,^{6–10} see Ref. 11 for review and more references. IR divergences of a scattering amplitude can be found in the eikonal approximation. It turns the amplitude into a product of straight semi-infinite Wilson lines along its external momenta. However, it introduces UV divergences which were absent in the original amplitude. These UV divergences are equal to the IR divergences of the amplitude with the opposite sign, because eikonal diagrams contain no dimensionful parameters.

2. Wilson Lines and HQET

Wilson lines are nonlocal objects. It is easier to understand their properties in the language of heavy quark effective theory (HQET). HQET is a usual local quantum field theory, and renormalization properties of Wilson lines can be obtained from renormalization of local operators in HQET. Renormalization theory of local operators is discussed in many quantum field theory textbooks.

Suppose we have QCD with n_f flavors plus a single heavy colored particle (in some representation R of the gauge group). The momentum of this particle can be decomposed as $P = Mv + p$, where M is its on-shell mass, v is a reference velocity ($v^2 = 1$) and p is called the residual momentum of this heavy particle. If the characteristic residual momentum p , characteristic momenta of light particles p_i and light particle masses m_i are all small ($p \ll M$, $p_i \ll M$ and $m_i \ll M$), then the system can be described by the HQET Lagrangian (see e.g. Refs. 12–14). This heavy particle can be, for example, a heavy quark (its flavor is *not* counted in n_f). At the leading order

in $1/M$, the heavy-particle spin does not interact with gluons and can be freely rotated (heavy quark symmetry). Moreover, it can be switched off (superflavor symmetry¹⁵).

The HQET Lagrangian is

$$L = h_{v0}^* iD \cdot v h_{v0} + L_{\text{QCD}}, \quad D^\mu h_{v0} = (\partial^\mu - ig_0 A_0^{\mu a} t_R^a) h_{v0} \quad (2.1)$$

(we can include several HQET fields with several velocities if we need: $\sum_i h_{v_i 0}^* iD \cdot v_i h_{v_i 0}$). The heavy (static) particle is described by the scalar field h_v in the color representation R ,

$$h_{v0} = Z_h^{1/2}(\alpha_s(\mu), a(\mu)) h_v(\mu), \quad (2.2)$$

where $h_v(\mu)$ is the $\overline{\text{MS}}$ -renormalized field. The momentum-space propagator of the field h_{v0} depends only on the residual energy $\omega = p \cdot v$,

$$\overrightarrow{\cancel{p}} = iS_{h0}(p \cdot v), \quad S_{h0}(\omega) = \frac{1}{\omega} \quad (2.3)$$

(the unit color matrix $\mathbf{1}_R$ is assumed). The $h_v^* h_v A$ vertex is

$$\overrightarrow{\cancel{p}} \overleftarrow{\cancel{v}} = i g_0 v^\mu t_R^a. \quad (2.4)$$

If we denote the sum of one-particle-irreducible (1PI) self-energy diagrams by $-i\Sigma_h(\omega)$, then the full propagator (i.e. the sum of all propagator diagrams) is

$$\overrightarrow{\cancel{p}} = iS_h(\omega), \quad S_h(\omega) = \frac{1}{\omega - \Sigma_h(\omega)}. \quad (2.5)$$

The renormalization factor Z_h is given by

$$\log \frac{S_h(\omega)}{S_{h0}(\omega)} = \log Z_h + \mathcal{O}(\varepsilon^0), \quad (2.6)$$

where $S_h(\omega)$ is expressed via the renormalized quantities $\alpha_s(\mu)$, $a(\mu)$. The HQET field $h_v(\mu)$ anomalous dimension is

$$\gamma_h(\alpha_s(\mu)) = \frac{d \log Z_h(\alpha_s(\mu), a(\mu))}{d \log \mu}. \quad (2.7)$$

We can also use the coordinate space,

$$\overrightarrow{\cancel{x}} = \theta(x \cdot v) \delta(x_\perp). \quad (2.8)$$

In the v -rest frame, the free propagator is $\delta(\mathbf{x}) S_{h0}(x^0)$, $iS_{h0}(t) = \theta(t)$. The full propagator

$$\overrightarrow{\cancel{x}} \overrightarrow{\cancel{y}} = \overrightarrow{\cancel{x}} \times \left\langle P \exp \left[ig_0 \int_x^y dx_\mu A_0^{a\mu}(x) t_R^a \right] \right\rangle, \quad (2.9)$$

A. Grozin

where the integral is taken along the straight line from x to y . In the v -rest frame $S_h(t) = S_{h0}(t)W(t)$, where

$$W(t) = \left\langle P\exp \left[ig_0 \int_0^t dt v_\mu A_0^{a\mu}(vt)t^a \right] \right\rangle \quad (2.10)$$

is the straight Wilson line along v of length t . Assuming $t > 0$, we have

$$\log W(t) = \log Z_h + \mathcal{O}(\varepsilon^0). \quad (2.11)$$

So, the factor Z_h describes renormalization of a finite-length Wilson line. In other words, $Z_h^{1/2}$ describes renormalization of an end of a Wilson line.

Transition of a heavy particle with a velocity v into a heavy particle with a velocity v' (e.g. decay of a heavy quark into another heavy quark plus colorless particles) in HQET framework is described by the current

$$J_0 = h_{v'0}^* h_{v0} = Z_J(\alpha_s(\mu), \varphi) J(\mu) \quad (2.12)$$

$[J(\mu)]$ is the $\overline{\text{MS}}$ -renormalized current, $\cosh \varphi = v \cdot v'$. Its anomalous dimension

$$\Gamma(\alpha_s(\mu), \varphi) = \frac{d \log Z_J(\alpha_s(\mu), \varphi)}{d \log \mu} \quad (2.13)$$

is called the cusp anomalous dimension. The current J is colorless, and hence Z_J and Γ are gauge-invariant. Dependence of the Isgur–Wise function on μ is determined¹⁶ by $\Gamma(\alpha_s, \varphi)$. The $1/\varepsilon$ IR divergence of massive QCD form factors is given by it.

Let $V(\omega, \omega', \varphi) = 1 + \Lambda(\omega, \omega', \varphi)$ be the sum of 1PI vertex diagrams of J_0 (1 is the tree-level diagram; ω and ω' are the incoming residual energy and the outgoing one). From each diagram for Σ_h we can get a set of diagrams for Λ by inserting the J_0 -vertex into each internal HQET line in turn. The correlator of J_0 , h_v^* , $h_{v'}$ is $V(\omega, \omega', \varphi) \cdot iS_h(\omega) \cdot iS_h(\omega')$; on the other hand, it is $Z_h Z_J$ times the finite correlator of the three renormalized operators. Recalling the fact that $S_h(\omega)$ is Z_h times the finite renormalized propagator, we have

$$\log V(\omega, \omega', \varphi) = \log Z_J(\varphi) - \log Z_h + \mathcal{O}(\varepsilon^0). \quad (2.14)$$

It is sufficient to calculate a single-scale vertex function $V(\omega, \omega, \varphi)$ in order to obtain Z_J . At $\varphi = 0$, we have the HQET Ward identities

$$\Lambda(\omega, \omega, 0) = -\frac{\Sigma_h(\omega) - \Sigma_h(\omega)}{\omega - \omega'} \quad \text{or} \quad V(\omega, \omega, 0) = \frac{S_h^{-1}(\omega) - S_h^{-1}(\omega')}{\omega - \omega'}. \quad (2.15)$$

Therefore, $\log V(\omega, \omega, 0) = -\log Z_h + \mathcal{O}(\varepsilon^0)$, $Z_J(\alpha_s, 0) = 1$ and

$$\Gamma(\alpha_s, 0) = 0. \quad (2.16)$$

In coordinate space, the Green's function $\langle h_{v'0}(x') J_0(0) h_{v0}^*(x) \rangle$ ($x^0 < 0 < x'^0$) is equal to the obvious δ -functions times the Wilson line $W(t, t', \varphi)$: the straight segment along v of length t , the angle φ and the straight segment along v' of length t' .

The corresponding renormalized Green's function is finite, and so

$$\log W(t, t', \varphi) = \log Z_J(\varphi) + \log Z_h + \mathcal{O}(\varepsilon^0). \quad (2.17)$$

At $\varphi = 0$ the Wilson line is straight: $W(t, t', 0) = W(t + t')$, and we again obtain $Z_J(0) = 1$.

At $\varphi \rightarrow 0$ the cusp anomalous dimension is a regular Taylor series in φ^2 ,

$$\Gamma(\alpha_s, \varphi) = \sum_{n=1}^{\infty} B_n(\alpha_s) \varphi^{2n}, \quad (2.18)$$

$B_1(\alpha_s)$ is usually called the Bremsstrahlung function. If our Wilson line interacts with QED with $n_f = 0$ (i.e. the free electromagnetic field), and we have a classical pointlike charge which is at rest in some reference frame at both $t \rightarrow \pm\infty$, then the energy of the emitted radiation is

$$\Delta E = 2\pi B_1(\alpha) \int_{-\infty}^{+\infty} dt (-a^2(t)), \quad (2.19)$$

where a^μ is the acceleration. In this theory $B_1(\alpha) = \alpha/(3\pi)$ exactly, and (2.19) is just the classical dipole radiation formula. The theory is conformally invariant, α does not run. The formula (2.19) is also valid¹⁷ in $\mathcal{N} = 4$ supersymmetric Yang–Mills (SYM), which is also conformally invariant. It cannot be generalized to other theories, because in them $B_1(\alpha_s(\mu))$ depends on μ .

At $\varphi \rightarrow \infty$,¹⁸

$$\Gamma(\alpha_s, \varphi) = K(\alpha_s)\varphi + \mathcal{O}(\varphi^0), \quad (2.20)$$

where K is called the light-like cusp anomalous dimension. It is related¹⁹ to renormalization properties of Wilson lines with light-like segments. The coefficients of $1/(1-x)_+$ in DGLAP kernels [as well as those of $1/(x-y)_+$ in ERBL kernels] are determined^{20,21} by the light-like cusp anomalous dimension. IR $1/\varepsilon^2$ divergences of form factor of massless particles are also determined by $K(\alpha_s)$.

If a worldline of finite length consists of straight segments with angles φ_i between them, its renormalization factor is $Z_h \prod Z_J(\varphi_i)$ [two ends contribute $Z_h^{1/2}$ each, each cusp contributes $Z_J(\varphi_i)$]. The same is true if the segments are not straight but just some smooth curves. We can approximate a smooth curve of length t by a broken line with $N \rightarrow \infty$ segments of length $\Delta t = t/N$ each. Cusp angles are $\Delta\varphi_i \sim 1/N$, so the contributions to $\log Z_J$ are $\sim 1/N^2$ each; there are N such contributions. Such Wilson lines can be described by the HQET field h which lives on the worldline. The HQET Lagrangian was actually used as a technical device for investigating Wilson lines^{22,23} (see Ref. 5 for review).

We can also understand this fact from another point of view. UV divergences come from small distances, where any smooth line is straight. The only possible UV divergence is the residual mass $\Sigma_h(0)$. This is a linear UV divergence. In dimensional regularization it is discarded: the residual mass $\Sigma_h(0)$ has dimensionality of mass, and we cannot construct any nonzero result for it by dimensions counting

A. Grozin

(in regularizations based on momentum cutoff Λ_{UV} , the UV-divergent residual mass is $\propto \Lambda_{\text{UV}}$).

3. Exponentiation

A Wilson line (of any shape) interacting with the free electromagnetic field (QED with $n_f = 0$) is given by the simple exponentiation formula. Let

$$w(t) = \overbrace{\quad}^{0 t_1 t_2 t} \quad (3.1)$$

be the one-loop contribution to $W(t)$. Here we use diagrams for Wilson lines, not for HQET propagators, so that the factors $\theta(x \cdot v)\delta(x_\perp)$ are not included. This diagram is an integral in t_1, t_2 such that $0 < t_1 < t_2 < t$. Let's calculate w^2 . It is an integral in t_1, t_2, t'_1, t'_2 such that $0 < t_1 < t_2 < t, 0 < t'_1 < t'_2 < t$. This integration region can be subdivided into six subregions corresponding to six diagrams,

$$\begin{aligned} & \overbrace{\quad}^{0 t_1 t_2 t} \times \overbrace{\quad}^{0 t'_1 t'_2 t} \\ &= \overbrace{\quad}^{0 t_1 t_2 t} + \overbrace{\quad}^{0 t_1 t_2 t} + \overbrace{\quad}^{0 t_1 t_2 t} \\ &+ \overbrace{\quad}^{0 t_1 t_2 t} + \overbrace{\quad}^{0 t_1 t_2 t} + \overbrace{\quad}^{0 t_1 t_2 t}. \end{aligned} \quad (3.2)$$

This is twice the two-loop contribution to $W(t)$. Continuing this drawing exercise we see that the three-loop contribution is $w^3/3!$, etc. The exact expression for the full Wilson line is²⁴

$$\overbrace{\quad}^{0 t} = \exp \overbrace{\quad}^{0 t}, \quad W(t) = e^{w(t)}. \quad (3.3)$$

So, we have $w = \log Z_h + \mathcal{O}(\varepsilon^0)$, $\log Z_h$ is *exactly* one-loop,

$$\gamma_h(\alpha) = 2(a - 3) \frac{\alpha}{4\pi}. \quad (3.4)$$

There are no higher-loop corrections. The same is true for $\Gamma(\alpha, \varphi)$ because exponentiation works for Wilson lines of any shapes, including those with cusps [this exact Γ is given below in (4.1)].

In QED with $n_f > 0$, the situation is more complicated: we don't know the exact results, just perturbative series. However, these series have a simple structure,

$$\begin{aligned} & \overbrace{\quad}^{0 t} = \exp \left[\overbrace{\quad}^{0 t} + \overbrace{\quad}^{0 t} + \dots \right], \\ & W = \exp[w_2 + w_4 + \dots], \end{aligned} \quad (3.5)$$

where the shaded blobs are the sums of connected diagrams with 2, 4, ... external photon lines (odd numbers of lines are forbidden by C -conservation),

$$\begin{aligned} w_2 &= \text{Diagram with one shaded blob} \\ &= \text{Diagram with two shaded blobs} + \text{Diagram with three shaded blobs} + \text{Diagram with four shaded blobs} + \dots, \end{aligned} \quad (3.6)$$

$$w_4 = \text{Diagram with one shaded blob} = \text{Diagram with two shaded blobs} + \dots \quad (3.7)$$

and so on (the shaded blobs here are not necessarily one-particle-irreducible). Diagrams in (3.6) and (3.7) are called *c-webs* (connected webs).

We have, for example,

$$\text{Diagram with two c-webs} \times \text{Diagram with one c-web} = \dots + \text{Diagram with three c-webs} + \dots,$$

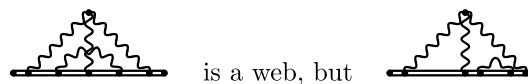
and these diagrams (containing two c-webs each) are already accounted for in the expansion of the exponent (3.5).

The sums of connected diagrams with $2n$ external (off-shell) photon legs at each order are gauge-invariant due to the QED Ward identity, except the free photon propagator. Hence all c-webs are gauge-invariant except the first one in (3.6). This one-loop c-web is linear in $e_0^2 a_0$; but $e_0^2 a_0 = e^2(\mu) a(\mu)$ because $Z_\alpha = Z_A^{-1}$ in QED. Therefore, the only gauge-dependent term in γ_h is the one-loop term given by (3.4); all higher-loop corrections are gauge-invariant.

In non-Abelian theories,^{25,26}

$$W = \exp \left[\sum \bar{C}_i w_i \right], \quad (3.8)$$

where w_i are *webs*, and \bar{C}_i are color-connected parts of their color factors C_i . Let's draw all gluon lines in a diagram for W on a single side of its HQET line. If we remove this HQET line, we obtain a diagram with gluon external lines which can be connected (c-web) or not. When this diagram is connected *if we count the line crossings as connections*, the diagram is called a web. For example,



is a web, but is not. (3.9)

If color factors of each web were the same as for the diagram where all its c-webs are separated, the contributions of webs would be accounted for in the exponent of the sum of c-webs. This is true in QED. In non-Abelian theories color factors are more complicated. For example, let's consider the first diagram in (3.9). It is a web

A. Grozin

but not a c-web: it contains two c-webs. Its color factor C is given by the color diagram which looks the same as this diagram in (3.9). It is not equal to $C_1 C_2$, the product of the color factors of these two c-webs taken separately. Let's pull these two c-webs apart, interchanging the vertices on the HQET line belonging to different c-webs according to the obvious commutator identity

$$\text{Diagram (3.10)}$$

This color factor C becomes

The first term consists of two separate c-webs, it is $C_1 C_2$; this contribution has already been accounted for in the expansion of the exponent. The second term is a connected color diagram, the connected part \bar{C} of the color factor C . This contribution is not yet accounted for. Therefore, we add this web with the color factor \bar{C} to the exponent in (3.8).

Let's define

$$\begin{aligned} \text{Tr } t_R^a t_R^b &= T_R \delta^{ab}, \quad t_R^a t_R^a = C_R \mathbf{1}_R, \quad N_R = \text{Tr } \mathbf{1}_R, \\ d_{RR'} &= \frac{d_R^{abcd} d_{R'}^{abcd}}{N_R}, \quad d_R^{abcd} = \text{Tr } t_R^{(a} t_{R'}^b t_{R'}^c t_R^{d)}, \end{aligned} \quad (3.11)$$

where brackets mean symmetrization (note that $\text{Tr } t_R^a t_R^a = C_R N_R = T_R N_A$, and hence $C_R = T_R N_A / N_R$; in particular, $C_A = T_A$). For $SU(N_c)$ gauge group with the standard normalization $T_F = \frac{1}{2}$, they are

$$\begin{aligned} C_F &= \frac{N_c^2 - 1}{2N_c}, \quad C_A = N_c, \quad d_{FF} = \frac{(N_c^2 - 1)(N_c^4 - 6N_c^2 + 18)}{96N_c^3}, \\ d_{AF} &= \frac{N_c}{N_c^2 - 1} d_{FA} = \frac{N_c(N_c^2 + 6)}{48}, \quad d_{AA} = \frac{N_c^2(N_c^2 + 36)}{24}. \end{aligned} \quad (3.12)$$

In QED $T_F = 1$, $C_R = Z^2$, $C_F = 1$, $C_A = 0$, $d_{RF} = Z^4$ and $d_{RA} = 0$, where Z is the charge of the infinitely heavy particle (in units of e).

The possible color structures of γ_h and Γ without n_f are, due to the non-Abelian exponentiation, C_R at one loop; $C_R C_A$ at two loops; $C_R C_A^2$ at three loops; $C_R C_A^3$ and d_{RA} at four loops. Color structures containing C_F are forbidden. As soon as there is at least one quark loop in the diagram (i.e. at least one power of n_f in the color structure), all possible color factors are allowed: gluons attached to quark loops are not restricted by exponentiation. Up to three loops, all color structures are proportional to C_R . The R -dependence of γ_h and Γ is given by the factor C_R — Casimir scaling. At four loops, the quartic Casimirs d_{RA} , d_{RF} appear. They are not proportional to C_R , and Casimir scaling breaks down.

4. History and the Current Status of Calculations

The one-loop cusp anomalous dimension follows from classical electrodynamics. When an infinitely heavy charged particle instantly changes its velocity, it either remains itself (probability $|F|^2$) or emits one or more photons. Up to the order α ,

$$\left| \begin{array}{c} \diagup \\ \diagdown \end{array} + \begin{array}{c} \diagup \\ \diagdown \end{array} \right|^2 + \int \left| \begin{array}{c} \diagup \\ \diagdown \end{array} + \begin{array}{c} \diagup \\ \diagdown \end{array} \right|^2 = 1.$$

In classical electrodynamics, the spectrum of the emitted radiation is^{27,28}

$$dE = \frac{e^2}{2\pi^2} (\varphi \coth \varphi - 1) d\omega,$$

and hence the probability of photon emission is dE/ω . In dimensional regularization, by dimensions counting, this probability becomes $C(\varepsilon)dE/\omega^{1+2\varepsilon}$ with $C(0) = 1$. Hence the form factor is

$$F = 1 - \frac{C(\varepsilon)}{2} \int_{\lambda}^{\infty} \frac{e^2}{2\pi^2} (\varphi \coth \varphi - 1) \frac{d\omega}{\omega^{1+2\varepsilon}} = 1 - 2 \frac{\alpha}{4\pi\varepsilon} (\varphi \coth \varphi - 1 + \mathcal{O}(\varepsilon))$$

(where λ is an IR cutoff), and the cusp anomalous dimension is

$$\Gamma = 4 \frac{\alpha}{4\pi} (\varphi \coth \varphi - 1). \quad (4.1)$$

The one-loop cusp anomalous dimension should be included in The Guinness Book of Records as the anomalous dimension known for the longest time (probably > 100 years). In QCD, it includes the obvious extra factor C_R . Of course, there are very many ways to obtain (4.1), using momentum or coordinate space.

After a wrong calculation,²⁹ the two-loop γ_h (with $n_f = 0$) has been calculated in Ref. 30. The full result (with n_f) has been obtained in Ref. 31 as a by-product of a two-loop calculation of the on-shell renormalization constant Z_Q^{os} of the field of a massive quark, essentially from the requirement that the renormalized QCD/HQET matching constant (5.4) is finite (though this was not explicitly stated in the article), and reproduced^{32,33} by direct HQET calculations. At three loops, it has been calculated in Ref. 34, again as a by-product of the Z_Q^{os} calculation, now at three loops; the result has been confirmed³⁵ by a direct HQET calculation.

The first attempt³⁰ to calculate the cusp anomalous dimension at two loops (at $n_f = 0$) was unsuccessful: the authors were unable to eliminate complicated double and triple integrals. A usable result (at $n_f = 0$) has been obtained in Refs. 7, 6 and 18. It contains three single integrals [two of them were calculated¹⁴ in terms of Li_2 and Li_3 , the formula (7.15)]. The (rather simple) n_f -term was added in Ref. 20. The calculation^{6,7,18} was repeated several times.^{36,37} The most nice form of the result

A. Grozin

(no integrals, just Li_2 and Li_3) is³⁷

$$\begin{aligned}
 \Gamma &= 4C_R \frac{\alpha_s}{4\pi} \left\{ \varphi \coth \varphi - 1 + \frac{\alpha_s}{4\pi} \left[C_A \left[\frac{2}{3}\pi^2 - \frac{49}{9} + 2\varphi^2 \right. \right. \right. \\
 &\quad + \coth \varphi \left(2\text{Li}_2(e^{-2\varphi}) - 4\varphi \log(1 - e^{-2\varphi}) - \frac{\pi^2}{3} - \frac{2}{3}\pi^2\varphi + \frac{67}{9}\varphi - 2\varphi^2 - \frac{2}{3}\varphi^3 \right) \\
 &\quad \left. \left. \left. + \coth^2 \varphi \left(2\text{Li}_3(e^{-2\varphi}) + 2\varphi \text{Li}_2(e^{-2\varphi}) - 2\zeta_3 + \frac{\pi^2}{3}\varphi + \frac{2}{3}\varphi^3 \right) \right] \right. \\
 &\quad \left. \left. - \frac{20}{9}T_F n_f (\varphi \coth \varphi - 1) \right] + \mathcal{O}(\alpha_s^2) \right\} \\
 &= 4C_R \frac{\alpha_s}{4\pi} \left\{ \varphi \coth \varphi - 1 + \frac{\alpha_s}{4\pi} \left[C_A \left[2 \left(1 + \frac{2}{3}\varphi^2 \right) - \frac{1}{3}(\varphi \coth \varphi - 1) \right. \right. \right. \\
 &\quad \times \left(2\pi^2 - \frac{67}{3} + 2\varphi^2 \right) + \coth \varphi (\varphi \coth \varphi + 1) (\text{Li}_2(1 - e^{2\varphi}) - \text{Li}_2(1 - e^{-2\varphi})) \\
 &\quad \left. \left. \left. - 2\coth^2 \varphi (\text{Li}_3(1 - e^{2\varphi}) + \text{Li}_3(1 - e^{-2\varphi})) \right] \right. \\
 &\quad \left. \left. - \frac{20}{9}T_F n_f (\varphi \coth \varphi - 1) \right] + \mathcal{O}(\alpha_s^2) \right\} \tag{4.2}
 \end{aligned}$$

(the last form is explicitly even in φ).

Table 1. Four-loop contributions to γ_h , Γ and its limiting cases.

Color	Example	γ_h	$\varphi \ll 1$	$\Gamma(\varphi)$	1L	$\varphi \gg 1$
$C_R(T_F n_f)^3$		Ref. 44	Ref. 14	Ref. 14	✓	Refs. 45 and 46
$C_R C_F (T_F n_f)^2$		Refs. 39 and 47	Refs. 39 and 47	Refs. 39 and 47	✓	Refs. 39, 47 and 48
$C_R C_A (T_F n_f)^2$		Refs. 49 and 50	Ref. 50	Ref. 50		Refs. 48, 51 and 52
$C_R C_F^2 T_F n_f$		Ref. 53	Ref. 53	Ref. 53	✓	Ref. 53
$C_R C_F C_A T_F n_f$		Ref. 50	Ref. 50	Ref. 50		Refs. 50 and 55
$C_R C_A^2 T_F n_f$		Ref. 50	Ref. 50			Refs. 54 and 55
$d_R F n_f$		Ref. 56	Refs. 56 and 50	Ref. 57		Refs. 58 and 59
$n_f^1, N_c \rightarrow \infty$		Ref. 50	Ref. 50			Refs. 51, 60 and 61
$C_R C_A^3$		Ref. 62	Ref. 62			Refs. 54 and 55
d_{RA}		Ref. 62	Ref. 62			Refs. 54 and 55
$n_f^0, N_c \rightarrow \infty$		Ref. 62	Ref. 62			Refs. 60 and 61

At three loops, the cusp anomalous dimension has been obtained in Refs. 38 and 39 (the results are given in Sec. 8 below). Results for supersymmetric QCD extensions have been also obtained.³⁹

The light-like cusp anomalous dimension (2.20) at three loops has been obtained in the course of calculating the three-loop DGLAP evolution kernels⁴⁰ (recently confirmed in Ref. 41) and confirmed in massless form-factor calculations.^{42,43}

The status of four-loop calculations is summarized in Table 1. The column 1L shows the color structures which have the simple one-loop φ -dependence $\varphi \coth \varphi - 1$. For several color structures the exact angle dependence is not known. A simple interpolation formula [in terms of the variable $\beta = \tanh(\varphi/2)$] for the four-loop cusp anomalous dimension has been proposed.⁶³ It is based on the known asymptotics $\beta \rightarrow 0$ and $\beta \rightarrow 1$. Such approximate formulas give a good precision at two and three loops,^{37,64} so it seems reasonable to hope that it also works well at four loops.

Some simple classes of contributions are also known at higher loops (Secs. 10–14).

5. HQET Field Anomalous Dimension

It is convenient to calculate the HQET self-energy $\Sigma_h(\omega)$ at $\omega < 0$, below the mass shell, where the result is analytical. The power of (-2ω) in each term of the

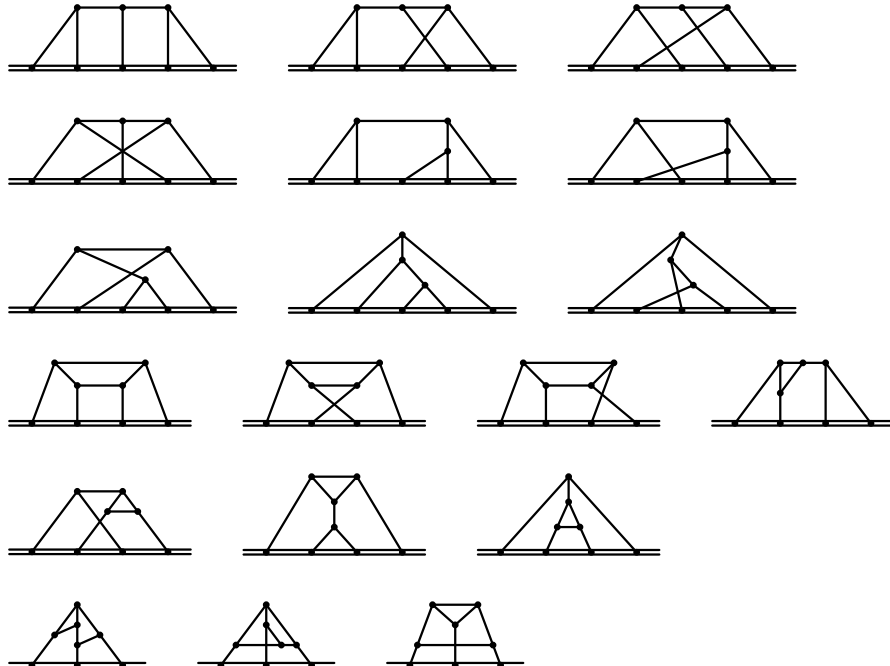


Fig. 1. Families of four-loop HQET self-energy Feynman integrals. Double lines are HQET ones, solid lines are massless.

A. Grozin

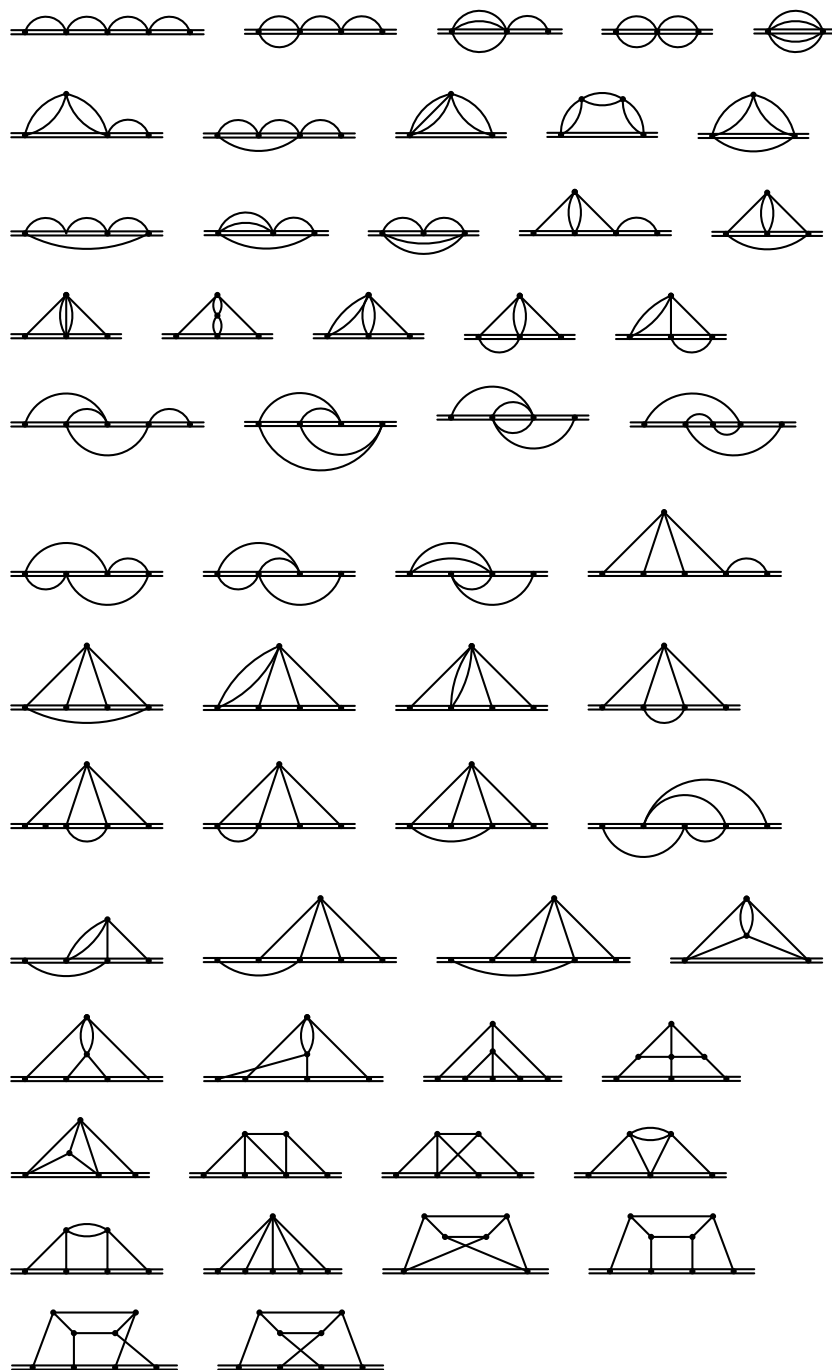


Fig. 2. Master integrals for four-loop HQET self-energy diagrams.

perturbative expansion is fixed by dimensions counting, so we can set $\omega = -\frac{1}{2}$ during the calculation. Many diagrams have linear dependent HQET denominators which can be killed by partial fractioning. At three loops, all four families of integrals reduce⁶⁵ to eight master integrals: five trivial, two are expressed^{65–67} via the hypergeometric functions ${}_3F_2$ of unit argument and for the last one, several terms of ε -expansion are known⁶⁸ (see Ref. 69 for review). At four loops, we are left with 19 families (Fig. 1). The families 10–12 were considered in Ref. 56, the family 1 (and one subfamily, i.e. a family with a contracted line) in Ref. 50. There are 54 master integrals (Fig. 2): 13 recursively one-loop (expressible via Γ -functions); 10 can be calculated using the formulas from Refs. 65–67 (in one case, the hypergeometric function happens to be expressible via Γ -functions); and for two integrals, several terms of ε -expansions are known from Ref. 68. The ε -expansions of all master integrals up to weight 12 have been obtained⁷⁰ using the DRA method.⁷¹

The complete result for the HQET field anomalous dimension up to four loops is⁶²

$$\begin{aligned} \gamma_h = & 2C_R(a-3)\frac{\alpha_s}{4\pi} + C_R\left(\frac{\alpha_s}{4\pi}\right)^2 \left[C_A\left(\frac{a^2}{2} + 4a - \frac{179}{6}\right) + \frac{32}{3}T_F n_f \right] \\ & + C_R\left(\frac{\alpha_s}{4\pi}\right)^3 \left\{ C_A^2 \left[\frac{5}{8}a^3 + \frac{3}{4}\left(\zeta_3 + \frac{13}{4}\right)a^2 + \left(6\zeta_3 - \frac{4}{45}\pi^4 + \frac{271}{16}\right)a \right. \right. \\ & \left. \left. - \frac{123}{4}\zeta_3 - \frac{4}{15}\pi^4 - \frac{23815}{216}\right] + C_A T_F n_f \left(-\frac{17}{2}a + 96\zeta_3 + \frac{782}{27} \right) \right. \\ & \left. - 6C_F T_F n_f (16\zeta_3 - 17) + \frac{160}{27}(T_F n_f)^2 \right\} + \left(\frac{\alpha_s}{4\pi}\right)^4 \left\{ C_R C_A^3 \left[\left(\frac{5}{3}\zeta_5 + \frac{\zeta_3}{6} + \frac{19}{2} \right) \right. \right. \\ & \times \frac{a^4}{16} + \left(21\zeta_3 - \frac{\pi^4}{30} + \frac{149}{3} \right) \frac{a^3}{16} - \left(\frac{169}{4}\zeta_5 - \frac{13}{3}\pi^2\zeta_3 - \frac{653}{4}\zeta_3 + \frac{121}{90}\pi^4 - \pi^2 \right. \\ & \left. - \frac{6707}{48} \right) \frac{a^2}{12} - \left(\frac{272}{9}\zeta_5 - \frac{11}{4}\zeta_3^2 - \frac{164}{27}\pi^2\zeta_3 - \frac{3839}{48}\zeta_3 - \frac{472}{8505}\pi^6 + \frac{9109}{4320}\pi^4 \right. \\ & \left. + \frac{2}{9}\pi^2 - \frac{1690475}{15552} \right) a + \frac{3859}{12}\zeta_5 + \frac{451}{4}\zeta_3^2 - \frac{709}{36}\pi^2\zeta_3 - \frac{212237}{288}\zeta_3 \\ & \left. + \frac{850}{1701}\pi^6 - \frac{10501}{2160}\pi^4 + \frac{781}{36}\pi^2 - \frac{471001}{648} \right] + d_{RA} \left[(5\zeta_5 - 7\zeta_3) \frac{a^4}{4} - 3\zeta_3 a^3 \right. \\ & \left. - \frac{3}{2}(25\zeta_5 - \zeta_3)a^2 + \left(540\zeta_5 + 24\zeta_3^2 - \frac{128}{3}\pi^2\zeta_3 - 11\zeta_3 - \frac{884}{2835}\pi^6 + \frac{16}{3}\pi^2 \right) a \right. \\ & \left. - \frac{4815}{4}\zeta_5 - 384\zeta_3^2 + \frac{320}{3}\pi^2\zeta_3 + \frac{569}{4}\zeta_3 + \frac{224}{405}\pi^6 + \frac{128}{15}\pi^4 - \frac{16}{3}\pi^2 \right] \\ & + C_R C_A^2 T_F n_f \left[\left(-\frac{7}{3}\zeta_3 + \frac{\pi^4}{180} - \frac{109}{36} \right) a^2 + \left(\frac{4}{9}\zeta_5 - \frac{16}{27}\pi^2\zeta_3 - 82\zeta_3 \right. \right. \\ & \left. \left. + \frac{\pi^4}{15} - \frac{37957}{1944} \right) a - \frac{1534}{3}\zeta_5 - 96\zeta_3^2 + \frac{104}{9}\pi^2\zeta_3 + \frac{5506}{3}\zeta_3 - \frac{3097}{540}\pi^4 \right. \end{aligned}$$

A. Grozin

$$\begin{aligned}
 & -\frac{16}{3}\pi^2 + \frac{30617}{81} \Big] + C_R C_F C_A T_F n_f \left[\left(88\zeta_3 + \frac{4}{15}\pi^4 - \frac{767}{6} \right) a - 480\zeta_5 \right. \\
 & - 928\zeta_3 + \frac{88}{15}\pi^4 + \frac{21703}{27} \Big] + 16C_R C_F^2 T_F n_f \left(60\zeta_5 - 37\zeta_3 - \frac{35}{3} \right) \\
 & + 64d_{RF} n_f \left(-5\zeta_5 + \frac{8}{3}\pi^2\zeta_3 + 4\zeta_3 - \frac{8}{3}\pi^2 \right) + 2C_R C_A (T_F n_f)^2 \\
 & \times \left[\frac{4}{3} \left(4\zeta_3 - \frac{269}{81} \right) a - 192\zeta_3 + \frac{16}{15}\pi^4 - \frac{1027}{81} \right] + 32C_R C_F (T_F n_f)^2 \\
 & \times \left(12\zeta_3 - \frac{\pi^4}{15} - \frac{103}{27} \right) - \frac{256}{27} C_R (T_F n_f)^3 (3\zeta_3 - 1) \Big\} + \dots
 \end{aligned} \tag{5.1}$$

The terms up to α_s^3 agree with Refs. 34 and 35. Some color structures of the α_s^4 contribution were known earlier, see Table 1. In QED, the only gauge-dependent term is the one-loop one; if $n_f = 0$, all contributions but the one-loop one vanish (Sec. 3).

Curiously, the difference of γ_h (with $R = F$) and γ_q is gauge-invariant up to two loops, linear in a at α_s^3 and quadratic in a at α_s^4 ,

$$\begin{aligned}
 \gamma_h - \gamma_q = & -6C_F \frac{\alpha_s}{4\pi} + C_F \left(\frac{\alpha_s}{4\pi} \right)^2 \left(3C_F - \frac{127}{3}C_A + \frac{44}{3}T_F n_f \right) \\
 & + C_F \left(\frac{\alpha_s}{4\pi} \right)^3 \left\{ C_A^2 \left[\left(\frac{9}{2}\zeta_3 - \frac{4}{45}\pi^4 + \frac{1}{2} \right) a - \frac{27}{2}\zeta_3 - \frac{4}{15}\pi^4 - \frac{6410}{27} \right] \right. \\
 & - C_F C_A \left(24\zeta_3 - \frac{143}{2} \right) - 3C_F^2 + 8C_A T_F n_f \left(12\zeta_3 + \frac{313}{27} \right) \\
 & - 96C_F T_F n_f (\zeta_3 - 1) + \frac{40}{27} (T_F n_f)^2 \Big\} + \left(\frac{\alpha_s}{4\pi} \right)^4 \left\{ C_F C_A^3 \left[\left(\frac{7}{4}\zeta_5 + \frac{13}{9}\pi^2\zeta_3 \right. \right. \right. \\
 & + \frac{43}{6}\zeta_3 - \frac{191}{540}\pi^4 + \frac{\pi^2}{3} + \frac{5}{3} \Big) \frac{a^2}{4} + \left(\frac{637}{36}\zeta_5 + \frac{11}{4}\zeta_3^2 + \frac{164}{27}\pi^2\zeta_3 + \frac{139}{6}\zeta_3 \right. \\
 & + \frac{472}{8505}\pi^6 - \frac{4409}{2160}\pi^4 - \frac{2}{9}\pi^2 + \frac{433}{72} \Big) a + \frac{27871}{48}\zeta_5 + \frac{451}{4}\zeta_3^2 - \frac{709}{36}\pi^2\zeta_3 \\
 & - \frac{39089}{72}\zeta_3 + \frac{850}{1701}\pi^6 - \frac{6389}{1080}\pi^4 + \frac{781}{36}\pi^2 - \frac{1233089}{648} \Big] \\
 & - C_F^2 C_A^2 \left[(10\zeta_5 - 7\zeta_3 + 6)a + 1570\zeta_5 - 421\zeta_3 - \frac{22}{15}\pi^4 - \frac{23885}{18} \right] \\
 & + C_F^3 C_A \left(2880\zeta_5 - 1696\zeta_3 - \frac{5131}{6} \right) - C_F^4 \left(1280\zeta_5 - 800\zeta_3 - \frac{1027}{4} \right) \\
 & + 2d_{RA} \left[-2(5\zeta_5 + \zeta_3)a^2 + \left(325\zeta_5 + 12\zeta_3^2 - \frac{64}{3}\pi^2\zeta_3 - 56\zeta_3 - \frac{442}{2835}\pi^6 \right. \right. \\
 & \left. \left. + \frac{8}{3}\pi^2 - 1 \right) a - 495\zeta_5 - 192\zeta_3^2 + \frac{160}{3}\pi^2\zeta_3 - 68\zeta_3 + \frac{112}{405}\pi^6 + \frac{64}{15}\pi^4 \right]
 \end{aligned}$$

$$\begin{aligned}
& - \frac{8}{3} \pi^2 + 67 \Big] + C_F C_A^2 T_F n_f \left[\left(\frac{4}{9} \zeta_5 - \frac{16}{27} \pi^2 \zeta_3 - 8 \zeta_3 + \frac{11}{45} \pi^4 - \frac{4}{9} \right) a \right. \\
& - \frac{1054}{3} \zeta_5 - 96 \zeta_3^2 + \frac{104}{9} \pi^2 \zeta_3 + \frac{5515}{3} \zeta_3 - \frac{289}{54} \pi^4 - \frac{16}{3} \pi^2 + \frac{85730}{81} \Big] \\
& - 2 C_F^2 C_A T_F n_f \left(400 \zeta_5 + 464 \zeta_3 - \frac{8}{3} \pi^4 - \frac{10931}{27} \right) + 8 C_F^3 T_F n_f \\
& \times \left(120 \zeta_5 - 58 \zeta_3 - \frac{89}{3} \right) - 64 d_{FF} n_f \left(5 \zeta_5 - \frac{8}{3} \pi^2 \zeta_3 - 4 \zeta_3 + \frac{8}{3} \pi^2 + 4 \right) \\
& - 32 C_F C_A (T_F n_f)^2 \left(14 \zeta_3 - \frac{\pi^4}{15} + \frac{229}{81} \right) + 32 C_F^2 (T_F n_f)^2 \\
& \times \left(14 \zeta_3 - \frac{\pi^4}{15} - \frac{160}{27} \right) - \frac{16}{9} C_F (T_F n_f)^3 \left(16 \zeta_3 - \frac{13}{9} \right) \Big\} + \dots
\end{aligned} \tag{5.2}$$

(see Refs. 72 and 73 for γ_q). In QED, the only gauge-dependent term in γ_h is the one-loop one, the same is true for γ_q (see Ref. 74), and $\gamma_h - \gamma_q$ is gauge-invariant to all orders. The on-shell renormalization constant of a heavy quark field Z_Q^{os} has the same pattern of a -dependence.

As a check of calculations, the hhg vertex at $p_g = 0$ has also been calculated in Ref. 62. It has a single structure $\Gamma(\omega) v^\mu t_R^a$. Infrared divergences are absent, therefore $\log \Gamma(\omega) = \log Z_\Gamma(\alpha_s, a) + \mathcal{O}(\varepsilon^0)$, where Z_Γ contains ultraviolet divergences. We have $Z_\alpha(\alpha_s) = Z_A^{-1}(\alpha_s, a)(Z_\Gamma(\alpha_s, a)Z_h(\alpha_s, a))^{-2}$, and hence

$$\begin{aligned}
\beta(\alpha_s) &= \frac{1}{2} \frac{d \log Z_\alpha(\alpha_s)}{d \log \mu} = \sum_{L=1}^{\infty} \beta_{L-1} \left(\frac{\alpha_s}{4\pi} \right)^L \\
&= -\gamma_\Gamma(\alpha_s, a) - \gamma_h(\alpha_s, a) - \frac{1}{2} \gamma_A(\alpha_s, a).
\end{aligned} \tag{5.3}$$

The well-known result for the four-loop β -function^{75,76} is reproduced using the four-loop γ_A ^{75,76}. This is a strong check of the calculation⁶² of γ_h .

If we consider QCD with n_f light flavors and one heavy flavor Q , then, in situations accessible for the HQET approach, the QCD heavy quark field Q can be expressed via the HQET field h_v via the matching relation^{74,77}

$$Q(\mu) = z(\mu) h_v(\mu) + \mathcal{O}\left(\frac{1}{M}\right). \tag{5.4}$$

The matching coefficient $z(\mu)$ can be obtained from the on-shell renormalization constant of the field Q in the $(n_f + 1)$ -flavor QCD

$$Z_Q^{\text{os}} = 1 + \sum_{L=1}^{\infty} \left(4 \frac{g_0^2 M^{-2\varepsilon}}{(4\pi)^{d/2} \varepsilon} e^{-\gamma\varepsilon} \right)^L Z_L, \quad Z_L = \sum_{n=0}^{\infty} Z_{L,n}(\xi) \varepsilon^n, \tag{5.5}$$

A. Grozin

where $g_0 = g_0^{(n_f+1)}$, $\xi = 1 - a_0^{(n_f+1)}$ and M is the on-shell mass of Q . The renormalized matching coefficient $z(\mu)$ must be finite. This requirement was used⁷⁷ to obtain analytical expressions for $Z_{4,n}$ with $n < 4$, see Tables I and II. However, analytical expressions for the color structures $C_F C_A^3$ and d_{FA} in $Z_{4,3}$ remained unknown (Table II), because the corresponding terms in γ_h were not known. Now we are in a position to complete Table II of Ref. 77:

$$\begin{aligned}
 Z_{4,3} = & C_F C_A^3 \left[\frac{1}{16} \left(\frac{2387}{3} a_4 + \frac{2387}{72} a_1^4 + \frac{2849}{36} \pi^2 a_1^2 - \frac{15907}{72} \pi^2 a_1 - \frac{102349}{384} \zeta_5 \right. \right. \\
 & + \frac{231}{256} \zeta_3^2 + \frac{44671}{576} \pi^2 \zeta_3 + \frac{5389931}{6912} \zeta_3 + \frac{787}{181440} \pi^6 - \frac{5659447}{414720} \pi^4 - \frac{275029}{10368} \pi^2 \\
 & - \frac{155786381}{124416} \Big) + \frac{\xi}{256} \left(\frac{1757}{192} \zeta_5 - \frac{11}{32} \zeta_3^2 + \frac{169}{48} \pi^2 \zeta_3 - \frac{3389}{96} \zeta_3 - \frac{59}{8505} \pi^6 \right. \\
 & + \frac{34433}{51840} \pi^4 - \frac{353}{144} \pi^2 - \frac{6629}{576} \Big) - \frac{\xi^2}{8192} \left(\frac{203}{12} \zeta_5 + \frac{17}{3} \pi^2 \zeta_3 - \frac{355}{6} \zeta_3 + \frac{59}{60} \pi^4 \right. \\
 & - \frac{13}{3} \pi^2 - 19 \Big) \Big] - d_{FA} \left[\frac{1}{16} \left(\frac{45}{16} \zeta_5 + \frac{45}{16} \zeta_3^2 - \frac{\pi^2}{2} \zeta_3 + \frac{63}{32} \zeta_3 - \frac{19}{10080} \pi^6 \right. \right. \\
 & - \frac{\pi^4}{15} - \frac{33}{32} \Big) + \frac{\xi}{16} \left(\frac{305}{64} \zeta_5 + \frac{3}{16} \zeta_3^2 - \frac{\pi^2}{3} \zeta_3 - \frac{15}{16} \zeta_3 - \frac{221}{90720} \pi^6 + \frac{\pi^2}{24} - \frac{1}{64} \right) \\
 & \left. \left. + \frac{\xi^2}{512} (5\zeta_5 + \zeta_3) \right] + \dots \right. \\
 = & C_F C_A^3 (-123.3401041 + 0.1197511751\xi - 0.005818521661\xi^2) \\
 & + d_{FA} (0.3701524967 + 0.1134626128\xi - 0.01247401500\xi^2) + \dots, \tag{5.6}
 \end{aligned}$$

where $a_n = \text{Li}_n(\frac{1}{2})$ (in particular, $a_1 = \log 2$), and dots mean other color structures (Table II in Ref. 77). The corresponding numerical results from Tables V–VII of Ref. 49 are

$$\begin{aligned}
 Z_{4,3} = & C_F C_A^3 [-123.354 \pm 0.086 + (0.11976 \pm 0.00013)\xi - (0.005817 \pm 0.000025)\xi^2] \\
 & + d_{FA} [0.40 \pm 0.21 + (0.1135 \pm 0.0025)\xi - (0.01250 \pm 0.00061)\xi^2] + \dots .
 \end{aligned}$$

Our analytical results (5.6) agree with them within the stated uncertainties. This is a good check of the new⁶² $C_R C_A^3$ - and d_{RA} -terms in (5.1).

6. Cusp Anomalous Dimension at Small Angles

When calculating $V(\omega, \omega, \varphi)$, we write

$$v' = v + \delta v, \quad \delta v = v(\cosh \varphi - 1) + n \sinh \varphi, \quad v \cdot n = 0, \quad n^2 = -1. \tag{6.1}$$

We expand the integrands in δv and average over direction of n in the $(d-1)$ -dimensional subspace orthogonal to v (this method of calculating the small-angle cusp anomalous dimension was first used at two loops⁷⁸).

The complete result for the first two terms of the small-angle expansion (2.18) of the cusp anomalous dimension up to four loops is⁶²

$$\begin{aligned}
\Gamma(\alpha_s, \varphi) = & 4 \frac{\alpha_s}{4\pi} (\varphi \coth \varphi - 1) \left\{ C_R - \frac{2}{3} C_R \frac{\alpha_s}{4\pi} \left[C_A \left(\pi^2 - \frac{47}{3} \right) + \frac{10}{3} T_F n_f \right] \right. \\
& + C_R \left(\frac{\alpha_s}{4\pi} \right)^2 \left[\frac{C_A^2}{3} \left(10\zeta_3 + 2\pi^4 - \frac{340}{9}\pi^2 + \frac{473}{2} \right) - \frac{2}{3} C_A T_F n_f \right. \\
& \times \left(28\zeta_3 - \frac{40}{9}\pi^2 + \frac{389}{9} \right) + C_F T_F n_f \left(16\zeta_3 - \frac{55}{3} \right) - \frac{16}{27} (T_F n_f)^2 \Big] \\
& + \left(\frac{\alpha_s}{4\pi} \right)^3 \left[-\frac{C_R C_A^3}{3} \left(310\zeta_5 + \frac{64}{3}\pi^2\zeta_3 - \frac{4756}{9}\zeta_3 + \frac{20}{9}\pi^6 - \frac{4841}{90}\pi^4 \right. \right. \\
& \left. \left. + \frac{35906}{81}\pi^2 - \frac{89011}{54} \right) - \frac{16}{3} d_{RA} \pi^2 \left(34\zeta_3 - \frac{2}{15}\pi^4 - \frac{8}{3}\pi^2 + \frac{1}{3} \right) \right. \\
& + \frac{C_R C_A^2 T_F n_f}{3} \left(440\zeta_5 + \frac{224}{3}\pi^2\zeta_3 - \frac{14444}{9}\zeta_3 - \frac{88}{9}\pi^4 + \frac{14768}{81}\pi^2 \right. \\
& \left. - \frac{48161}{54} \right) + C_R C_F C_A T_F n_f \left(80\zeta_5 - \frac{64}{3}\pi^2\zeta_3 + \frac{2720}{9}\zeta_3 - \frac{44}{45}\pi^4 \right. \\
& \left. + \frac{220}{9}\pi^2 - \frac{25943}{81} \right) - 2 C_R C_F^2 T_F n_f \left(80\zeta_5 - \frac{148}{3}\zeta_3 - \frac{143}{9} \right) \\
& + \frac{16}{3} d_{RF} n_f \pi^2 \left(16\zeta_3 - \frac{5}{3}\pi^2 - \frac{10}{3} \right) + \frac{C_R C_A (T_F n_f)^2}{27} \\
& \times \left(2240\zeta_3 - \frac{56}{5}\pi^4 - \frac{608}{9}\pi^2 + \frac{1835}{3} \right) - \frac{8}{9} C_R C_F (T_F n_f)^2 \\
& \times \left. \left(80\zeta_3 - \frac{2}{5}\pi^4 - \frac{299}{9} \right) + \frac{64}{27} C_R (T_F n_f)^3 \left(2\zeta_3 - \frac{1}{3} \right) \right] \Big\} + \varphi^4 \left(\frac{\alpha_s}{4\pi} \right)^2 \\
& \times \left\{ \frac{4}{135} C_R C_A - \frac{16}{3} C_R C_A \frac{\alpha_s}{4\pi} \left[C_A \left(\frac{23}{25}\zeta_3 - \frac{\pi^2}{27} - \frac{1531}{2025} \right) + \frac{2}{81} T_F n_f \right] \right. \\
& + \frac{4}{9} \left(\frac{\alpha_s}{4\pi} \right)^2 \left[\frac{C_R C_A^3}{15} \left(2816\zeta_5 + \frac{1864}{15}\pi^2\zeta_3 - \frac{1194292}{225}\zeta_3 - \frac{907}{225}\pi^4 \right. \right. \\
& \left. \left. - \frac{16858}{405}\pi^2 + \frac{5696611}{2025} \right) - 16 d_{RA} \left(14\zeta_5 - \frac{268}{75}\pi^2\zeta_3 - \frac{566}{45}\zeta_3 + \frac{53}{225}\pi^4 \right. \right. \\
& \left. \left. + \frac{848}{405}\pi^2 - \frac{8}{27} \right) + \frac{2}{15} C_R C_A^2 T_F n_f \left(32\zeta_5 - \frac{64}{15}\pi^2\zeta_3 + \frac{39368}{75}\zeta_3 - \frac{514}{225}\pi^4 \right. \right. \\
& \left. \left. + \frac{361}{135}\pi^2 - \frac{874967}{2025} \right) + \frac{2}{3} C_R C_F C_A T_F n_f \left(\frac{16}{5}\zeta_3 - \frac{11}{3} \right) \right. \\
& \left. - 16 d_{RF} n_f \left(16\zeta_5 - \frac{16}{75}\pi^2\zeta_3 - \frac{284}{25}\zeta_3 - \frac{8}{75}\pi^4 + \frac{23}{25}\pi^2 + \frac{23}{25} \right) \right. \\
& \left. + \frac{304}{1215} C_R C_A (T_F n_f)^2 \right] \Big\} + \mathcal{O}(\varphi^6, \alpha_s^5). \tag{6.2}
\end{aligned}$$

A. Grozin

The terms up to α_s^3 agree with the results^{38,39} expanded in φ^2 [see (8.12)]. Some color structures of the α_s^4 contribution were known earlier, see Table 1. For some of them, the full φ -dependence is known; for some, one more term in the φ^2 -expansion is known⁵⁰ in addition to the terms presented in (6.2). In the Abelian case $d_{RF}n_f\alpha^4$ is the only term which does not have the simple one-loop angle dependence⁵³ [note that there is a typo in the formula (4.2) in this paper].

In the first curly bracket in (6.2), the highest weight of constants in the α_s^L -term is $2(L - 1)$. In the second curly bracket terms with this highest weight are absent.

In $\mathcal{N} = 4$ SYM, supersymmetric Wilson lines are usually discussed. They interact not only with gluons but also with scalars. A cusp on a supersymmetric Wilson line is characterized by the geometric angle φ and the internal angle ϑ (we'll consider the case $\vartheta = 0$). In the case of $SU(N_c)$ gauge group in the large- N_c limit, the Bremsstrahlung function (the φ^2 -term) is known exactly in coupling.¹⁷ The full φ -dependence is known up to four loops.⁷⁹ The result has the structure

$$\Gamma = \sum_{L=1}^{\infty} \Gamma_L \left(\frac{N_c \alpha_s}{2\pi} \right)^L, \quad \Gamma_L = \sum_{n=1}^L \Gamma_{Ln} \tanh^n \frac{\varphi}{2}.$$

Up to three loops, the large- N_c results are sufficient for reconstructing the complete results for the arbitrary gauge groups via Casimirs. However, at four loops $d_{RA}/(C_R C_A^3) = 1/24 + \mathcal{O}(1/N_c^2)$ (the $1/N_c^2$ -term depends on R), and we know only a certain linear combination of the coefficients of $C_R C_A^3$ and d_{RA} . The Bremsstrahlung function is known for an arbitrary gauge group via Casimirs up to (in principle) an arbitrarily high order.⁸⁰ Expanding the results of Ref. 79 up to φ^4 and replacing the φ^2 -term by the result of Ref. 80, we have

$$\begin{aligned} \Gamma = & \frac{\alpha_s}{2\pi} \varphi \tanh \frac{\varphi}{2} \left[C_R - \frac{1}{6} C_R C_A \pi \alpha_s + \frac{1}{24} C_R C_A^2 (\pi \alpha_s)^2 - \left(\frac{5}{24} C_R C_A^3 - \frac{d_{RA}}{5} \right) \right. \\ & \times \left. \frac{(\pi \alpha_s)^3}{18} \right] + \frac{N_c \alpha_s \varphi^4}{2\pi} \left[\frac{1}{6} - \frac{3}{2} \zeta_3 \frac{N_c \alpha_s}{2\pi} + \left(\frac{45}{4} \zeta_5 + \frac{2}{3} \pi^2 \zeta_3 - \frac{2}{45} \pi^4 \right) \left(\frac{N_c \alpha_s}{2\pi} \right)^2 \right] \\ & + \mathcal{O}(\varphi^6, \alpha_s^5). \end{aligned} \quad (6.3)$$

The $\mathcal{O}(\varphi)$ -terms in Γ_{L1} contain only maximum-weight contributions, and produce the first bracket in (6.3); it is homogeneous in weight. The $\mathcal{O}(\varphi^3)$ -terms in Γ_{L1} and the $\mathcal{O}(\varphi^2)$ -terms in Γ_{L2} contain only lower-weight contributions, and produce the second square bracket in (6.3); it is not homogeneous and only known in the $N_c \rightarrow \infty$ limit. If we keep only maximum-weight terms, this second bracket vanishes, just like the second curly bracket in the QCD result (6.2). If we keep only the maximum-weight terms in the first curly bracket in (6.2), we obtain exactly the first square bracket in the supersymmetric result (6.3). So, the principle of maximal transcendentality^{81,82} works for the Bremsstrahlung function up to four loops.

The HQET field anomalous dimension γ_h (5.1) has the same pattern of weights as the first curly bracket in (6.2). If we retain only the highest weights $2(L - 1)$ in

γ_h (5.1), we get

$$2C_F(a-3)\frac{\alpha_s}{4\pi} - \frac{4}{15}\left(\frac{a}{3}+1\right)\pi^4\left(\frac{\alpha_s}{4\pi}\right)^3 + \left(\frac{\alpha_s}{4\pi}\right)^4\left\{C_RC_A^3\left[\left(\frac{11}{4}\zeta_3^2 + \frac{472}{8505}\pi^6\right)a + \frac{451}{4}\zeta_3^2 + \frac{850}{1701}\pi^6\right] + 4d_{RA}\left[\left(6\zeta_3^2 - \frac{221}{2835}\pi^6\right)a - 8\left(12\zeta_3^2 - \frac{7}{405}\pi^6\right)\right] - 96\zeta_3^2C_RC_AT_Fn_f\right\} + \dots$$

(the α_s^2 -term is absent because the corresponding term in γ_h contains no π^2). All terms are linear in a here. It would be interesting to understand whether this expression is somehow related to the anomalous dimension of an end of Wilson line in the $\mathcal{N} = 4$ SYM. The term with n_f does not look encouraging in this respect.

7. Light-Like Cusp Anomalous Dimension

The full result up to four loops has been obtained in Ref. 54 and confirmed in Ref. 55 from form factor calculations,

$$\begin{aligned} K(\alpha_s) = & 4\frac{\alpha_s}{4\pi}\left\{C_R - C_R\frac{\alpha_s}{4\pi}\left[\frac{C_A}{3}\left(\pi^2 - \frac{67}{3}\right) + \frac{20}{9}T_Fn_f\right] + C_R\left(\frac{\alpha_s}{4\pi}\right)^2\right. \\ & \times \left[\frac{C_A^2}{3}\left(22\zeta_3 + \frac{11}{15}\pi^4 - \frac{134}{9}\pi^2 + \frac{245}{2}\right) - \frac{2}{3}C_AT_Fn_f\left(28\zeta_3 - \frac{20}{9}\pi^2\right.\right. \\ & \left.\left.+ \frac{209}{9}\right) + C_FT_Fn_f\left(16\zeta_3 - \frac{55}{3}\right) - \frac{16}{27}(T_Fn_f)^2\right] + \left(\frac{\alpha_s}{4\pi}\right)^3 \\ & \times \left[-C_RC_A^3\left(\frac{902}{9}\zeta_5 + 4\zeta_3^2 + \frac{44}{9}\pi^2\zeta_3 - \frac{5236}{27}\zeta_3 + \frac{626}{2835}\pi^6 - \frac{451}{90}\pi^4\right.\right. \\ & \left.\left.+ \frac{11050}{243}\pi^2 - \frac{42139}{162}\right) + 8d_{RA}\left(\frac{110}{3}\zeta_5 - 12\zeta_3^2 + \frac{4}{3}\zeta_3 - \frac{31}{945}\pi^6 - \frac{2}{3}\pi^2\right)\right. \\ & \left.+ \frac{C_RC_A^2T_Fn_f}{9}\left(1048\zeta_5 + 112\pi^2\zeta_3 - \frac{11552}{3}\zeta_3 - \frac{44}{15}\pi^4 + \frac{5080}{27}\pi^2 - \frac{24137}{18}\right)\right. \\ & \left.+ C_RC_FC_AT_Fn_f\left(80\zeta_5 - \frac{32}{3}\pi^2\zeta_3 + \frac{1856}{9}\zeta_3 - \frac{44}{45}\pi^4 + \frac{110}{9}\pi^2 - \frac{17033}{81}\right)\right. \\ & \left.- 2C_RC_F^2T_Fn_f\left(80\zeta_5 - \frac{148}{3}\zeta_3 - \frac{143}{9}\right) - \frac{32}{3}d_{RF}n_f(10\zeta_5 + 2\zeta_3 - \pi^2)\right. \\ & \left.+ \frac{C_RC_A(T_Fn_f)^2}{27}\left(2240\zeta_3 - \frac{56}{5}\pi^4 - \frac{304}{9}\pi^2 + \frac{923}{3}\right) - \frac{8}{9}C_RC_F(T_Fn_f)^2\right. \\ & \left.\left.\times \left(80\zeta_3 - \frac{2}{5}\pi^4 - \frac{299}{9}\right) + \frac{64}{27}C_R(T_Fn_f)^3\left(2\zeta_3 - \frac{1}{3}\right)\right] + \mathcal{O}(\alpha_s^4)\right\}. \quad (7.1) \end{aligned}$$

The terms up to α_s^3 agree with Ref. 40. Some color structures of the α_s^4 -contribution were known earlier, see Table 1. The four-loop $C_RC_FC_AT_Fn_f$ -term in Ref. 54 was

A. Grozin

derived from a conjecture, see Sec. 8 for details; in Ref. 55 it was confirmed by a direct calculation. In QED with $n_f = 0$ only the one-loop term remains.

In $\mathcal{N} = 4$ SYM with $SU(N_c)$ gauge group in the large- N_c limit, the light-like anomalous dimension is known⁸³ exactly in $g^2 N_c$; results up to four loops were derived in Refs. 84, 85 and 79. Up to three loops, these results are sufficient for reconstructing the full result for an arbitrary gauge group expressed via Casimirs. At four loops, there are two different Casimirs; the full analytical result has been obtained in Refs. 54 and 86,

$$K(\alpha_s) = 4 \frac{\alpha_s}{4\pi} \left\{ C_R - \frac{\pi^2}{3} C_R C_A \frac{\alpha_s}{4\pi} + \frac{11}{45} \pi^4 C_R C_A^2 \left(\frac{\alpha_s}{4\pi} \right)^2 - \left(\frac{\alpha_s}{4\pi} \right)^3 \right. \\ \times \left[2C_R C_A^3 \left(2\zeta_3^2 + \frac{313}{2835} \pi^6 \right) + 8d_{RA} \left(12\zeta_3^2 + \frac{31}{945} \pi^6 \right) \right] + \mathcal{O}(\alpha_s^4) \right\}. \quad (7.2)$$

If we keep only the maximum-weight terms in the QCD result (7.1), we obtain exactly the SYM result (7.2). So, the principle of maximal transcendentality^{81,82} works for the light-like cusp anomalous dimension up to four loops.

8. A Conjecture Which Sometimes Works

An interesting property of Γ up to three loops has been noticed in Refs. 38 and 39. Let's introduce a new coupling A instead of $\alpha_s/(4\pi)$,

$$K(\alpha_s) = 4C_R A, \quad A = \frac{\alpha_s}{4\pi} \left[1 + K_2 \frac{\alpha_s}{4\pi} + K_3 \left(\frac{\alpha_s}{4\pi} \right)^2 + \dots \right], \\ K_2 = C_A K_A + T_F n_f K_f, \\ K_3 = C_A^2 K_{AA} + C_A T_F n_f K_{Af} + C_F T_F n_f K_{Ff} + (T_F n_f)^2 K_{ff}, \quad \dots, \quad (8.1)$$

where $K(\alpha_s)$ is the light-like cusp anomalous dimension [see (7.1)], and re-express $\Gamma(\alpha_s, \varphi)$ via it,

$$\Gamma(\alpha_s, \varphi) = \Omega(A, \varphi) = C_R [\Omega_1(\varphi) A + \Omega_2(\varphi) A^2 + \Omega_3(\varphi) A^3 + \dots]. \quad (8.2)$$

Then the function Ω does not depend on n_f , i.e. on the number of matter spinor fields in fundamental representation. Moreover, it remains the same in a generic gauge theory with any numbers of fermions and scalars (including supersymmetric QCD extensions). It contains only the adjoint-representation color structures,

$$\Omega_2(\varphi) = C_A \Omega_A(\varphi), \quad \Omega_3(\varphi) = C_A^2 \Omega_{AA}(\varphi), \quad \dots \quad (8.3)$$

If we write $\Gamma(\alpha_s, \varphi)$ as

$$\Gamma(\alpha_s, \varphi) = C_R \frac{\alpha_s}{4\pi} \left[\Gamma_1(\varphi) + \Gamma_2(\varphi) \frac{\alpha_s}{4\pi} + \Gamma_3(\varphi) \left(\frac{\alpha_s}{4\pi} \right)^2 + \dots \right], \\ \Gamma_2(\varphi) = C_A \Gamma_A(\varphi) + T_F n_f \Gamma_f(\varphi), \\ \Gamma_3(\varphi) = C_A^2 \Gamma_{AA}(\varphi) + C_A T_F n_f \Gamma_{Af}(\varphi) + C_F T_F n_f \Gamma_{Ff}(\varphi) \\ + (T_F n_f)^2 \Gamma_{ff}(\varphi), \quad \dots,$$

then

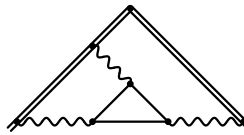
$$\Gamma_1(\varphi) = \Omega_1(\varphi), \quad \Gamma_A(\varphi) = \Omega_A(\varphi) + K_A \Omega_1(\varphi), \quad (8.4)$$

$$\Gamma_{AA}(\varphi) = \Omega_{AA}(\varphi) + 2K_A \Omega_A(\varphi) + K_{AA} \Omega_1(\varphi), \quad (8.5)$$

$$\Gamma_f(\varphi) = K_f \Omega_1(\varphi), \quad \Gamma_{Ff}(\varphi) = K_{Ff} \Omega_1(\varphi), \quad \Gamma_{ff}(\varphi) = K_{ff} \Omega_1(\varphi), \quad (8.6)$$

$$\Gamma_{Af}(\varphi) = 2K_f \Omega_A(\varphi) + K_{Af} \Omega_1(\varphi). \quad (8.7)$$

For purely gluonic structures Γ_X ($X = 1, A, AA$), using (8.4)–(8.5) we can express Ω_X via Γ_X and lower-loop results. For the Abelian structures $X = 1, f, Ff, ff$, the terms Γ_X are given by diagrams with a single two-leg c-webs (see Sec. 10), and hence have the pure one-loop angle dependence $\Omega_1(\varphi) = 4(\varphi \coth \varphi - 1)$. In these cases, the coefficient of Ω_1 is fixed by the $\varphi \rightarrow \infty$ limit to be K_X ; the relations (8.6) hold by construction, and contain no interesting information. The relation (8.7) is the only interesting one. It expresses the contribution of highly nontrivial three-loop diagrams



to Γ via lower-loop contributions. The φ -dependence of Γ_{Af} is very nontrivial; it seems absolutely impossible that the relation (8.7) holds accidentally, it must have some explanation (which is not yet known).

The result of the calculation^{38,39} is

$$\begin{aligned} \Omega_1 &= 4\tilde{A}_1, \quad \Omega_A = 8\left(\tilde{A}_3 + \tilde{A}_2 + \frac{\pi^2}{6}\tilde{A}_1\right), \\ \Omega_{AA} &= 16\left(\tilde{A}_5 + \tilde{A}_4 - \tilde{A}_2 + \tilde{B}_5 + \tilde{B}_3 + \frac{\pi^2}{3}(\tilde{A}_3 + \tilde{A}_2) - \frac{\pi^4}{180}\tilde{A}_1\right), \end{aligned} \quad (8.8)$$

where $\tilde{A}_i = A_i(x) - A_i(1)$, $\tilde{B}_i = B_i(x) - B_i(1)$, $x = e^{-\varphi}$,

$$\begin{aligned} A_1(x) &= \frac{\xi}{2}H_1(y), \\ A_2(x) &= \frac{1}{2}H_{1,1}(y) + \frac{\pi^2}{3} - \xi\left[H_{0,1}(y) + \frac{1}{2}H_{1,1}(y)\right], \\ A_3(x) &= -\xi\left[\frac{1}{4}H_{1,1,1}(y) + \frac{\pi^2}{6}H_1(y)\right] + \xi^2\left[\frac{1}{2}H_{1,0,1}(y) + \frac{1}{4}H_{1,1,1}(y)\right], \\ A_4(x) &= -\frac{1}{4}H_{1,1,1,1}(y) - \frac{\pi^2}{6}H_{1,1}(y) + \xi\left[2H_{1,1,0,1}(y) + \frac{3}{2}H_{0,1,1,1}(y) + \frac{7}{4}H_{1,1,1,1}(y) \right. \\ &\quad \left. + \frac{\pi^2}{3}H_{0,1}(y) + \frac{\pi^2}{6}H_{1,1}(y) + 3\zeta_3 H_1(y)\right] - \xi^2\left[2H_{1,0,0,1}(y) + 2H_{0,1,0,1}(y) \right. \\ &\quad \left. + 2H_{1,1,0,1}(y) + H_{1,0,1,1}(y) + H_{0,1,1,1}(y) + \frac{3}{2}H_{1,1,1,1}(y)\right], \end{aligned}$$

A. Grozin

$$\begin{aligned}
 A_5(x) &= \xi \left[\frac{5}{8} H_{1,1,1,1,1}(y) + \frac{\pi^2}{4} H_{1,1,1}(y) + \frac{\pi^4}{12} H_1(y) \right] - \xi^2 [H_{1,1,1,0,1}(y) \\
 &\quad + \frac{3}{4} H_{1,0,1,1,1}(y) + H_{0,1,1,1,1}(y) + \frac{11}{8} H_{1,1,1,1,1}(y) + \frac{\pi^2}{6} H_{1,0,1}(y) \\
 &\quad + \frac{\pi^2}{3} H_{0,1,1}(y) + \frac{\pi^2}{4} H_{1,1,1}(y) + \frac{3}{2} \zeta_3 H_{1,1}(y) \Big] + \xi^3 [H_{1,1,0,0,1}(y) \\
 &\quad + H_{1,0,1,0,1}(y) + H_{1,1,1,0,1}(y) + \frac{1}{2} H_{1,1,0,1,1}(y) + \frac{1}{2} H_{1,0,1,1,1}(y) \\
 &\quad + \frac{3}{4} H_{1,1,1,1,1}(y) \Big], \\
 B_3(x) &= -H_{1,0,1}(y) + \frac{1}{2} H_{0,1,1}(y) - \frac{1}{4} H_{1,1,1}(y) \\
 &\quad + \xi \left[2H_{0,0,1}(y) + H_{1,0,1}(y) + H_{0,1,1}(y) + \frac{1}{4} H_{1,1,1}(y) \right], \\
 B_5(x) &= \frac{x}{1-x^2} \left[-4H_{-1,0,-1,0,0}(x) + 4H_{-1,0,1,0,0}(x) - 4H_{1,0,-1,0,0}(x) \right. \\
 &\quad + 4H_{1,0,1,0,0}(x) + 4H_{-1,0,0,0,0}(x) + 4H_{1,0,0,0,0}(x) \\
 &\quad \left. + 2\zeta_3 H_{-1,0}(x) + 2\zeta_3 H_{1,0}(x) - \frac{\pi^4}{60} H_{-1}(x) - \frac{\pi^4}{60} H_1(x) \right],
 \end{aligned}$$

$\xi = (1+x^2)/(1-x^2)$, $y = 1-x^2$. Here, $H_{...}(x)$ are harmonic polylogarithms.⁸⁷ Symbolic manipulations and numerical evaluation of these functions are available in **Mathematica**^{88,89} and **Maple**.⁹⁰ Numerical evaluation of multiple polylogarithms (including harmonic ones) was implemented⁹¹ in C++ and used in **GiNaC**⁹² (<https://ginac.de/>). Numerical evaluation of harmonic polylogarithms was implemented in **Fortran** up to weight 4^{93,94} and then up to weight 8.⁹⁵

At large φ , we have

$$\begin{aligned}
 A_1 &= \varphi + \dots, \quad A_2 = \frac{\pi^2}{6} + \dots, \quad A_3 = -\frac{\pi^2}{6} \varphi - \zeta_3 + \dots, \quad A_4 = \frac{19}{180} \pi^4 + \dots, \\
 A_5 &= \frac{11}{180} \pi^4 \varphi + \frac{9}{2} \zeta_5 - \frac{\pi^2}{5} \zeta_3 + \dots, \quad B_3 = \frac{7}{2} \zeta_3 + \dots, \quad B_5 = 0 + \dots,
 \end{aligned} \tag{8.9}$$

where dots mean exponentially suppressed terms. Subtracting A_i , B_i at $\varphi = 0$ [see (8.11)] to obtain \tilde{A}_i , \tilde{B}_i , we get

$$\begin{aligned}
 \Omega_1 &= 4(\varphi - 1) + \dots, \quad \Omega_A = 8(1 - \zeta_3) + \dots, \\
 \Omega_{AA} &= 8(9\zeta_5 - \pi^2\zeta_3 - 2\zeta_3 + \pi^2 - 4) + \dots.
 \end{aligned} \tag{8.10}$$

By construction, only the one-loop term Ω_1 contains the linearly growing contribution φ , all higher terms are $\mathcal{O}(\varphi^0)$. Using the formulas (8.4)–(8.7), it is easy to reconstruct the $\mathcal{O}(\varphi^0)$ -terms in the large- φ asymptotics (2.20) up to three loops.

At small φ , we have

$$\begin{aligned}
A_1 &= 1 + \frac{\varphi^2}{3} - \frac{\varphi^4}{45} + \frac{2}{945} \varphi^6 - \frac{\varphi^8}{4725} + \frac{2}{93555} \varphi^{10} + \mathcal{O}(\varphi^{12}), \\
A_2 &= \frac{\pi^2}{3} - 2 + \frac{\varphi^2}{9} - \frac{14}{675} \varphi^4 + \frac{304}{99225} \varphi^6 - \frac{22}{55125} \varphi^8 + \frac{26104}{540280125} \varphi^{10} + \mathcal{O}(\varphi^{12}), \\
A_3 &= -\frac{\pi^2}{3} + 1 - \left(\pi^2 - \frac{7}{2} \right) \frac{\varphi^2}{9} + \left(\frac{\pi^2}{3} - \frac{2}{5} \right) \frac{\varphi^4}{45} - \frac{2}{2835} \left(\pi^2 + \frac{19}{35} \right) \varphi^6 \\
&\quad + \left(\pi^2 + \frac{67}{35} \right) \frac{\varphi^8}{14175} - \frac{2}{93555} \left(\frac{\pi^2}{3} + \frac{1949}{1925} \right) \varphi^{10} + \mathcal{O}(\varphi^{12}), \\
A_4 &= 2 \left(3\zeta_3 + \frac{\pi^2}{3} - 3 \right) + \left(2\zeta_3 - \frac{\pi^2}{27} - \frac{91}{54} \right) \varphi^2 - \left(2\zeta_3 - \frac{14}{135} \pi^2 - \frac{1789}{1350} \right) \frac{\varphi^4}{15} \\
&\quad + \left(4\zeta_3 - \frac{304}{945} \pi^2 - \frac{250121}{66150} \right) \frac{\varphi^6}{315} - \left(2\zeta_3 - \frac{22}{105} \pi^2 - \frac{296647}{99225} \right) \frac{\varphi^8}{1575} \\
&\quad + \left(4\zeta_3 - \frac{26104}{51975} \pi^2 - \frac{352666739}{40020750} \right) \frac{\varphi^{10}}{31185} + \mathcal{O}(\varphi^{12}), \\
A_5 &= -3\zeta_3 + \frac{\pi^4}{6} - \frac{2}{3} \pi^2 + 2 - \left(2\zeta_3 - \frac{\pi^4}{18} + \frac{5}{27} \pi^2 - \frac{65}{54} \right) \varphi^2 \\
&\quad - \left(\zeta_3 + \frac{\pi^4}{54} - \frac{41}{405} \pi^2 - \frac{1649}{2025} \right) \frac{\varphi^4}{5} + \left(2\zeta_3 + \frac{\pi^4}{45} - \frac{349}{1575} \pi^2 - \frac{6401}{18375} \right) \frac{\varphi^6}{63} \\
&\quad - \left(\zeta_3 + \frac{\pi^4}{126} - \frac{32}{245} \pi^2 + \frac{38959}{138915} \right) \frac{\varphi^8}{225} \\
&\quad + \left(2\zeta_3 + \frac{\pi^4}{81} - \frac{5683}{18711} \pi^2 + \frac{232902262}{180093375} \right) \frac{\varphi^{10}}{3465} + \mathcal{O}(\varphi^{12}), \\
B_3 &= 4 + \frac{5}{54} \varphi^2 - \frac{889}{40500} \varphi^4 + \frac{80299}{20837250} \varphi^6 - \frac{357533}{625117500} \varphi^8 + \frac{10632271}{138671898750} \varphi^{10} \\
&\quad + \mathcal{O}(\varphi^{12}), \\
B_5 &= \frac{3}{2} \zeta_3 - \left(\zeta_3 + \frac{1}{6} \right) \frac{\varphi^2}{3} + \left(11\zeta_3 + \frac{31}{12} \right) \frac{\varphi^4}{225} - \left(202\zeta_3 + \frac{143}{3} \right) \frac{\varphi^6}{33075} \\
&\quad + \left(13\zeta_3 + \frac{7739}{2916} \right) \frac{\varphi^8}{18375} - \left(\frac{2026}{7} \zeta_3 + \frac{1261}{27} \right) \frac{\varphi^{10}}{3675375} + \mathcal{O}(\varphi^{12}),
\end{aligned} \tag{8.11}$$

and hence

$$\begin{aligned}
\Omega_1 &= 4 \left(\frac{\varphi^2}{3} - \frac{\varphi^4}{45} + \frac{2}{945} \varphi^6 - \frac{\varphi^8}{4725} + \frac{2}{93555} \varphi^{10} \right) + \mathcal{O}(\varphi^{12}), \\
\Omega_4 &= 4 \left[-\left(\frac{\pi^2}{9} - 1 \right) \varphi^2 + (\pi^2 - 8) \frac{\varphi^4}{135} - \frac{2}{2835} \left(\pi^2 - \frac{38}{5} \right) \varphi^6 + \left(\pi^2 - \frac{262}{35} \right) \right. \\
&\quad \times \left. \frac{\varphi^8}{14175} - \frac{2}{280665} \left(\pi^2 - \frac{262}{35} \right) \varphi^{10} \right] + \mathcal{O}(\varphi^{12}),
\end{aligned}$$

A. Grozin

$$\begin{aligned}
 \Omega_{AA} = & 4 \left[- \left(4\zeta_3 - \frac{\pi^4}{5} + \frac{2}{3}\pi^2 + \frac{20}{3} \right) \frac{\varphi^2}{3} - \left(\frac{256}{5}\zeta_3 + \frac{\pi^4}{5} - \frac{28}{9}\pi^2 - \frac{706}{15} \right) \frac{\varphi^4}{45} \right. \\
 & + \frac{2}{945} \left(\frac{2536}{35}\zeta_3 + \frac{\pi^4}{5} - \frac{62}{9}\pi^2 - \frac{10826}{315} \right) \varphi^6 \\
 & - \left(\frac{368}{49}\zeta_3 + \frac{\pi^4}{63} - \frac{76}{81}\pi^2 - \frac{33398}{35721} \right) \frac{\varphi^8}{375} \\
 & \left. + \frac{2}{467775} \left(\frac{32248}{55}\zeta_3 + \pi^4 - \frac{3994}{45}\pi^2 + \frac{36182402}{363825} \right) \varphi^{10} \right] + \mathcal{O}(\varphi^{12}). \tag{8.12}
 \end{aligned}$$

It is easy to reconstruct small- φ expansions of all color structures of Γ up to three loops up to φ^{10} (more terms can be added if desired).

If has been conjectured^{38,39} that this structure holds at higher orders. At four loops, we have

$$\begin{aligned}
 K_4 = & C_A^3 K_{AAA} + \frac{d_{RA}}{C_R} K_{dRA} \\
 & + C_A^2 T_F n_f K_{AAf} + C_F C_A T_F n_f K_{FAf} + C_F^2 T_F n_f K_{FFf} + \frac{d_{RF}}{C_R} n_f K_{dRF} \\
 & + C_A (T_F n_f)^2 K_{Aff} + C_F (T_F n_f)^2 K_{FFF} + (T_F n_f)^3 K_{fff}.
 \end{aligned}$$

The quartic-Casimir terms here do not look nice because the “universal” coupling A depends on R . We should, probably, suppose

$$\Omega_4(\varphi) = C_A^3 \Omega_{AAA}(\varphi) + \frac{d_{RA}}{C_R} \Omega_{dRA}(\varphi)$$

(it is also R -dependent). Then for

$$\begin{aligned}
 \Gamma_4 = & C_A^3 \Gamma_{AAA} + \frac{d_{RA}}{C_R} \Gamma_{dRA} \\
 & + C_A^2 T_F n_f \Gamma_{AAf} + C_F C_A T_F n_f \Gamma_{FAf} + C_F^2 T_F n_f \Gamma_{FFf} + \frac{d_{RF}}{C_R} n_f \Gamma_{dRF} \\
 & + C_A (T_F n_f)^2 \Gamma_{Aff} + C_F (T_F n_f)^2 \Gamma_{FFF} + (T_F n_f)^3 \Gamma_{fff}
 \end{aligned}$$

the conjecture results in

$$\begin{aligned}
 \Gamma_{AAA} &= \Omega_{AAA} + 3K_A \Omega_{AA} + (2K_{AA} + K_A^2) \Omega_A + K_{AAA} \Omega_1, \\
 \Gamma_{dRA} &= \Omega_{dRA} + K_{dRA} \Omega_1,
 \end{aligned} \tag{8.13}$$

$$\Gamma_{FFF} = K_{FFF} \Omega_1, \quad \Gamma_{FFF} = K_{FFF} \Omega_1, \quad \Gamma_{fff} = K_{fff} \Omega_1, \tag{8.14}$$

$$\begin{aligned}
 \Gamma_{AAf} &= 3K_f \Omega_{AA} + 2(K_{Af} + K_A K_f) \Omega_A + K_{AAF} \Omega_1, \\
 \Gamma_{dRF} &= K_{RF} \Omega_1,
 \end{aligned} \tag{8.15}$$

$$\begin{aligned}
 \Gamma_{FAf} &= 2K_{Ff} \Omega_A + K_{FAf} \Omega_1, \\
 \Gamma_{Aff} &= (2K_{ff} + K_f^2) \Omega_A + K_{Aff} \Omega_1.
 \end{aligned} \tag{8.16}$$

The Abelian terms Γ_{FFf} , Γ_{Fff} and Γ_{fff} are given by the diagrams containing a single two-leg c-web, and hence have the one-loop φ -dependence $\Omega_1(\varphi)$ (see Sec. 10). So, the relations (8.14) hold by construction.

The first two terms of the small- φ expansion of Γ_{dRF} have been obtained in Ref. 56. It has been proved that the relation (8.15) for Γ_{dRF} does not hold. Later, the third term of this expansion⁵⁰, the large- φ limit^{58,59} and, finally, the full φ -dependence⁵⁷ have been obtained. The φ -dependence is *extremely* complicated, and certainly does not satisfy the relation in (8.15). The relation (8.15) for Γ_{AAf} is also wrong, as demonstrated in Ref. 50 by the calculation of two terms in the small- φ expansion. These two structures get contributions from diagrams containing a light-quark box. Maybe, such diagrams are the reason for breaking the conjecture.

However, the two remaining structures, Γ_{FAf} and Γ_{Aff} , pass all existing tests, and seem to agree⁵⁰ with the relations (8.16). For Γ_{Aff} , three terms of the small- φ expansion⁵⁰ and the large- φ limit^{48,51,52} are known, so that there are three analytical checks of the corresponding relation in (8.16). For Γ_{FAf} , two terms of the small- φ expansion are known⁵⁰; the large- φ limit K_{FAf} was only known numerically at the moment.⁶¹ So, there was only one analytical and one numerical check. The analytical form of K_{FAf} has been predicted⁵⁰ on the basis of the conjecture, and later confirmed⁵⁵ by a direct calculation. It seems that there can be little doubt that the relations (8.16) for the full φ -dependence of Γ_{FAf} and Γ_{Aff} are valid. If we believe in this statement, we can get many terms of small- φ expansions of these structures using (8.12), and their large- φ asymptotics including the $\mathcal{O}(\varphi^0)$ -terms using (8.10).

9. Euclidean Angle Near π

In a paper,⁹⁶ the authors have noticed that the two-loop cusp anomalous dimension Γ at Euclidean angle $\phi \rightarrow \pi$ is related to the one-loop static quark–antiquark potential $V(r)$,

$$\Gamma(\pi - \delta) = \frac{rV(r)}{\delta}. \quad (9.1)$$

The proof of these relations to all orders given in this paper is incorrect: we shall see that it breaks down for the three-loop Γ .

In fact, this relation follows from conformal symmetry^{38,39} (which is broken in QCD by the conformal anomaly). Let's consider the Euclidean space with the metric

$$ds^2 = dx_0^2 + d\mathbf{x}^2.$$

In spherical coordinates,

$$x_0 = r \cos \delta, \quad \mathbf{x} = r \mathbf{n} \sin \delta, \quad ds^2 = dr^2 + r^2(d\delta^2 + \sin^2 \delta d\mathbf{n}^2).$$

We assume $\delta \ll 1$ and introduce the new coordinates y by

$$r = e^{y_0}, \quad \mathbf{y} = \delta \mathbf{n}, \quad ds^2 = e^{2y_0}(dy_0^2 + d\mathbf{y}^2).$$

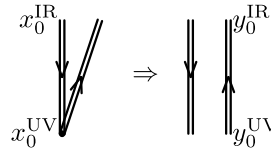
This metric is conformally flat.

A. Grozin

Let's consider a Wilson line in x -space having the shape of a small angle δ (the x_0 -axis is directed upward). We introduce a UV cutoff x_0^{UV} close to the angle and an IR cutoff x_0^{IR} far from it. Then

$$\log W = \Gamma \log \frac{x_0^{\text{IR}}}{x_0^{\text{UV}}}. \quad (9.2)$$

In y -space, it looks like a pair of antiparallel lines at a distance \mathbf{y} from each other:



and

$$\log W = V(\mathbf{y})(y_0^{\text{IR}} - y_0^{\text{UV}}). \quad (9.3)$$

If our theory is conformally invariant, these Wilson lines coincide, and

$$\Gamma(\pi - \delta) = \frac{yV(y)}{\delta}, \quad (9.4)$$

where $y = |\mathbf{y}|$. Due to conformal symmetry, $V(y) = \text{const}/y$. We can also re-write this relation in momentum space,

$$\Gamma(\pi - \delta) = \frac{\mathbf{q}^2 V(\mathbf{q})}{4\pi\delta} \quad (9.5)$$

[the momentum-space potential is $V(\mathbf{q}) = \text{const}/|\mathbf{q}|^2$]. In $\mathcal{N} = 4$ SYM (which is conformally symmetric), the three-loop $\Gamma(\pi - \delta)$ ^{38,39} agrees with the two-loop V .⁹⁷

Let's introduce the conformal anomaly $\Delta(\alpha_s)$ by

$$4\pi\Delta(\alpha_s(|\mathbf{q}|)) = [\delta\Gamma(\alpha_s(|\mathbf{q}|), \pi - \delta)]_{\delta \rightarrow 0} - \frac{\mathbf{q}^2 V(\alpha_s(|\mathbf{q}|), \mathbf{q})}{4\pi}. \quad (9.6)$$

In QCD at three loops Δ can be obtained from the general result (8.8) using the asymptotics $\phi = \pi - \delta$, $\delta \rightarrow 0$ of A_i , B_i [see (A.13) in Ref. 50]. The result is³⁹

$$\Delta(\alpha_s) = \frac{4}{27}\beta_0 C_R (47C_A - 28T_F n_f) \left(\frac{\alpha_s}{4\pi} \right)^3 + \mathcal{O}(\alpha_s^4). \quad (9.7)$$

It vanishes when $\beta_0 = 0$. In QCD (as well as in QED and many other gauge theories) conformal symmetry is anomalous, broken by the β -function. Therefore, it seems reasonable to assume³⁹ that, similarly to the Crewther relation,^{98–100} the conformal anomaly has the form

$$\Delta(\alpha_s) = \beta(\alpha_s) C(\alpha_s). \quad (9.8)$$

In addition to the α_s^2 -term (9.7) of C , several color structures of the α_s^3 -term are known⁵⁰ [the three-loop $V(\mathbf{q})$ ^{101–103} is used],

$$C(\alpha_s) = \frac{4}{27} C_R (47C_A - 28T_F n_f) \left(\frac{\alpha_s}{4\pi} \right)^2$$

$$\begin{aligned}
 & + 4C_R \left[x_{AA} C_A^2 - \left(5\zeta_3 + \frac{\pi^4}{6} - \frac{79}{648} \right) C_A T_F n_f + \frac{2}{3} \left(19\zeta_3 + \frac{\pi^4}{10} - \frac{1711}{48} \right) \right. \\
 & \times C_F T_F n_f + \frac{8}{9} \left(\zeta_3 + \frac{58}{27} \right) (T_F n_f)^2 \left. \right] \left(\frac{\alpha_s}{4\pi} \right)^3 + \mathcal{O}(\alpha_s^4),
 \end{aligned} \tag{9.9}$$

where x_{AA} is unknown (and, in fact, ill-defined, see Sec. 9.1).

The coefficient of C_F in the α_s^2 -term of C , as well as that of C_F^2 in the α_s^3 -term of C , vanishes; this follows from a more general result (Sec. 13). The coefficient of $(T_F n_f)^2$ in the α_s^3 -term of C follows from Γ_{fff} which is known (Sec. 11); the factorized form (9.8) requires a definite result for Γ_{Aff} in the limit $\delta \rightarrow 0$ which agrees with the conjecture (8.16). This is one more confirmation of this conjecture for Γ_{Aff} [if we believe in (9.8)]. The coefficient of $C_F T_F n_f$ in the α_s^3 -term of C follows from Γ_{fff} which is known (Sec. 12); the factorized form (9.8) requires a definite result for Γ_{FAf} in the limit $\delta \rightarrow 0$ which agrees with the conjecture (8.16). This is one more confirmation of this conjecture for Γ_{FAf} [if we believe in (9.8)]. The coefficient of $C_A T_F n_f$ in the α_s^3 -term of C follows from the conjectured (8.16) result for Γ_{Aff} in the limit $\delta \rightarrow 0$. If we believe in (9.8), there is no $d_{RF} n_f$ -term in $\Delta(\alpha_s)$ at four loops; the full φ -dependence of this structure is known⁵⁷, but it is *extremely* complicated, and this conjecture has not been explicitly checked yet.

In a recent paper,¹⁰⁴ it was proposed to represent $C(\alpha_s)$ in the form

$$C(\alpha_s) = \sum_{n=0}^{\infty} C_n(\alpha_s) [\beta(\alpha_s)]^n, \tag{9.10}$$

where $C_n(\alpha_s)$ are series in α_s whose coefficients don't contain $T_F n_f$. In fact, an arbitrary series

$$C(\alpha_s) = \sum_{n=1}^{\infty} P_n(T_F n_f) \left(\frac{\alpha_s}{4\pi} \right)^{n+1} \tag{9.11}$$

[where $P_n(x)$ is a polynomial of degree n] can be reduced to the form (9.10) by a simple algorithm. In P_1 , we express $T_F n_f$ via

$$\beta(\alpha_s) - \sum_{n=1}^{\infty} \beta_n \left(\frac{\alpha_s}{4\pi} \right)^{n+1}$$

(note that $\beta_{n \geq 1}$ is a polynomial in $T_F n_f$ of degree n) and update $P_{\geq 2}(T_F n_f)$ by incorporating this sum. Then we repeat the same step for P_2 , and so on. At the N th step, three kinds of terms appear:

- $[\beta(\alpha_s)]^m$ with coefficients not containing $\beta_{\geq 1}$ ($m \in [0, N]$); these terms become a part of the final result.
- $[\beta(\alpha_s)]^m$ times some series having the form (9.11) ($m \in [1, N-1]$); for these series, we call the algorithm recursively.
- Terms without $\beta(\alpha_s)$ containing $\beta_{\geq 1}$; they are absorbed into $P_{\geq N+1}(T_F n_f)$.

A. Grozin

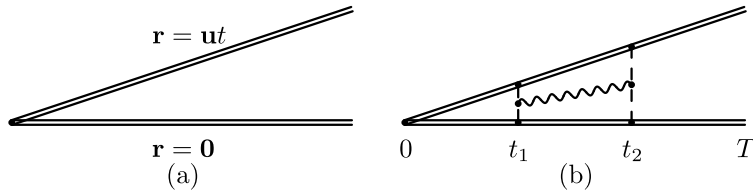


Fig. 3. (a) The Wilson line describing production of a heavy quark-antiquark pair with a small relative velocity \mathbf{u} . (b) The first transverse-gluon contribution.

As a result, we get the desired form (9.10), and this representation is unique. This is not a physical statement, but a simple algebraic fact. Let's stress that here we discuss the dependence on $T_F n_f$ only; n_f can appear in other contexts, such as $d_F^{abcd} n_f$ (light-by-light).

9.1. $C_R C_A^3 \alpha_s^4 \log(\delta)/\delta$ -term

At four loops, a $C_R C_A^3 \alpha_s^4 \log(\delta)/\delta$ -term appears¹⁰⁵ in $\Gamma(\pi - \delta)$. It is similar to the three-loop $\log(\mu r)$ -term in the potential.^{106,107}

Let's consider a cusped Wilson line in Minkowski space [Fig. 3(a)]. It is formed by the static quark and antiquark worldlines $\mathbf{r} = \mathbf{0}$ and $\mathbf{r} = \mathbf{u}t$, where \mathbf{u} is a small relative velocity ($u = |\mathbf{u}| \ll 1$). At the end of the calculation, we'll analytically continue the result to Euclidean space ($u = i\delta$). We neglect all terms suppressed by powers of u . It is convenient to use Coulomb gauge. The static quark and antiquark interact by exchanging instantaneous Coulomb gluons,

$$V(\mathbf{q}) = -C_F \frac{g_0^2}{\mathbf{q}^2}, \quad V(\mathbf{r}) = -C_F \kappa_0 \frac{g_0^2}{4\pi} \frac{1}{r^{1-2\varepsilon}} \quad (9.12)$$

(the power of r is obvious from dimensions counting). Here and below, $\kappa_i = 1 + \mathcal{O}(\varepsilon)$ are some normalization factors (we don't need their exact form).

Transverse gluons interact only with Coulomb ones, but not with the static quarks. The first transverse-gluon contribution is shown in Fig. 3(b). Here T is an infrared cutoff. We use the method of regions to analyze this contribution. In the ultrasoft region $t_1 \sim t_2 \sim t_2 - t_1$; Coulomb-gluon characteristic momentum is $q \sim 1/(ut_{1,2})$, and the transverse-gluon characteristic momentum is $k \sim 1/t_{1,2} \ll q$. In the soft region $t_2 - t_1 \sim ut_{1,2}$, and $k \sim 1/(t_2 - t_1) \sim q$. To determine the coefficient of the logarithm in the $1/\delta$ -term in $\Gamma(\pi - \delta)$, it turns out to be sufficient to consider the ultrasoft region. Neglecting k in the three-gluon vertex, we obtain in momentum and coordinate spaces

$= f^{aa_1 a_2} g_0^3 \frac{2q^i}{(\mathbf{q}^2)^2},$

$= i f^{aa_1 a_2} \kappa_0 \frac{g_0^3}{4\pi} \frac{r^i}{r^{1-2\varepsilon}}.$

(9.13)

The ratio of the Wilson line [Fig. 3(b)] to the one without the transverse-gluon correction is $1 + R_{\text{us}} + R_{\text{soft}}$. The ultrasoft contribution is

$$R_{\text{us}} = \int_0^T dt_2 \int_0^{t_2} dt_1 K(t_1, t_2), \quad (9.14)$$

where

$$K(t_1, t_2) = \frac{1}{4} C_F C_A^2 \kappa_0^2 \frac{g_0^6}{(4\pi)^2} \frac{r_1^i}{r_1^{1-2\varepsilon}} \frac{r_2^j}{r_2^{1-2\varepsilon}} D^{ij}(v(t_2 - t_1)) \exp \left[-i \int_{t_1}^{t_2} dt \Delta V(ut) \right] \quad (9.15)$$

[$v = (1, \mathbf{0})$ is the four-velocity of our small dipole]. During the time interval between t_1 and t_2 , the static quark–antiquark pair is in the adjoint color state instead of the singlet one, and their leading-order interaction potential $V_o(r)$ is obtained from the expression for the singlet potential $V(r)$ (9.12) by replacing the color factor C_F with $C_F - C_A/2$. Therefore, we get the integral of $\Delta V(r) = V_o(r) - V(r)$. The characteristic sizes of the regions of the transverse-gluon emission and absorption are $\sim ut_{1,2}$; we neglect them, so that this gluon propagates between the points vt_1 and vt_2 :

$$D^{ij}(vt) = 8(i/2)^{2\varepsilon} \frac{\Gamma(2-\varepsilon)}{3-2\varepsilon} \frac{t^{-2+2\varepsilon}}{(4\pi)^{2-\varepsilon}} \delta^{ij}. \quad (9.16)$$

We obtain

$$K(t_1, t_2) = \frac{2}{3} C_F C_A^2 \kappa_1 \frac{g_0^6}{(4\pi)^4} u^{4\varepsilon} t_1^{2\varepsilon} t_2^{2\varepsilon} (t_2 - t_1)^{-2+2\varepsilon} \exp \left[-\frac{i}{4} C_A \kappa_0 \frac{g_0^2}{4\pi} \frac{t_2^{2\varepsilon} - t_1^{2\varepsilon}}{\varepsilon u^{1-2\varepsilon}} \right]. \quad (9.17)$$

Now we consider just a single Coulomb-gluon exchange between t_1 and t_2 ,

$$K^{(1)}(t_1, t_2) = -\frac{i}{6} C_F C_A^3 \kappa_2 \frac{g_0^8}{(4\pi)^5} \frac{t_1^{2\varepsilon} t_2^{2\varepsilon} (t_2^{2\varepsilon} - t_1^{2\varepsilon}) (t_2 - t_1)^{-2+2\varepsilon}}{\varepsilon u^{1-6\varepsilon}}. \quad (9.18)$$

Calculating the integral (9.14) by the substitutions $t_1 = xt_2$, we obtain

$$\int_0^1 dx x^{2\varepsilon} (1 - x^{2\varepsilon}) (1 - x)^{-2+2\varepsilon} = \frac{\Gamma(1+2\varepsilon)}{1-2\varepsilon} \left[3 \frac{\Gamma(1+4\varepsilon)}{\Gamma(1+6\varepsilon)} - 2 \frac{\Gamma(1+2\varepsilon)}{\Gamma(1+4\varepsilon)} \right] = 1 + \mathcal{O}(\varepsilon), \quad (9.19)$$

and therefore

$$R_{\text{us}}^{(1)} = -\frac{i}{48} C_F C_A^3 \kappa_3 \frac{g_0^8}{(4\pi)^5} \frac{T^{8\varepsilon}}{\varepsilon^2 u^{1-6\varepsilon}}. \quad (9.20)$$

The soft contribution is nearly local in time ($t_2 - t_1 \sim ut_{1,2} \ll t_{1,2}$), and can be described by a soft potential. For a single Coulomb exchange between t_1 and t_2 , it is

$$V_{\text{soft}}^{(1)}(r) = c C_F C_A^3 \frac{g_0^8}{r^{1-8\varepsilon}} \quad (9.21)$$

by counting dimensions, so that

$$R_{\text{soft}}^{(1)} = -i \int_0^T dt V_{\text{soft}}^{(1)}(ut) = -ic C_F C_A^3 \frac{g_0^8 T^{8\varepsilon}}{8\varepsilon u^{1-8\varepsilon}}. \quad (9.22)$$

A. Grozin

The double pole $1/\varepsilon^2$ should cancel in $R^{(1)} = R_{\text{us}}^{(1)} + R_{\text{soft}}^{(1)}$; this fixes the $1/\varepsilon$ -term in c , and we obtain

$$\begin{aligned} R^{(1)} &= -\frac{i}{48} C_F C_A^3 \frac{g_0^8 T^{8\varepsilon}}{(4\pi)^5} \frac{\kappa_3 u^{6\varepsilon} - \kappa_4 u^{8\varepsilon}}{\varepsilon^2 u} \\ &= \frac{i}{24} C_F C_A^3 \frac{\alpha_s^4(\mu)(\mu T)^{8\varepsilon}}{4\pi} \frac{\log u + \text{const.}}{\varepsilon u}. \end{aligned} \quad (9.23)$$

This leads to the following contribution to Γ :

$$\Delta\Gamma = -\frac{i}{3} C_F C_A^3 \frac{\alpha_s^4}{4\pi} \frac{\log u + \text{const.}}{u}. \quad (9.24)$$

Finally, analytically continuing it to Euclidean space ($\varphi_E = \pi + i\varphi_M$, $\varphi_M = u$) and replacing $C_F \rightarrow C_R$, we obtain¹⁰⁵

$$\Delta\Gamma(\pi - \delta) = -\frac{1}{3} C_F C_A^3 \frac{\alpha_s^4}{4\pi} \frac{\log \delta + \text{const.}}{\delta}. \quad (9.25)$$

This contribution does not allow us to take the limit $\delta \rightarrow 0$ in (9.6). Higher orders in α_s will contain higher powers of $\log \delta$. Hopefully, summing terms with the leading powers of $\log \delta$ to all orders will produce a finite result for $\delta\Gamma(\pi - \delta)$, in which $\log \alpha_s$ will appear in place of $\log \delta$.

10. Higher-Loop Abelian Results: Two-Leg c-Webs

In general, $\log W$ is given by the sum of webs (3.8). For some families of Abelian color structures, only two-leg c-webs (3.6) contribute. We can work in QED. The full photon propagator is

$$\begin{aligned} \overbrace{\hspace{1cm}}^k = iD^{\mu\nu}(k), \\ D^{\mu\nu}(k) = \frac{D_0^{\mu\nu}(k)}{1 - \Pi(k^2)}, \quad D_0^{\mu\nu}(k) = \frac{1}{-k^2} \left(g^{\mu\nu} + \frac{k^\mu k^\nu}{-k^2} \right) \end{aligned} \quad (10.1)$$

(only the zero-order propagator is gauge-dependent; here and below, we use Landau gauge). The photon self-energy is the sum of 1PI diagrams,

$$\begin{aligned} \overbrace{\hspace{1cm}}^k = i(k^2 g^{\mu\nu} - k^\mu k^\nu) \Pi(k^2), \quad \Pi(k^2) = \sum_{L=1}^{\infty} \Pi_{L-1}(k^2), \\ \Pi_{L-1}(k^2) = \Pi_{L-1}[A_0(-k^2)^{-2\varepsilon}]^L, \quad A_0 = e^{-\gamma\varepsilon} \frac{e_0^2}{(4\pi)^{d/2}}. \end{aligned} \quad (10.2)$$

The $\overline{\text{MS}}$ charge renormalization is

$$A_0 = \mu^{2\varepsilon} \frac{\alpha(\mu)}{4\pi} Z_\alpha(\alpha(\mu)). \quad (10.3)$$

We can select a subset S of Abelian color structures of the gluon propagator which satisfies two conditions:

- (1) the contributions of the color structures $C_R \times S$ to bare $\log W$ are given by two-leg c-webs only [see (3.5)];
- (2) no color factor $C \notin S$ being multiplied by a color factor in Z_α can produce a color factor $C' \in S$.

The contribution of the color structures S to the gluon propagator is

$$\begin{aligned} D_S^{\mu\nu}(k) &= \sum_{L=0}^{\infty} d_S^{(L)} D_L^{\mu\nu}(k) A_0^L, \\ D_L^{\mu\nu}(k) &= \frac{1}{(-k^2)^{1+L\varepsilon}} \left(g^{\mu\nu} + \frac{k^\mu k^\nu}{-k^2} \right), \end{aligned} \quad (10.4)$$

where $d_S^{(L)}$ are products of some color structures of $\Pi_{L'}$. In coordinate space,

$$\begin{aligned} D_{L-1}^{\mu\nu}(x) &= \frac{i}{(4\pi)^{d/2}} \frac{\Gamma(1-u)}{\Gamma(2+u-\varepsilon)} \\ &\times \frac{2^{1-2u}}{(-x^2)^{1-u}} \left[(1+2(u-\varepsilon))g^{\mu\nu} - 2(1-u) \frac{x^\mu x^\nu}{-x^2} \right]. \end{aligned} \quad (10.5)$$

Here and below

$$u = L\varepsilon. \quad (10.6)$$

10.1. HQET field anomalous dimension

For a straight Wilson line in Euclidean time ($t = -i\tau$),

$$\begin{aligned} \overbrace{0}^{} \overbrace{t}^{} &= \overbrace{0}^{} \overbrace{t}^{} \times w_S(t), \\ w_S(\tau) &= \sum_{L=1}^{\infty} d_S^{(L-1)} w_L [A_0(\tau/2)^{2\varepsilon} e^{\gamma\varepsilon}]^L, \quad w_L = -e^{\gamma(\varepsilon-2u)} \frac{(3-2\varepsilon)\Gamma(-u)}{(1-2u)\Gamma(2+u-\varepsilon)}. \end{aligned} \quad (10.7)$$

A finite t provides an IR cutoff; the region $t_2 - t_1 \rightarrow 0$ gives a UV divergence. Re-expressing $w_S(\tau)$ via $\alpha_s(\mu)$ using (10.3) [say, with $\mu = (2/\tau)e^{-\gamma}$] and using $w_S(\tau) = (\log Z_h)_S + \mathcal{O}(\varepsilon^0)$ (2.11), we obtain $(\log Z_h)_S$ (it does not depend on τ) and hence $(\gamma_h)_S$.

Alternatively, we can work in momentum space. The Fourier image of $w_S(t)$ (10.7) is

$$\begin{aligned} \overbrace{\omega}^{} \overbrace{\omega}^{} &= \overbrace{\omega}^{} \overbrace{\omega}^{} \times \tilde{w}_S(\omega), \\ \tilde{w}_S(\omega) &= \sum_{L=1}^{\infty} d_S^{(L-1)} \tilde{w}_L [A_0(-2\omega)^{-2\varepsilon}]^L, \quad \tilde{w}_L = -e^{\gamma\varepsilon} \frac{(3-2\varepsilon)\Gamma(-u)\Gamma(1+2u)}{(1-2u)\Gamma(2+u-\varepsilon)}. \end{aligned} \quad (10.8)$$

A. Grozin

This result can be derived in momentum space using¹⁴

$$\frac{1}{i\pi^{d/2}} \int \frac{d^d k}{[-2(k \cdot v + \omega)]^{n_1} (-k^2)^{n_2}} = I(n_1, n_2) (-2\omega)^{d-n_1-2n_2},$$

$$I(n_1, n_2) = \frac{\Gamma(n_1 + 2n_2 - d)\Gamma(\frac{d}{2} - n_2)}{\Gamma(n_1)\Gamma(n_2)}, \quad (10.9)$$

or by Fourier transforming (10.7). Now a nonzero ω provides an IR cutoff; the region $k \rightarrow \infty$ gives a UV divergence which coincides with that of (10.7). Re-expressing $\tilde{w}_S(\tau)$ via $\alpha_s(\mu)$ using (10.3) (say, with $\mu = -2\omega$) and using $\tilde{w}_S(\omega) = (\log Z_h)_S + \mathcal{O}(\varepsilon^0)$, we obtain $(\log Z_h)_S$ (it does not depend on ω) and hence $(\gamma_h)_S$.

The renormalization constant can be written as

$$(\log Z_h)_S = \sum_{n=1}^{\infty} \frac{z_{hn}}{\varepsilon^n}, \quad z_{hn} = \mathcal{O}(\alpha_s^n). \quad (10.10)$$

Only z_{h1} is needed in order to obtain

$$\gamma_h(\alpha_s) = -2 \frac{dz_{h1}(\alpha_s)}{d \log \alpha_s}; \quad (10.11)$$

higher z_{hn} contain no new information, and are uniquely reconstructed from z_{h1} using self-consistency conditions.

10.2. Cusp anomalous dimension

For a cusped Wilson line, we have ($-t < 0 < t'$)

$$(\log W(t, t', \varphi))_S = w_S(t, t', \varphi)$$

$$= \begin{array}{c} \text{Diagram: two triangles connected at their top vertices, each with a wavy line entering from the left and a straight line exiting to the right. The top vertex is labeled '0'. The bottom-left vertex is labeled '-vt' and the bottom-right vertex is labeled 'v't'.} \\ + \end{array} \quad (10.12)$$

$$+ \begin{array}{c} \text{Diagram: two triangles connected at their top vertices, each with a wavy line entering from the right and a straight line exiting to the left. The top vertex is labeled '0'. The bottom-left vertex is labeled '-vt' and the bottom-right vertex is labeled 'v't'.} \\ - \end{array}$$

and

$$w_S(t, t', \varphi) - w_S(t, t', 0) = \begin{array}{c} \text{Diagram: two triangles connected at their top vertices, each with a wavy line entering from the left and a straight line exiting to the right. The top vertex is labeled '0'. The bottom-left vertex is labeled '-vt' and the bottom-right vertex is labeled 'v't'.} \\ - \begin{array}{c} \text{Diagram: a single horizontal line segment with a wavy line attached to its left end, labeled '0'. The line segment has endpoints '-vt' and 'vt'.} \end{array} \end{array} \quad (10.13)$$

Let's denote $(-t < -t_1 < 0 < t_2 < t')$

$$\begin{array}{c}
 \text{Diagram: Two vertices connected by a wavy line. The left vertex has a horizontal line to } -vt_1 \text{ and a diagonal line to } v't_2. The right vertex has a horizontal line to } v't' \text{ and a diagonal line to } -vt. \\
 = \quad \text{Diagram: Two vertices connected by a straight line. The left vertex has a horizontal line to } -vt \text{ and a diagonal line to } v't'. \text{ The right vertex has a horizontal line to } v't' \text{ and a diagonal line to } 0. \\
 \times V_S(t, t', \varphi), \\
 V_S(\tau, \tau', \varphi) = \sum_{L=1}^{\infty} d_S^{(L-1)} V_L(\tau'/\tau, \varphi) [A_0 (\tau \tau'/4)^{\varepsilon} e^{\gamma \varepsilon}]^L.
 \end{array} \tag{10.14}$$

When expressed via the renormalized quantities, $V_S(t, t', \varphi) = (\log Z_J(\varphi))_S + (\log Z_h)_S + \mathcal{O}(\varepsilon^0)$. Therefore, $\bar{V}_S(t, t', \varphi) = V_S(t, t', \varphi) - V_S(t, t', 0) = (\log Z_J(\varphi))_S + \mathcal{O}(\varepsilon^0)$, where $(\log Z_J(\varphi))_S$ does not depend on t and t' and is gauge-invariant. Note that

$$V_S(t, t', 0) = w_S(t+t') - w_S(t) - w_S(t') = -(\log Z_h)_S + \mathcal{O}(\varepsilon^0). \tag{10.15}$$

For calculating the anomalous dimension we need finite τ, τ' as IR regulators. We may set $\tau' = \tau$ in order to have a simpler single-scale problem,⁵³

$$V_L(1, \varphi) = -2e^{\gamma(\varepsilon-2u)} \frac{\Gamma(1-u)}{\Gamma(2+u-\varepsilon)} [I_1(u, \varphi)(2+u-2\varepsilon) \cosh \varphi + I_2(u, \varphi)(1-u)], \tag{10.16}$$

$$\begin{aligned}
 I_1(u, \varphi) &= \int_0^1 dt_1 \int_0^1 dt_2 (e^{\varphi/2} t_1 + e^{-\varphi/2} t_2)^{-1+u} (e^{-\varphi/2} t_1 + e^{\varphi/2} t_2)^{-1+u} \\
 &= \frac{e^{-2u\varphi}}{4u^2 \sinh \varphi} (g_1(u, \varphi) - g_2(u, \varphi)), \\
 I_2(u, \varphi) &= \int_0^1 dt_1 \int_0^1 dt_2 (e^{\varphi/2} t_1 + e^{-\varphi/2} t_2)^u (e^{-\varphi/2} t_1 + e^{\varphi/2} t_2)^{-2+u} \\
 &= \frac{1}{2u(1-u)} \left[1 + \frac{e^{-2u\varphi}}{2 \sinh \varphi} (e^{-\varphi} g_1(u, \varphi) - e^{\varphi} g_2(u, \varphi)) \right], \\
 I_1(u, 0) &= I_2(u, 0) = \frac{2 - 2^{2u}}{2u(1-2u)}, \tag{10.17}
 \end{aligned}$$

$$g_1(u, \varphi) = (e^\varphi + 1)^{2u} f_1(u, 1 - e^\varphi) - f_1(u, 1 - e^{2\varphi}),$$

$$g_2(u, \varphi) = (e^\varphi + 1)^{2u} f_2(u, 1 - e^\varphi) - f_2(u, 1 - e^{2\varphi}),$$

$$f_1(u, x) = {}_2F_1\left(\begin{matrix} -2u, -u \\ 1 - 2u \end{matrix} \middle| x\right) = 1 + 2 \operatorname{Li}_2(x) u^2 + \mathcal{O}(u^3),$$

$$\begin{aligned}
 f_2(u, x) &= {}_2F_1\left(\begin{matrix} -2u, 1 - u \\ 1 - 2u \end{matrix} \middle| x\right) = 1 + 2 \log(1-x) u \\
 &\quad + (\log^2(1-x) - 2 \operatorname{Li}_2(x)) u^2 + \mathcal{O}(u^3).
 \end{aligned}$$

Using (10.17) we get the equality (10.15). The UV divergence ($u = L\varepsilon, \varepsilon \rightarrow 0$) of $V_L(1, \varphi)$ (10.16) is

$$V_L(1, \varphi) = -\frac{2\varphi \coth \varphi + 1}{u} + \mathcal{O}(1). \tag{10.18}$$

A. Grozin

Alternatively, we can work in momentum space. The Fourier image of $V_S(t, t', \varphi)$ (10.14) is

$$\begin{aligned} & \text{Diagram: Two external lines labeled } \omega \text{ and } \omega' \text{ meeting at a vertex with a wavy line between them.} = \text{Diagram: Two external lines labeled } \omega \text{ and } \omega' \text{ meeting at a vertex with a solid line between them.} \times \tilde{V}_S(\omega, \omega', \varphi), \\ \tilde{V}_S(\omega, \omega', \varphi) &= \text{Diagram: Two external lines labeled } \omega \text{ and } \omega' \text{ meeting at a vertex with a wavy line between them.} = \sum_{L=1}^{\infty} d_S^{(L-1)} \tilde{V}_L(\omega'/\omega, \varphi) [A_0(4\omega\omega')^{-\varepsilon}]^L. \end{aligned} \quad (10.19)$$

We have $\tilde{V}_S(\omega, \omega', \varphi) = \tilde{V}_S(\omega, \omega', \varphi) - \tilde{V}_S(\omega, \omega', 0) = (\log Z_J(\varphi))_S + \mathcal{O}(\varepsilon^0)$, where $(\log Z_J(\varphi))_S$ does not depend on ω and ω' and is gauge-invariant. Note that

$$\tilde{V}_S(\omega, \omega', 0) = -\frac{\omega \tilde{w}_S(\omega) - \omega' \tilde{w}_S(\omega')}{\omega - \omega'} = -(\log Z_h)_S + \mathcal{O}(\varepsilon^0) \quad (10.20)$$

[this result can be derived by separating partial fractions in the loop integrand or by Fourier transforming (10.15)].

The scalar Feynman integrals in $\tilde{V}_L(y, \varphi)$ can be reduced¹⁰⁸ to three master integrals, among which two are trivial (10.9) and one nontrivial,

$$\begin{aligned} \tilde{V}_L(y, \varphi) &= -\frac{2e^{\gamma\varepsilon}}{(1+u-\varepsilon)(2\cosh\varphi-y-y^{-1})} \{2[(1-\varepsilon)(2\cosh\varphi-y-y^{-1})\cosh\varphi \\ &\quad + u(\cosh\varphi-y)(\cosh\varphi-y^{-1})]I(y) + [(\cosh\varphi-y)y^{-u} \\ &\quad + (\cosh\varphi-y^{-1})y^u]I(2, 1+u-\varepsilon)\}, \\ I(y) &= \frac{(4\omega\omega')^u}{i\pi^{d/2}} \int \frac{d^d k}{[-2(k \cdot v + \omega)][-2(k \cdot v' + \omega')](-k^2)^{1+u-\varepsilon}}. \end{aligned} \quad (10.21)$$

In anomalous dimension calculations, nonzero ω, ω' are needed only as IR regulators, and we may set $\omega' = \omega$ in order to have a simpler single-scale problem. The master integral $I(1)$ (10.21) is then expressed¹⁰⁸ via a hypergeometric function, and the result is⁴⁷

$$\begin{aligned} \tilde{V}_L(1, \varphi) &= -2e^{\gamma\varepsilon} \frac{I(2, 1+u-\varepsilon)}{1+u-\varepsilon} \{[(2+u-2\varepsilon)\cosh\varphi-u]F(u, \varphi) + 1\}, \\ F(u, \varphi) &= {}_2F_1\left(\begin{matrix} 1, 1-u \\ \frac{3}{2} \end{matrix} \middle| \frac{1-\cosh\varphi}{2}\right), \quad F(0, \varphi) = \frac{\varphi}{\sinh\varphi}. \end{aligned} \quad (10.22)$$

At $\varphi = 0$ [$F(u, \varphi) = 1$] we get (10.20) (at $\omega' = \omega$ it becomes a derivative). The UV divergence of $\tilde{V}_L(1, \varphi)$ (10.22) is the same as that of $V_L(1, \varphi)$ (10.18).

The hypergeometric function $F(u, \varphi)$ (10.22) has been expanded¹⁰⁹ in u to all orders,^a the coefficients are expressed via Nielsen polylogarithms $S_{nm}(x)$. The result¹⁰⁹ is written for the case of a Euclidean angle, its analytical continuation to Minkowski angles is¹¹¹

^aThere is a typo in this formula. It has been corrected in Ref. 110 and in v4 of the arXiv preprint.

$$F(u, \varphi) = \frac{1}{\sinh \varphi (2 \cosh(\varphi/2))^{2u}} \left[\frac{\sinh(\varphi u)}{u} - e^{-\varphi u} \sum_{n=1}^{\infty} u^n \sum_{m=1}^n (-2)^{n-m} S_{m,n-m+1}(-e^{\varphi}) + e^{\varphi u} \sum_{n=1}^{\infty} u^n \sum_{m=1}^n (-2)^{n-m} S_{m,n-m+1}(-e^{-\varphi}) \right]. \quad (10.23)$$

It is possible to re-express this expansion in terms of Nielsen polylogarithms of just one argument (see Ref. 112 or <http://functions.wolfram.com/Zeta-FunctionsandPolylogarithms/PolyLog3/17/01/>), but then the symmetry $\varphi \rightarrow -\varphi$ will not be explicit.

10.3. Potential

We shall need also some formulas for the static quark–antiquark potential in order to discuss the conformal anomaly $\Delta(\alpha_s)$. The Wilson loop in Fig. 4(a) described the following sequence of events: a static (HQET) particle in a color representation R and its antiparticle are created at a distance \mathbf{r} at the moment $t = 0$; they stay at these positions for a time $T \gg r$; and finally, they are annihilated at the moment T . This pair has the energy $V(\mathbf{r})$, and for large T we have

$$\log W = -iV(\mathbf{r})T. \quad (10.24)$$

Due to exponentiation (Sec. 3), $\log W$ is equal to the sum of webs. Here, we shall consider Abelian color structures for which only two-leg webs [Figs. 4(b) and 4(c)] contribute. We are not interested in contributions where the gluon is attached to the lower horizontal Wilson line or to the upper one — such contributions don’t scale as T . The diagram in Fig. 4(b) describes not a quark–antiquark potential but the

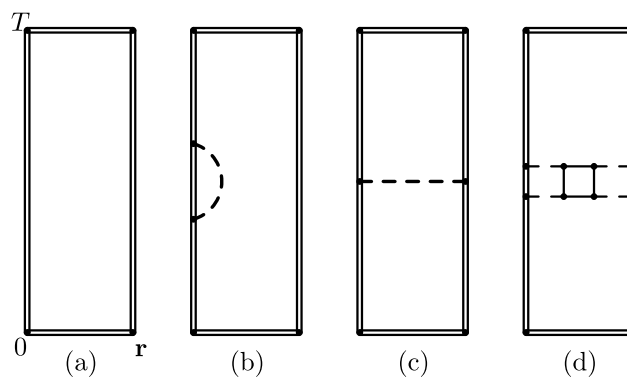


Fig. 4. The Wilson loop determining the quark–antiquark potential.

A. Grozin

residual mass term of an HQET particle; it vanishes in dimensional regularization. The first contribution of a four-leg web is shown in Fig. 4(d).

It is convenient to use the Coulomb gauge. The full Coulomb photon propagator is

$$D(q) = \frac{1}{1 - \Pi(q^2)} \frac{1}{\mathbf{q}^2}. \quad (10.25)$$

The photon self-energy $\Pi(q^2)$ is gauge-invariant in QED, so we may use the same $\Pi(q^2)$ (10.2) as in covariant gauges. Integration in one of the two times in Fig. 4(c) gives T ; integration in the other time gives

$$V(\mathbf{r}) = -e_0^2 \int_{-\infty}^{+\infty} dt D(t, \mathbf{r}) = \int \frac{d^{d-1}\mathbf{q}}{(2\pi)^{d-1}} e^{i\mathbf{q}\cdot\mathbf{r}} V(\mathbf{q}), \quad (10.26)$$

where the momentum-space potential is

$$V(\mathbf{q}) = -e_0^2 D(q), \quad q = (0, \mathbf{q}). \quad (10.27)$$

It is finite, because in QED $Z_\alpha = Z_A^{-1}$. The contribution of a subset S of color structures is

$$V_S(\mathbf{q}) = -(4\pi)^{d/2} e^{\gamma\varepsilon} \sum_{L=1}^{\infty} \frac{d_S^{(L-1)}}{(\mathbf{q}^2)^{1+(L-1)\varepsilon}} A_0^L. \quad (10.28)$$

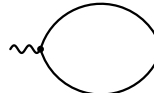
11. Leading Large- β_0 Order

Let's consider terms with the leading powers of n_f to all orders in α_s : $S = \{(T_F n_f)^L, L \geq 0\}$. It is sufficient to consider QED: $C_F = T_F = 1$, $C_A = 0$ and $\beta_0 = -\frac{4}{3}n_f$. Let's introduce

$$b = \beta_0 \frac{\alpha}{4\pi}. \quad (11.1)$$

We assume $b \sim 1$ and take into account all powers of b ; $1/\beta_0 \ll 1$ is our small parameter, and we consider only a few terms in expansions in $1/\beta_0$. This large- β_0 limit is reviewed in Chap. 8 of Ref. 14.

The photon self-energy $\Pi_0(k^2)$ at the leading large- β_0 ($L\beta_0$) order is ~ 1 ,



$$\Rightarrow \Pi_0(k^2) = \Pi_0 A_0 (-k^2)^{-\varepsilon}, \quad \Pi_0 = \beta_0 \frac{D(\varepsilon)}{\varepsilon}, \quad (11.2)$$

$$D(\varepsilon) = e^{\gamma\varepsilon} \frac{(1-\varepsilon)\Gamma(1+\varepsilon)\Gamma^2(1-\varepsilon)}{(1-2\varepsilon)(1-\frac{2}{3}\varepsilon)\Gamma(1-2\varepsilon)} = 1 + \frac{5}{3}\varepsilon + \dots$$

The charge renormalization in the $\overline{\text{MS}}$ scheme (10.3) is

$$\beta_0 A_0 = b Z_\alpha(b) \mu^{2\varepsilon}. \quad (11.3)$$

At the $L\beta_0$ order, we can solve the RG equation (the β -function is b)

$$\frac{d \log Z_\alpha(b)}{d \log b} = -\frac{b}{\varepsilon + b}$$

and obtain

$$Z_\alpha(b) = \frac{1}{1 + b/\varepsilon}. \quad (11.4)$$

11.1. HQET field anomalous dimension

The diagrams for w_S and V_S include only Π_0 -insertions in the photon propagator (Fig. 5): $d_S^{(L)} = \Pi_0^L$. We can write the two-leg web $\tilde{w}(\omega)$ in the form

$$\tilde{w}(\omega) = \frac{1}{\beta_0} \sum_{L=1}^{\infty} \frac{\tilde{f}(\varepsilon, L\varepsilon)}{L} [\Pi_0(k^2)]^L + \mathcal{O}\left(\frac{1}{\beta_0^2}\right) \quad (k^2 = (-2\omega)^2), \quad (11.5)$$

$$\tilde{f}(\varepsilon, u) = \frac{u\tilde{w}_L}{D(\varepsilon)} = \frac{3(1 - \frac{2}{3}\varepsilon)^2 \Gamma(2 - 2\varepsilon) \Gamma(1 - u) \Gamma(1 + 2u)}{(1 - \varepsilon)(1 - 2u) \Gamma^2(1 - \varepsilon) \Gamma(1 + \varepsilon) \Gamma(2 + u - \varepsilon)}. \quad (11.6)$$

Expressing it via $\alpha(\mu)$ using (11.3) with $\mu = (-2\omega)D(\varepsilon)^{-1/(2\varepsilon)} \rightarrow (-2\omega)e^{-5/6}$ using (11.4), we have

$$\tilde{w}(\omega) = \frac{1}{\beta_0} \sum_{L=1}^{\infty} \frac{\tilde{f}(\varepsilon, L\varepsilon)}{L} \left(\frac{b}{\varepsilon + b}\right)^L + \mathcal{O}\left(\frac{1}{\beta_0^2}\right). \quad (11.7)$$

The function $\tilde{f}(\varepsilon, u)$ (11.6) is regular at $\varepsilon = u = 0$,

$$\tilde{f}(\varepsilon, u) = \sum_{n=0}^{\infty} \sum_{m=0}^{\infty} \tilde{f}_{nm} \varepsilon^n u^m. \quad (11.8)$$

We also expand $[b/(\varepsilon + b)]^L$ in b and get a quadruple series for $\tilde{w}(\omega)$. When selecting ε^{-1} -terms in order to obtain z_{h1} , all coefficients but \tilde{f}_{n0} cancel,

$$z_{h1}(b) = -\frac{1}{\beta_0} \sum_{n=0}^{\infty} \frac{\tilde{f}_{n0}}{n+1} (-b)^{n+1} + \mathcal{O}\left(\frac{1}{\beta_0^2}\right),$$

so that

$$\gamma_h(b) = -2 \frac{b}{\beta_0} \tilde{f}(-b, 0) + \mathcal{O}\left(\frac{1}{\beta_0^2}\right). \quad (11.9)$$

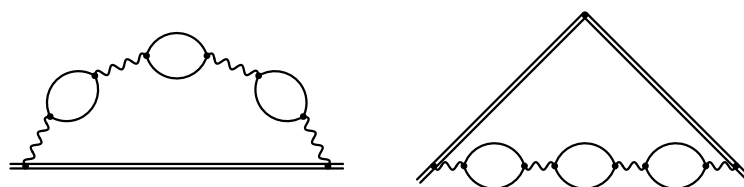


Fig. 5. Typical diagrams for γ_h and $\Gamma(\varphi)$ at $L\beta_0$ order.

A. Grozin

Finally, we obtain⁴⁴

$$\gamma_h(b) = -6 \frac{b}{\beta_0} \gamma_0(b) + \mathcal{O}\left(\frac{1}{\beta_0^2}\right), \quad (11.10)$$

$$\begin{aligned} \gamma_0(b) &= \frac{(1 + \frac{2}{3}b)^2 \Gamma(2 + 2b)}{(1 + b)^2 \Gamma^3(1 + b) \Gamma(1 - b)} = 1 + \frac{4}{3}b - \frac{5}{9}b^2 - 2\left(\zeta_3 - \frac{1}{3}\right)b^3 \\ &\quad + \left(\frac{\pi^4}{10} - 8\zeta_3 - \frac{7}{3}\right)\frac{b^4}{3} - 2\left(3\zeta_5 - \frac{\pi^4}{45} - \frac{5}{9}\zeta_3 - \frac{4}{9}\right)b^5 \\ &\quad + \left(2\zeta_3^2 + \frac{2}{189}\pi^6 - 8\zeta_5 - \frac{\pi^4}{54} - \frac{4}{3}\zeta_3 - 1\right)b^6 + \mathcal{O}(b^7). \end{aligned} \quad (11.11)$$

It is absolutely trivial to extend this expansion to any desired order. This is the Landau-gauge result; in order to obtain the result in an arbitrary covariant gauge, one should add the trivial one-loop term proportional to a . Restoring the color factors

$$\gamma_h = -6C_R \frac{\alpha_s}{4\pi} \gamma_0(b) + \dots, \quad b = -\frac{4}{3}T_F n_f, \quad (11.12)$$

we reproduce the corresponding terms in (5.1).

Alternatively, we can work in coordinate space,

$$\begin{aligned} w(\tau) &= \frac{1}{\beta_0} \sum_{L=1}^{\infty} \frac{f(\varepsilon, L\varepsilon)}{L} [\Pi_0(k^2) e^{\gamma\varepsilon}]^L + \mathcal{O}\left(\frac{1}{\beta_0^2}\right) \quad (k^2 = (2/\tau)^2), \\ f(\varepsilon, u) &= \frac{uw_L}{D(\varepsilon)} = \frac{3(1 - \frac{2}{3}\varepsilon)^2 \Gamma(2 - 2\varepsilon) \Gamma(1 + u)}{(1 - \varepsilon)(1 - 2u) \Gamma^2(1 - \varepsilon) \Gamma(1 + \varepsilon) \Gamma(2 + u - \varepsilon)}, \end{aligned}$$

see (10.7). Choosing $\mu = (2/\tau)e^{-\gamma}D(\varepsilon)^{1/(2\varepsilon)} \rightarrow (2/\tau)e^{-\gamma-5/6}$, we obtain

$$w(\tau) = \frac{1}{\beta_0} \sum_{L=1}^{\infty} \frac{f(\varepsilon, L\varepsilon)}{L} \left(\frac{b}{\varepsilon + b}\right)^L + \mathcal{O}\left(\frac{1}{\beta_0^2}\right);$$

$f(-b, 0) = \tilde{f}(-b, 0)$, so we get the result (11.11) again.

11.2. Cusp anomalous dimension

We can write $\tilde{V}(\omega, \omega, \varphi)$ in the form $[\tilde{V}(\varphi) = \tilde{V}(1, \varphi) - \tilde{V}(1, 0)]$

$$\begin{aligned} \tilde{V}(\omega, \omega, \varphi) &= \frac{1}{\beta_0} \sum_{L=1}^{\infty} \frac{\tilde{f}(\varepsilon, L\varepsilon, \varphi)}{L} [\Pi_0(k^2)]^L + \mathcal{O}\left(\frac{1}{\beta_0^2}\right) \quad (k^2 = (-2\omega)^2), \\ \tilde{f}(\varepsilon, u, \varphi) &= \frac{u\tilde{V}(\varphi)}{D(\varepsilon)} = -\frac{(1 - \frac{2}{3}\varepsilon)\Gamma(2 - 2\varepsilon)\Gamma(1 - u)\Gamma(1 + 2u)}{(1 - \varepsilon)\Gamma^2(1 - \varepsilon)\Gamma(1 + \varepsilon)\Gamma(2 + u - \varepsilon)} \\ &\quad \times [(2 + u - 2\varepsilon)\cosh\varphi - u]F(u, \varphi) - 2(1 - \varepsilon)], \end{aligned} \quad (11.13)$$

see (10.22). We re-express the result via the renormalized b ,

$$\tilde{V}(\omega, \omega, \varphi) = \frac{1}{\beta_0} \sum_{L=1}^{\infty} \frac{\tilde{f}(\varepsilon, L\varepsilon, \varphi)}{L} \left(\frac{b}{\varepsilon + b}\right)^L + \mathcal{O}\left(\frac{1}{\beta_0^2}\right),$$

expand $\tilde{f}(\varepsilon, u, \varphi)$ in ε and u and $[b/(\varepsilon + b)]^L$ in b . When selecting ε^{-1} -terms in order to obtain z_{J1} , all coefficients but $f_{n0}(\varphi)$ cancel,

$$\begin{aligned} z_{J1}(b, \varphi) &= -\frac{1}{\beta_0} \sum_{n=0}^{\infty} \frac{\tilde{f}_{n0}(\varphi)}{n+1} (-b)^{n+1} + \mathcal{O}\left(\frac{1}{\beta_0^2}\right), \\ \tilde{f}(\varepsilon, 0, \varphi) &= \sum_{n=0}^{\infty} \tilde{f}_{n0}(\varphi) \varepsilon^n = -2(\varphi \coth \varphi - 1) \hat{f}(\varepsilon), \\ \hat{f}(\varepsilon) &= \sum_{n=0}^{\infty} \hat{f}_n \varepsilon^n, \quad \tilde{f}_{n0}(\varphi) = -2(\varphi \coth \varphi - 1) \hat{f}_n. \end{aligned}$$

Therefore, at $L\beta_0$ order, we obtain^{45,46}

$$\begin{aligned} \Gamma(b, \varphi) &= 4(\varphi \coth \varphi - 1) \frac{b}{\beta_0} \Gamma_0(b) + \mathcal{O}\left(\frac{1}{\beta_0^2}\right), \\ \Gamma_0(b) &= \hat{f}(-b) = \frac{(1 + \frac{2}{3}b)\Gamma(2 + 2b)}{(1 + b)\Gamma^3(1 + b)\Gamma(1 - b)} = 1 + \frac{5}{3}b - \frac{b^2}{3} - \left(2\zeta_3 - \frac{1}{3}\right)b^3 \\ &\quad + \left(\frac{\pi^4}{10} - 10\zeta_3 - 1\right)\frac{b^4}{3} - \left(6\zeta_5 - \frac{\pi^4}{18} - \frac{2}{3}\zeta_3 - \frac{1}{3}\right)b^5 \\ &\quad + \left(2\zeta_3^2 + \frac{2}{189}\pi^6 - 10\zeta_5 - \frac{\pi^4}{90} - \frac{2}{3}\zeta_3 - \frac{1}{3}\right)b^6 + \mathcal{O}(b^7). \end{aligned} \tag{11.14}$$

It is absolutely trivial to extend this expansion to any desired order. Restoring the color factors (11.12), we reproduce the corresponding terms in (6.2).

Alternatively, we can work in coordinate space $[\bar{V}(\tau, \tau, \varphi) = V(\tau, \tau, \varphi) - V(\tau, \tau, 0)]$,

$$\begin{aligned} \bar{V}(\tau, \tau, \varphi) &= \frac{1}{\beta_0} \sum_{L=1}^{\infty} \frac{f(\varepsilon, L\varepsilon, \varphi)}{L} [\Pi_0(k^2) e^{\gamma\varepsilon}]^L + \mathcal{O}\left(\frac{1}{\beta_0^2}\right) \quad (k^2 = (2/\tau)^2), \\ f(\varepsilon, u) &= \frac{uw_L}{D(\varepsilon)} = e^{\gamma(\varepsilon-2u)} \frac{3(1 - \frac{2}{3}\varepsilon)^2 \Gamma(2 - 2\varepsilon) \Gamma(1 + u)}{(1 - \varepsilon)(1 - 2u) \Gamma^2(1 - \varepsilon) \Gamma(1 + \varepsilon) \Gamma(2 + u - \varepsilon)}, \end{aligned}$$

see (10.7). Choosing $\mu = (2/\tau)e^{-\gamma} D(\varepsilon)^{1/(2\varepsilon)} \rightarrow (2/\tau)e^{-\gamma-5/6}$, we obtain

$$\bar{V}(\tau, \tau, \varphi) = \frac{1}{\beta_0} \sum_{L=1}^{\infty} \frac{f(\varepsilon, L\varepsilon)}{L} \left(\frac{b}{\varepsilon + b}\right)^L + \mathcal{O}\left(\frac{1}{\beta_0^2}\right);$$

$f(-b, 0, \varphi) = \tilde{f}(-b, 0, \varphi)$, therefore we get the result (11.14) again.

11.3. Potential and conformal anomaly

Now we consider the potential $V(\mathbf{q})$ at the $L\beta_0$ order. Choosing $\mu = |\mathbf{q}|$ we have (10.28)

$$V(\mathbf{q}) = -\frac{(4\pi)^{d/2} e^{\gamma\varepsilon}}{\beta_0 D(\varepsilon) (\mathbf{q}^2)^{1-\varepsilon}} \varepsilon \sum_{L=1}^{\infty} \left(D(\varepsilon) \frac{b}{\varepsilon + b}\right)^L + \mathcal{O}\left(\frac{1}{\beta_0^2}\right).$$

A. Grozin

The sum here can be written as

$$\sum_{L=1}^{\infty} g(\varepsilon, L\varepsilon) \left(\frac{b}{\varepsilon + b} \right)^L, \quad g(\varepsilon, u) = D(\varepsilon)^{u/\varepsilon} = \sum_{n,m=0}^{\infty} g_{nm} \varepsilon^n u^m.$$

This sum is equal to

$$\frac{b}{\varepsilon} \sum_{n=0}^{\infty} n! g_{0n} b^n + \mathcal{O}(\varepsilon^0)$$

[$1/\varepsilon^n$ -terms with $n > 1$ vanish, so that $V(\mathbf{q})$ is automatically finite], where

$$g(0, u) = e^{\frac{5}{3}u}, \quad g_{0n} = \frac{1}{n!} \left(\frac{5}{3} \right)^n. \quad (11.15)$$

Therefore

$$V(\mathbf{q}) = -\frac{(4\pi)^2}{\mathbf{q}^2} \frac{b}{\beta_0} V_0(b) + \mathcal{O}\left(\frac{1}{\beta_0^2}\right), \quad V_0(b) = \frac{1}{1 - \frac{5}{3}b}. \quad (11.16)$$

The conformal anomaly (9.8) at the $L\beta_0$ order is

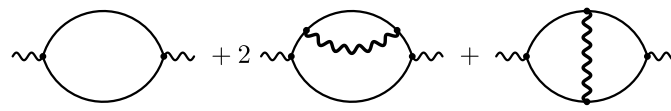
$$\begin{aligned} C &= \frac{b^2}{\beta_0} C_0(b) + \mathcal{O}\left(\frac{1}{\beta_0^2}\right), \\ C_0(b) &= \frac{V_0(b) - \Gamma_0(b)}{b^2} = \frac{28}{9} + 2 \left(\zeta_3 + \frac{58}{27} \right) b - \left(\frac{\pi^4}{10} - 10\zeta_3 - \frac{652}{27} \right) \frac{b^2}{3} \\ &\quad + \left(6\zeta_5 - \frac{\pi^4}{18} - \frac{2}{3}\zeta_3 + \frac{3044}{243} \right) b^3 - \left(2\zeta_3^2 + \frac{2}{189}\pi^6 - 10\zeta_5 - \frac{\pi^4}{90} \right. \\ &\quad \left. - \frac{2}{3}\zeta_3 - \frac{15868}{729} \right) b^4 + \dots. \end{aligned} \quad (11.17)$$

It is absolutely trivial to extend this expansion to any desired order. Restoring the color factors (11.12), we reproduce the $C_R T_F n_f \alpha_s^2$ - and $C_R (T_F n_f)^2 \alpha_s^3$ -terms in (9.9).

12. Next-To-Leading Large- β_0 Order

Now let's add to S the Abelian terms with next-to-leading powers of n_f : $\{C_F(T_F n_f)^{L-1}, L \geq 2\}$. It is sufficient to consider QED in the large- β_0 limit, but now we add the first $1/\beta_0$ -correction.

To obtain the photon propagator with the next-to-leading large- β_0 (NL β_0) accuracy, we need the photon self-energy up to $1/\beta_0$,



$$\Rightarrow \Pi_0(k^2) + \frac{\Pi_1(k^2)}{\beta_0} + \mathcal{O}\left(\frac{1}{\beta_0^2}\right), \quad (12.1)$$

where the photon propagators in Π_1 are taken at the $L\beta_0$ order. The $NL\beta_0$ contribution can be written in the form^{113,114}

$$\Pi_1(k^2) = 3\varepsilon \sum_{L=2}^{\infty} \frac{F(\varepsilon, L\varepsilon)}{L} \Pi_0(k^2)^L. \quad (12.2)$$

Using integration by parts, one can reduce it to

$$\begin{aligned} F(\varepsilon, u) &= \frac{2(1-2\varepsilon)^2(3-2\varepsilon)\Gamma^2(1-2\varepsilon)}{9(1-\varepsilon)(1-u)(2-u)\Gamma^2(1-\varepsilon)\Gamma^2(1+\varepsilon)} \\ &\times \left[-u \frac{2-3\varepsilon-\varepsilon^2+\varepsilon(2+\varepsilon)u-\varepsilon u^2}{\Gamma^2(1-\varepsilon)} I(1+u-2\varepsilon) \right. \\ &+ 2 \frac{2(1+\varepsilon)(3-2\varepsilon)-(4+11\varepsilon-7\varepsilon^2)u+\varepsilon(8-3\varepsilon)u^2-\varepsilon u^3}{(1-u)(2-u)(1-u-\varepsilon)(2-u-\varepsilon)} \\ &\times \left. \frac{\Gamma(1+u)\Gamma(1-u+\varepsilon)}{\Gamma(1-u-\varepsilon)\Gamma(1+u-2\varepsilon)} \right] = \sum_{n,m=0}^{\infty} F_{nm} \varepsilon^n u^m, \end{aligned} \quad (12.3)$$

where the integral

$$I(n) = \text{---} \circlearrowleft \text{---} = \frac{1}{\pi^d} \int \frac{d^d k_1 d^d k_2}{k_1^2 k_2^2 (k_1 + p)^2 (k_2 + p)^2 [(k_1 - k_2)^2]^n}$$

(Euclidean, $p^2 = 1$) can be expressed via a ${}_3F_2$ -function of unit argument^{115,116} (see the review¹¹⁷ for more references). The ${}_3F_2$ -function can be expanded up to any desired order using known algorithms, the coefficients are expressed via multiple ζ -values; therefore, the coefficients F_{nm} can be calculated to any desired order.

The function $F(\varepsilon, u)$ simplifies in some cases. In particular,¹¹³

$$F(\varepsilon, 0) = \frac{(1+\varepsilon)(1-2\varepsilon)^2(1-\frac{2}{3}\varepsilon)^2\Gamma(1-2\varepsilon)}{(1-\varepsilon)^2(1-\frac{1}{2}\varepsilon)\Gamma(1+\varepsilon)\Gamma^3(1-\varepsilon)}, \quad (12.4)$$

so that F_{n0} contain no multiple ζ -values, only ζ_n . Also¹¹⁴

$$F(0, u) = \frac{2}{3} \frac{\psi'\left(2-\frac{u}{2}\right) - \psi'\left(1+\frac{u}{2}\right) - \psi'\left(\frac{3-u}{2}\right) + \psi'\left(\frac{1+u}{2}\right)}{(1-u)(2-u)}, \quad (12.5)$$

so that F_{0m} contains¹¹⁴ only ζ_{2n+1} ,

$$\begin{aligned} F_{0m} &= -\frac{32}{3} \sum_{s=1}^{[(m+1)/2]} s(1-2^{-2s})(1-2^{2s-m-2})\zeta_{2s+1} \\ &+ \frac{4}{3}(m+1)(m+(m+6)2^{-m-3}). \end{aligned} \quad (12.6)$$

A. Grozin

The two-loop case is, of course, trivial,

$$F(\varepsilon, 2\varepsilon) = \frac{2}{9\varepsilon^2} \frac{3-2\varepsilon}{1-\varepsilon} \left[2 \frac{(1-2\varepsilon)^2(2-2\varepsilon+\varepsilon^2)}{(1-3\varepsilon)(2-3\varepsilon)} \right. \\ \times \left. \frac{\Gamma(1+2\varepsilon)\Gamma^2(1-2\varepsilon)}{\Gamma^2(1+\varepsilon)\Gamma(1-\varepsilon)\Gamma(1-3\varepsilon)} - 2 + \varepsilon - 2\varepsilon^2 \right].$$

Let's write the charge renormalization constant Z_α with the $\text{NL}\beta_0$ accuracy as

$$Z_\alpha(b) = \frac{1}{1+b/\varepsilon} \left[1 + \frac{Z_{\alpha 1}(b)}{\beta_0} + \mathcal{O}\left(\frac{1}{\beta_0^2}\right) \right], \\ Z_{\alpha 1}(b) = \frac{Z_{\alpha 11}(b)}{\varepsilon} + \frac{Z_{\alpha 12}(b)}{\varepsilon^2} + \dots, \quad Z_{\alpha 1n} = \mathcal{O}(b^{n+1}). \quad (12.7)$$

In the Abelian theory, $\log(1 - \Pi)$ expressed via renormalized b using (11.3) should be equal to $\log Z_\alpha + \mathcal{O}(\varepsilon^0)$. Equating the coefficients of ε^{-1} in the $1/\beta_0$ -terms in this relation, we see that $Z_{\alpha 11}$ (12.7) is given by the coefficient of ε^{-1} in

$$-\left(1 + \frac{b}{\varepsilon}\right)\Pi_1.$$

It is convenient to choose $\mu^2 = (-k^2)D(\varepsilon)^{-1/\varepsilon} \rightarrow (-k^2)e^{-5/3}$, then

$$\Pi_1 = 3\varepsilon \sum_{L=2}^{\infty} \frac{F(\varepsilon, L\varepsilon)}{L} \left(\frac{b}{\varepsilon+b}\right)^L.$$

We expand in b and expand $F(\varepsilon, u)$ in ε and u ; selecting the ε^{-1} -terms, we find that all coefficients but F_{n0} cancel,

$$Z_{\alpha 11} = -3 \sum_{n=0}^{\infty} \frac{F_{n0}(-b)^{n+2}}{(n+1)(n+2)}. \quad (12.8)$$

The β -function with $\text{NL}\beta_0$ accuracy is

$$\beta(b) = b + \frac{b^2}{\beta_0} B_1(b) + \mathcal{O}\left(\frac{1}{\beta_0^2}\right), \quad (12.9)$$

where^{113,114}

$$b^2 B_1(b) = -\frac{dZ_{\alpha 11}(b)}{d\log b}, \quad (12.10)$$

$$B_1(b) = 3 \sum_{n=0}^{\infty} \frac{F_{n0}(-b)^n}{n+1} \\ = 3 + \frac{11}{4}b - \frac{77}{36}b^2 - \left(3\zeta_3 + \frac{107}{48}\right)\frac{b^3}{2} + \left(\frac{\pi^4}{10} - 11\zeta_3 + \frac{251}{48}\right)\frac{b^4}{5} + \dots \quad (12.11)$$

[the coefficients F_{n0} follow from $F(\varepsilon, 0)$ (12.4)]. The corresponding terms in the five-loop QED β -function¹¹⁸ are reproduced. We shall need the full $Z_{\alpha 1}$, not just $Z_{\alpha 11}$;

integrating the RG equation with the $1/\beta_0$ -accuracy, we obtain

$$\begin{aligned} Z_{\alpha 1}(b) &= -\varepsilon \int_0^b \frac{b B_1(b) db}{(\varepsilon + b)^2} \\ &= -\frac{3}{2} \frac{b^2}{\varepsilon} + \frac{1}{2} (4 + F_{10}\varepsilon) \frac{b^3}{\varepsilon^2} - \frac{1}{4} (9 + 3F_{10}\varepsilon + F_{20}\varepsilon^2) \frac{b^4}{\varepsilon^3} + \dots \end{aligned}$$

12.1. HQET field anomalous dimension

At the $\text{NL}\beta_0$ order, we should expand the photon propagator $(1 - \Pi_0 - \Pi_1/\beta_0)^{-1}$ up to $1/\beta_0$ (Fig. 6). The photon propagator contains a single Π_1 -insertion and any number of Π_0 -insertions; the photon propagator inside Π_1 contains any number of Π_0 -insertions. The two-leg web $\tilde{w}(\omega)$ becomes

$$\begin{aligned} \tilde{w}(\omega) &= \frac{1}{\beta_0} \sum_{L=1}^{\infty} \frac{\tilde{f}(\varepsilon, L\varepsilon)}{L} \left(\frac{b}{\varepsilon + b} \right)^L \\ &\times \left[1 + L \frac{Z_{\alpha 1}}{\beta_0} + \frac{3\varepsilon}{\beta_0} \sum_{L'=2}^{L-1} \frac{L-L'}{L'} F(\varepsilon, L'\varepsilon) \right] + \mathcal{O}\left(\frac{1}{\beta_0^3}\right), \quad (12.12) \end{aligned}$$

where L' is the number of loops in the Π_1 -insertion, and the $1/\beta_0$ -correction $Z_{\alpha 1}$ to the charge renormalization (12.7) is taken into account. We expand in b and substitute the expansions (12.3) and (11.8); in z_{h1} , the coefficient of ε^{-1} , all \tilde{f}_{nm} except \tilde{f}_{n0} cancel. We obtain⁴⁷

$$\begin{aligned} \gamma_h(b) &= -6 \left[\frac{b}{\beta_0} \gamma_0(b) - \frac{b^3}{\beta_0^2} \gamma_1(b) \right] + \mathcal{O}\left(\frac{1}{\beta_0^3}\right), \\ \gamma_1(b) &= -\frac{3}{2} [F_{10} + 2F_{01} - 2\tilde{f}_{10}] + [2F_{20} + 3(F_{11} + F_{02}) + 3F_{01}\tilde{f}_{10} - 6\tilde{f}_{20}]b \\ &\quad - \left[\frac{3}{4} (3F_{30} + 4(F_{21} + F_{12} + F_{03})) + (F_{20} + 3(F_{11} + F_{02}))\tilde{f}_{10} \right. \\ &\quad \left. - \frac{3}{2} (F_{10} - 2F_{01})\tilde{f}_{20} - 9\tilde{f}_{30} \right] b^2 + \dots \end{aligned}$$

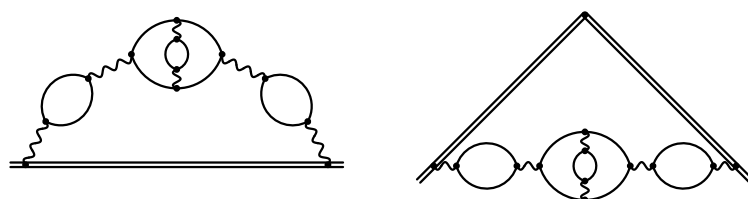


Fig. 6. Typical diagrams for γ_h and $\Gamma(\varphi)$ at $\text{NL}\beta_0$ order.

A. Grozin

$$\begin{aligned}
 &= 3 \left(4\zeta_3 - \frac{17}{4} \right) + \left(-\frac{\pi^4}{5} + 36\zeta_3 - \frac{103}{9} \right) b + \left(24\zeta_5 - \frac{3}{5}\pi^4 + \frac{59}{2}\zeta_3 \right. \\
 &\quad \left. + \frac{14579}{864} \right) b^2 + \left(-48\zeta_3^3 - \frac{2}{63}\pi^6 + 72\zeta_5 - \frac{44}{75}\pi^4 + \frac{3229}{45}\zeta_3 - \frac{5191}{540} \right) b^3 \\
 &\quad + \left(36\zeta_7 + \frac{8}{5}\pi^4\zeta_3 - 144\zeta_3^2 - \frac{2}{21}\pi^6 + 107\zeta_5 - \frac{946}{675}\pi^4 + \frac{9601}{180}\zeta_3 + \frac{22859}{8640} \right) b^4 \\
 &\quad + \left(-240\zeta_3\zeta_5 - \frac{4}{225}\pi^8 + 108\zeta_7 + \frac{24}{5}\pi^4\zeta_3 - \frac{664}{7}\zeta_3^2 - \frac{272}{1323}\pi^6 \right. \\
 &\quad \left. + \frac{18574}{63}\zeta_5 - \frac{119}{135}\pi^4 - \frac{6263}{63}\zeta_3 + \frac{16103}{1296} \right) b^5 + \dots
 \end{aligned} \tag{12.13}$$

This expansion can be extended to higher loops, but the complexity of expanding $F(\varepsilon, u)$ in ε, u to obtain F_{nm} quickly grows with $n + m$, so this extension is not quite trivial. Note that the last (eight-loop) term here contains F_{nm} with $n + m = 6$, $n > 0, m > 0$, each of them contains $\zeta_{5,3}$; but they enter as the combination $F_{51} + F_{42} + F_{33} + F_{24} + F_{15}$ in which this $\zeta_{5,3}$ cancels. Restoring the color factors, we reproduce the corresponding terms in (5.1).

12.2. Cusp anomalous dimension

The two-leg web $\tilde{V}(\omega, \omega, \varphi)$ is given by a formula similar to (12.12). The cusp anomalous dimension at $\text{NL}\beta_0$ order is determined by the same coefficients \hat{f}_n as at $\text{L}\beta_0$ order, plus the coefficients F_{nm} . We obtain⁴⁷

$$\begin{aligned}
 \Gamma(b, \varphi) &= 4(\varphi \cot \varphi - 1) \left[\frac{b}{\beta_0} \Gamma_0(b) - \frac{b^3}{\beta_0^2} \Gamma_1(b) \right] + \mathcal{O}\left(\frac{1}{\beta_0^3}\right), \\
 \Gamma_1(b) &= 12\zeta_3 - \frac{55}{4} + \left(-\frac{\pi^4}{5} + 40\zeta_3 - \frac{299}{18} \right) b \\
 &\quad + \left(24\zeta_5 - \frac{2}{3}\pi^4 + \frac{233}{6}\zeta_3 + \frac{15211}{864} \right) b^2 \\
 &\quad + \left(-48\zeta_3^2 - \frac{2}{63}\pi^6 + 80\zeta_5 - \frac{167}{225}\pi^4 + \frac{1168}{15}\zeta_3 - \frac{971}{240} \right) b^3 \\
 &\quad + \left(36\zeta_7 + \frac{8}{5}\pi^4\zeta_3 - 160\zeta_3^2 - \frac{20}{189}\pi^6 + \frac{377}{3}\zeta_5 - \frac{23}{15}\pi^4 + \frac{929}{12}\zeta_3 - \frac{8017}{1728} \right) b^4 \\
 &\quad + \left(-240\zeta_3\zeta_5 - \frac{4}{225}\pi^8 + 120\zeta_7 + \frac{16}{3}\pi^4\zeta_3 - \frac{2776}{21}\zeta_3^2 - \frac{914}{3969}\pi^6 \right. \\
 &\quad \left. + \frac{6826}{21}\zeta_5 - \frac{1793}{1350}\pi^4 - \frac{31693}{315}\zeta_3 + \frac{79433}{4320} \right) b^5 + \dots
 \end{aligned} \tag{12.14}$$

This expansion also can be extended to higher loops, but the complexity of calculations quickly grows. At eight loops, the same combination of F_{nm} with $n + m = 6$

appears, so that $\zeta_{5,3}$ cancels here, too. Restoring the color factors, we reproduce the corresponding terms in (6.2).

12.3. Potential and conformal anomaly

The static potential at the $N\beta_0$ level is

$$\begin{aligned} V(\mathbf{q}) &= -\frac{(4\pi)^2}{\beta_0 \mathbf{q}^2} \varepsilon \sum_{L=1}^{\infty} g(\varepsilon, L\varepsilon) \left(\frac{b}{\varepsilon + b} \right)^L \left[1 + L \frac{Z_{\alpha 1}}{\beta_0} \right. \\ &\quad \left. + \frac{3\varepsilon}{\beta_0} \sum_{L'=2}^{L-1} \frac{L-L'}{L'} F(\varepsilon, L'\varepsilon) \right] + \mathcal{O}\left(\frac{1}{\beta_0^3}\right) \\ &= -\frac{(4\pi)^2}{\mathbf{q}^2} \left[\frac{b}{\beta_0} V_0(b) - \frac{b^3}{\beta_0^2} V_1(b) \right] + \mathcal{O}\left(\frac{1}{\beta_0^3}\right), \end{aligned} \quad (12.15)$$

where

$$\begin{aligned} V_1(b) &= -\frac{3}{2} [F_{10} + 2F_{01} + 2g_{01}] + \frac{1}{2} [F_{20} - 6F_{02} - 6(F_{10} + 3F_{01})g_{01} - 30g_{02}]b \\ &\quad - \frac{1}{4} [F_{30} + 24F_{03} - 4(F_{20} + 12F_{02})g_{01} + 36(F_{10} + 4F_{01})g_{02} + 312g_{03}]b^2 \\ &\quad + \dots \end{aligned}$$

contains only the same coefficients g_{0n} (11.15) as the $L\beta_0$ result, and only F_{n0} and F_{0m} are involved [see (12.4)–(12.6)]. We obtain⁴⁷

$$\begin{aligned} V_1(b) &= 12\zeta_3 - \frac{55}{4} + \left(78\zeta_3 - \frac{7001}{72} \right)b + \left(60\zeta_5 + \frac{723}{2}\zeta_3 - \frac{147851}{288} \right)b^2 \\ &\quad + \left(770\zeta_5 + \frac{\pi^4}{200} + \frac{276901}{180}\zeta_3 - \frac{70418923}{25920} \right)b^3 + \left(1134\zeta_7 + \frac{32297}{5}\zeta_5 \right. \\ &\quad \left. + \frac{41}{1800}\pi^4 + \frac{402479}{60}\zeta_3 - \frac{1249510621}{77760} \right)b^4 + \left(21735\zeta_7 + \frac{\zeta_3^2}{7} + \frac{\pi^6}{1323} \right. \\ &\quad \left. + \frac{5911849}{126}\zeta_5 + \frac{41}{720}\pi^4 + \frac{48558187}{1512}\zeta_3 - \frac{10255708489}{93312} \right)b^5 + \dots \end{aligned} \quad (12.16)$$

Thus, we have reproduced the $C_F(T_F n_f)^2 \alpha_s^3$ - and $C_F^2 T_F n_f \alpha_s^3$ -terms in the two-loop potential,¹¹⁹ as well as the $C_F(T_F n_f)^3 \alpha_s^4$ - and $C_F^2 (T_F n_f)^2 \alpha_s^4$ -terms in the three-loop one.¹²⁰ This expansion can be easily extended to any order; it contains only ζ_n because only F_{n0} (12.4) and F_{0m} (12.6) are present. Note the pattern of the highest weights in (12.16): 3, 3, 5, 5, 7, 7, whereas one would expect 3, 4, 5, 6, 7, 8, as in (12.14) and (12.13).

Constructing $\Delta(\alpha_s)$ (9.6) from $\Gamma(\varphi)$ (12.14) and $V(\mathbf{q})$ (12.15) and dividing by $\beta(\alpha_s)$ (12.9), we obtain $C(\alpha_s)$ (9.8),

$$C = \frac{b^2}{\beta_0} C_0(b) - \frac{b^3}{\beta_0^2} C_1(b) + \mathcal{O}\left(\frac{1}{\beta_0^3}\right),$$

A. Grozin

$$\begin{aligned}
 C_1(b) = & \frac{\pi^4}{5} + 38\zeta_3 - \frac{1711}{24} + \left(36\zeta_5 + \frac{2}{3}\pi^4 + \frac{986}{3}\zeta_3 - \frac{110059}{216} \right)b \\
 & + \left(48\zeta_3^2 + \frac{2}{63}\pi^6 + 690\zeta_5 + \frac{233}{360}\pi^4 + \frac{53135}{36}\zeta_3 - \frac{13910875}{5184} \right)b^2 \\
 & + \left(1098\zeta_7 - \frac{8}{5}\pi^4\zeta_3 + 160\zeta_3^2 + \frac{20}{189}\pi^6 + \frac{95276}{15}\zeta_5 + \frac{292}{225}\pi^4 + \frac{596591}{90}\zeta_3 \right. \\
 & \left. - \frac{51895439}{3240} \right)b^3 + \left(240\zeta_3\zeta_5 + \frac{4}{225}\pi^8 + 21615\zeta_7 - \frac{16}{3}\pi^4\zeta_3 + \frac{370}{3}\zeta_3^2 \right. \\
 & \left. + \frac{113}{567}\pi^6 + \frac{419768}{9}\zeta_5 + \frac{1679}{1200}\pi^4 + \frac{23179201}{720}\zeta_3 - \frac{51249331081}{466560} \right)b^4 + \dots
 \end{aligned} \tag{12.17}$$

The first term in C_1 reproduces the $C_R C_F T_F n_f \alpha_s^3$ -term in (9.9).

13. Abelian Terms with $(T_F n_f)^1$

Finally, we consider Abelian color structures linear in $T_F n_f$: $S = \{1\} \cup \{C_L^{L-1} T_F n_f, L \geq 1\}$. We can work in QED. Writing the L -loop photon self-energy as

$$\Pi_{L-1} = \tilde{\Pi}_{L-1} n_f + (n_f^{>1}\text{-terms}),$$

we have the photon propagator

$$D^{\mu\nu}(k) = D_0^{\mu\nu}(k) + n_f \sum_{L=1}^{\infty} \tilde{\Pi}_{L-1} D_L^{\mu\nu}(k) A_0^L + (n_f^{>1}\text{-terms}). \tag{13.1}$$

In QED $\log(1 - \Pi(k^2)) = \log Z_\alpha + \mathcal{O}(\varepsilon^0)$; writing the L -loop β -function coefficient as $\beta_{L-1} = \bar{\beta}_{L-1} n_f + (n_f^{>1}\text{-terms})$, we see that $1/\varepsilon$ -terms in $\tilde{\Pi}_{L-1}$ are related to $\bar{\beta}_{L-1}$,

$$\tilde{\Pi}_{L-1} = \frac{\bar{\beta}_{L-1}}{L\varepsilon} + \bar{\Pi}_{L-1} + \mathcal{O}(\varepsilon). \tag{13.2}$$

Here, the β -function coefficients are¹²¹

$$\bar{\beta}_0 = -\frac{4}{3}, \quad \bar{\beta}_1 = -4, \quad \bar{\beta}_2 = 2, \quad \bar{\beta}_3 = 46; \tag{13.3}$$

and¹²²

$$\begin{aligned}
 \bar{\Pi}_0 &= -\frac{20}{9}, \quad \bar{\Pi}_1 = 16\zeta_3 - \frac{55}{3}, \quad \bar{\Pi}_2 = -2 \left(80\zeta_5 - \frac{148}{3}\zeta_3 - \frac{143}{9} \right), \\
 \bar{\Pi}_3 &= 2240\zeta_7 - 1960\zeta_5 - 104\zeta_3 + \frac{31}{3}.
 \end{aligned} \tag{13.4}$$

13.1. HQET field anomalous dimension

The web $\tilde{w}(\omega)$ (10.8) is

$$\begin{aligned}\tilde{w}(\omega) &= \tilde{w}_1 A_0 (-2\omega)^{-2\varepsilon} + n_f \sum_{L=2}^{\infty} \tilde{\Pi}_{L-2} \tilde{w}_L [A_0 (-2\omega)^{-2\varepsilon}]^L \\ &\quad + (n_f^{>1}\text{-terms}) + (w_{>2\text{ legs}}\text{-terms}),\end{aligned}\tag{13.5}$$

where (10.8)

$$\tilde{w}_L = \frac{3}{L\varepsilon} + \frac{1}{L} + 3 + \mathcal{O}(\varepsilon).\tag{13.6}$$

We re-express $\tilde{w}(\omega)$ via $\alpha(-2\omega)$ using (10.3),

$$Z_\alpha = 1 - \frac{n_f}{\varepsilon} \sum_{L=1}^{\infty} \frac{\bar{\beta}_{L-1}}{L} \left(\frac{\alpha}{4\pi}\right)^L + (n_f^{>1}\text{-terms})$$

(it is sufficient to include Z_α in the \tilde{w}_1 -term). Collecting the ε^{-1} -terms, we have

$$\begin{aligned}z_{h1} &= 3 \frac{\alpha}{4\pi} + n_f \sum_{L=2}^{\infty} \frac{3\bar{\Pi}_{L-2} - \bar{\beta}_{L-2}}{L} \left(\frac{\alpha}{4\pi}\right)^L \\ &\quad + (n_f^{>1}\text{-terms}) + (w_{>2\text{ legs}}\text{-terms}).\end{aligned}$$

Restoring the color factors, we finally obtain⁵³

$$\begin{aligned}\gamma_h &= -2C_R \frac{\alpha_s}{4\pi} \left[3 + T_F n_f \frac{\alpha_s}{4\pi} \sum_{L=0}^{\infty} (3\bar{\Pi}_L - \bar{\beta}_L) \left(C_F \frac{\alpha_s}{4\pi}\right)^L \right] + \dots \\ &= -2C_R \frac{\alpha_s}{4\pi} \left\{ 3 + T_F n_f \frac{\alpha_s}{4\pi} \left[-\frac{16}{3} + 3(16\zeta_3 - 17)C_F \frac{\alpha_s}{4\pi} \right. \right. \\ &\quad - 8 \left(60\zeta_5 - 37\zeta_3 - \frac{35}{3} \right) \left(C_F \frac{\alpha_s}{4\pi} \right)^2 \\ &\quad \left. \left. + 3(2240\zeta_7 - 1960\zeta_5 - 104\zeta_3 - 5) \left(C_F \frac{\alpha_s}{4\pi} \right)^3 + \mathcal{O}(\alpha_s^4) \right] \right\} + \dots,\end{aligned}\tag{13.7}$$

where dots mean other color structures. The corresponding terms from (5.1) are reproduced. This expansion cannot be extended without a highly nontrivial calculation of higher $\bar{\Pi}_L$ and $\bar{\beta}_L$.

This result can also be obtained in coordinate space: w_L (10.7) has the structure identical to (13.6), and if we express $w(\tau)$ via $\alpha((2/\tau)e^{-\gamma})$, the calculation is exactly the same as above.

13.2. Cusp anomalous dimension

The web $\tilde{\tilde{V}}(\varphi)$ (10.19) is

$$\tilde{\tilde{V}}(\varphi) = -2 \frac{\varphi \coth \varphi - 1}{L\varepsilon} + V(\varphi) + \mathcal{O}(\varepsilon),\tag{13.8}$$

A. Grozin

where $V(\varphi) = V(-\varphi)$ does not depend on L and hence $\bar{\beta}_{L-2}$ cancels in the calculation of z_{J1} [in contrast to z_{h1} where the corresponding term in (13.6) contains $1/L$, and $\bar{\beta}_{L-2}$ does not cancel],

$$z_{J1} = -2(\varphi \coth \varphi - 1) \frac{\alpha_s}{4\pi} \left[1 + n_f \frac{\alpha_s}{4\pi} \sum_{L=0}^{\infty} \frac{\bar{\Pi}_L}{L} \left(\frac{\alpha_s}{4\pi} \right)^L \right] \\ + (n_f^{>1}\text{-terms}) + (w_{>2 \text{ legs}}\text{-terms}).$$

Restoring color factors, we obtain⁵³

$$\Gamma(\varphi) = 4C_R(\varphi \coth \varphi - 1) \frac{\alpha_s}{4\pi} \left[1 + T_F n_f \frac{\alpha_s}{4\pi} \sum_{L=0}^{\infty} \bar{\Pi}_L \left(C_F \frac{\alpha_s}{4\pi} \right)^L \right] + \dots \\ = 4C_R(\varphi \coth \varphi - 1) \frac{\alpha_s}{4\pi} \left\{ 1 + T_F n_f \frac{\alpha_s}{4\pi} \left[-\frac{20}{9} + \left(16\zeta_3 - \frac{55}{3} \right) C_F \frac{\alpha_s}{4\pi} \right. \right. \\ \left. - 2 \left(80\zeta_5 - \frac{148}{3}\zeta_3 - \frac{143}{9} \right) \left(C_F \frac{\alpha_s}{4\pi} \right)^2 + \left(2240\zeta_7 - 1960\zeta_5 - 104\zeta_3 + \frac{31}{3} \right) \right. \\ \times \left. \left(C_F \frac{\alpha_s}{4\pi} \right)^3 + \mathcal{O}(\alpha_s^4) \right\} + \dots, \quad (13.9)$$

where dots mean other color structures. The corresponding terms from (6.2) are reproduced. This expansion cannot be extended without a highly nontrivial calculation of higher $\bar{\Pi}_L$ and $\bar{\beta}_L$.

This result can also be obtained in coordinate space: $\bar{V}(\varphi)$ (10.16) has the structure identical to (13.8), and if we express $\bar{V}(\tau, \tau, \varphi)$ via $\alpha((2/\tau)e^{-\gamma})$, the calculation is exactly the same as above.

13.3. Potential and conformal anomaly

Now we consider the $C_F^{L-1} T_F n_f \alpha_s^L$ -terms in the quark–antiquark potential. In Coulomb gauge, they are given by a single Coulomb-gluon propagator⁵³,

$$V(\mathbf{q}) = -C_R \frac{4\pi\alpha_s}{\mathbf{q}^2} \left[1 + T_F n_f \frac{\alpha_s}{4\pi} \sum_{L=0}^{\infty} \bar{\Pi}_L \left(C_F \frac{\alpha_s}{4\pi} \right)^L \right] + \dots \\ = -\frac{4\pi\alpha_s}{\mathbf{q}^2} C_R \left\{ 1 + T_F n_f \frac{\alpha_s}{4\pi} \left[-\frac{20}{9} + \left(16\zeta_3 - \frac{55}{3} \right) C_F \frac{\alpha_s}{4\pi} \right. \right. \\ \left. - 2 \left(80\zeta_5 - \frac{148}{3}\zeta_3 - \frac{143}{9} \right) \left(C_F \frac{\alpha_s}{4\pi} \right)^2 + \left(2240\zeta_7 - 1960\zeta_5 - 104\zeta_3 + \frac{31}{3} \right) \right. \\ \times \left. \left(C_F \frac{\alpha_s}{4\pi} \right)^3 + \mathcal{O}(\alpha_s^4) \right\} + \dots, \quad (13.10)$$

where $\alpha_s = \alpha_s(|\mathbf{q}|)$ and dots mean other color structures. The terms up to α_s^4 agree with Ref. 120.

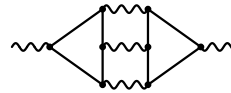
Comparing (13.10) with (13.9), we see that the $C_F^{L-1} T_F n_f$ color structures are absent in Δ to all orders in α_s . In particular, this explains the absence of C_F in the

bracket in (9.7). It is easy to prove by induction that $C_R C_F^{L-1} \alpha_s^L$ -terms are absent in $C(\alpha_s)$ (9.8) to all orders⁵³.

14. $C_R C_F^2 (T_F n_f)^2 \alpha_s^5$ and $C_R \bar{d}_F F n_f^2 \alpha_s^5$

In Secs. 11–13, we considered some families of Abelian color structures $C_R C_F^{L-n-1} (T_F n_f)^n \alpha_s^L$ in the HQET field anomalous dimension γ_h , the cusp anomalous dimension $\Gamma(\varphi)$ as well as the quark–antiquark potential $V(\mathbf{q})$ (and hence the conformal anomaly Δ). These families are shown in Fig. 7; some of them intersect, and we can compare the results of the corresponding approaches. We see that the only five-loop structure from this class not considered in the previous sections is $C_R C_F^2 (T_F n_f)^2 \alpha_s^5$. It can be considered using the general guidelines outlined in Sec. 10 if we choose $S = \{1, T_F n_f, C_F T_F n_f, C_F^2 T_F n_f, C_F^2 (T_F n_f)^2\}$.

The gluon self-energy diagram



and similar ones with permutations of vertices contain the color structure $\bar{d}_{FF} n_f^2$, where

$$\bar{d}_{FF} = \frac{d_F^{abcd} d_F^{abcd}}{N_A}. \quad (14.1)$$

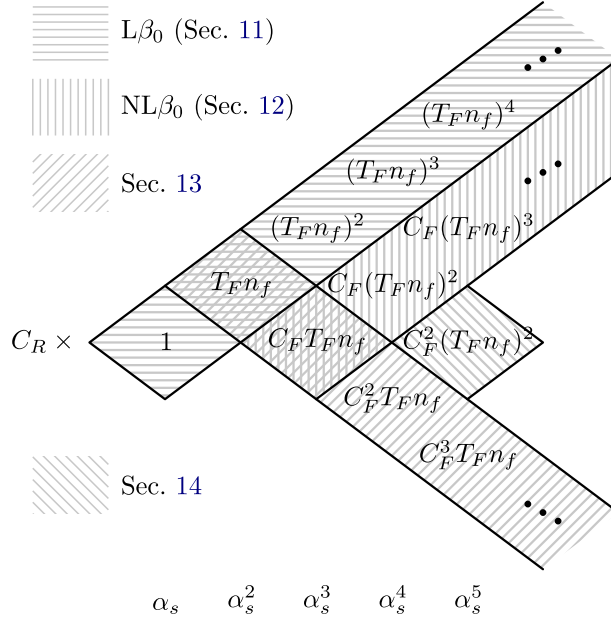


Fig. 7. Abelian color structures.

A. Grozin

Its contribution ($C_R \bar{d}_{FF} n_f^2 \alpha_s^5$) to γ_h and similar quantities can be obtained by setting $S = \{\bar{d}_{FF} n_f^2\}$.

Alternatively, we can just consider all $C_F^{L-n-1}(T_F n_f)^n$ up to $L = 5$ plus $\bar{d}_{FF} n_f^2$, and re-derive the corresponding results of Secs. 11–13 together with obtaining the two new results. The HQET field anomalous dimension is

$$\begin{aligned}
 \gamma_h = C_R \frac{\alpha_s}{4\pi} & \left\{ -6 + \frac{32}{3} T_F n_f \frac{\alpha_s}{4\pi} - 2T_F n_f \left(\frac{\alpha_s}{4\pi} \right)^2 \left[3C_F(16\zeta_3 - 17) - \frac{80}{27} T_F n_f^2 \right] \right. \\
 & + 16T_F n_f \left(\frac{\alpha_s}{4\pi} \right)^3 \left[C_F^2 \left(60\zeta_5 - 37\zeta_3 - \frac{35}{3} \right) \right. \\
 & - 2C_F T_F n_f \left(\frac{\pi^4}{15} - 12\zeta_3 + \frac{103}{27} \right) - \frac{16}{9} (T_F n_f)^2 \left(\zeta_3 - \frac{1}{3} \right) \\
 & - \left(\frac{\alpha_s}{4\pi} \right)^4 [6C_F^3 T_F n_f (2240\zeta_7 - 1960\zeta_5 - 104\zeta_3 - 5) \\
 & + C_F^2 (T_F n_f)^2 \left(1792\zeta_3^2 - \frac{640}{189}\pi^6 + \frac{17920}{3}\zeta_5 + \frac{88}{5}\pi^4 - \frac{68096}{9}\zeta_3 + \frac{59411}{27} \right) \\
 & + 32\bar{d}_{FF} n_f^2 \left(32\zeta_3^2 - 60\zeta_5 + \frac{2}{15}\pi^4 + \frac{157}{3}\zeta_3 - 43 \right) \\
 & + \frac{4}{3} C_F (T_F n_f)^3 \left(256\zeta_5 - \frac{32}{5}\pi^4 + \frac{944}{3}\zeta_3 + \frac{14579}{81} \right) \\
 & \left. \left. + \frac{256}{81} (T_F n_f)^4 \left(\frac{\pi^4}{5} - 16\zeta_3 - \frac{14}{3} \right) \right] \right\} + \dots, \tag{14.2}
 \end{aligned}$$

where dots mean other color structures. The corresponding parts of (11.11), (12.13) and (13.7) are reproduced; the $C_R C_F^2 (T_F n_f)^2 \alpha_s^5$ and $C_R \bar{d}_{FF} n_f^2 \alpha_s^5$ results are new.

The cusp anomalous dimension is

$$\begin{aligned}
 \Gamma(\varphi) = 4C_R(\varphi \coth \varphi - 1) \frac{\alpha_s}{4\pi} & \left\{ 1 - \frac{20}{9} T_F n_f \frac{\alpha_s}{4\pi} \right. \\
 & + T_F n_f \left(\frac{\alpha_s}{4\pi} \right)^2 \left[C_F \left(16\zeta_3 - \frac{55}{3} \right) - \frac{16}{27} T_F n_f \right] \\
 & + T_F n_f \left(\frac{\alpha_s}{4\pi} \right)^3 \left[-2C_F^2 \left(80\zeta_5 - \frac{148}{3}\zeta_3 - \frac{143}{9} \right) \right. \\
 & + \frac{8}{9} C_F T_F n_f \left(\frac{2}{5}\pi^4 - 80\zeta_3 + \frac{299}{9} \right) + \frac{64}{27} (T_F n_f)^2 \left(2\zeta_3 - \frac{1}{3} \right) \\
 & + \left(\frac{\alpha_s}{4\pi} \right)^4 \left[C_F^3 T_F n_f \left(2240\zeta_7 - 1960\zeta_5 - 104\zeta_3 + \frac{31}{3} \right) \right. \\
 & + \frac{C_F^2 (T_F n_f)^2}{3} \left(896\zeta_3^2 - \frac{320}{189}\pi^6 + 3200\zeta_5 + \frac{44}{5}\pi^4 - \frac{36512}{9}\zeta_3 + \frac{62971}{54} \right) \\
 & \left. \left. + 16\bar{d}_{FF} n_f^2 \left(\frac{32}{3}\zeta_3^2 - 20\zeta_5 + \frac{2}{45}\pi^4 + 21\zeta_3 - \frac{431}{27} \right) \right] \right\}
 \end{aligned}$$

$$\begin{aligned}
 & + \frac{2}{9} C_F (T_F n_f)^3 \left(256\zeta_5 - \frac{64}{9}\pi^4 + \frac{3728}{9}\zeta_3 + \frac{15211}{81} \right) \\
 & + \frac{128}{243} (T_F n_f)^4 \left(\frac{\pi^4}{5} - 20\zeta_3 - 2 \right) \Big] \Big\} + \dots , \tag{14.3}
 \end{aligned}$$

where dots mean other color structures. The corresponding parts of (11.14), (12.14) and (13.9) are reproduced; the $C_R C_F^2 (T_F n_f)^2 \alpha_s^5$ and $C_R \bar{d}_{FF} n_f^2 \alpha_s^5$ results are new.

The quark–antiquark potential is

$$\begin{aligned}
 V(\mathbf{q}) = & -C_R \frac{4\pi\alpha_s}{\mathbf{q}^2} \left\{ 1 - \frac{20}{9} T_F n_f \frac{\alpha_s}{4\pi} + T_F n_f \left(\frac{\alpha_s}{4\pi} \right)^2 \left[C_F \left(16\zeta_3 - \frac{55}{3} \right) + \frac{400}{81} T_F n_f \right] \right. \\
 & + T_F n_f \left(\frac{\alpha_s}{4\pi} \right)^3 \left[-2C_F^2 \left(80\zeta_5 - \frac{148}{3}\zeta_3 - \frac{143}{9} \right) \right. \\
 & \left. - \frac{2}{3} C_F T_F n_f \left(208\zeta_3 - \frac{7001}{27} \right) - \frac{8000}{729} (T_F n_f)^2 \right] \\
 & + \left(\frac{\alpha_s}{4\pi} \right)^4 \left[C_F^3 T_F n_f \left(2240\zeta_7 - 1960\zeta_5 - 104\zeta_3 + \frac{31}{3} \right) \right. \\
 & + C_F^2 (T_F n_f)^2 \left(512\zeta_3^2 + \frac{22400}{9}\zeta_5 - \frac{44}{135}\pi^4 - \frac{25792}{9}\zeta_3 + \frac{13025}{54} \right) \\
 & + 16\bar{d}_{FF} n_f^2 \left(\frac{32}{3}\zeta_3^2 - 20\zeta_5 + \frac{2}{45}\pi^4 + 21\zeta_3 - \frac{431}{27} \right) + \frac{2}{9} C_F (T_F n_f)^3 \\
 & \times \left. \left(640\zeta_5 + 3856\zeta_3 - \frac{147851}{27} \right) + \frac{160000}{6561} (T_F n_f)^4 \right\} + \dots , \tag{14.4}
 \end{aligned}$$

where $\alpha_s = \alpha_s(|\mathbf{q}|)$ and dots mean other color structures. The corresponding parts of (11.16), (12.16) and (13.10) are reproduced; the $C_R C_F^2 (T_F n_f)^2 \alpha_s^5$ and $C_R \bar{d}_{FF} n_f^2 \alpha_s^5$ results are new.

We can obtain $\Delta(\alpha_s)$ (9.6) from $\Gamma(\varphi)$ (14.3) and $V(\mathbf{q})$ (14.4). The $C_R \bar{d}_{FF} n_f^2 \alpha_s^5$ contribution has canceled, just like all $C_R C_F^{L-2} T_F n_f \alpha_s^L$ ones (Sec. 13), and for the same reason: there is just a single $\Pi(k^2)$ -insertion both in the diagram for $\Gamma(\varphi)$ and in the diagram for $V(\mathbf{q})$. If it had not canceled, it would be impossible to introduce $C(\alpha_s)$ (9.8). We obtain

$$\begin{aligned}
 C(\alpha_s) = & C_R T_F n_f \left(\frac{\alpha_s}{4\pi} \right)^2 \left\{ -\frac{112}{27} + \frac{\alpha_s}{4\pi} \left[C_F \left(\frac{4}{5}\pi^4 + 152\zeta_3 - \frac{1711}{6} \right) \right. \right. \\
 & + \frac{32}{9} T_F n_f \left(\zeta_3 + \frac{58}{27} \right) \Big] + \left(\frac{\alpha_s}{4\pi} \right)^2 \left[-C_F^2 \left(160\zeta_3^2 + \frac{80}{189}\pi^6 + \frac{3200}{3}\zeta_5 \right. \right. \\
 & \left. - \frac{74}{45}\pi^4 - \frac{8848}{9}\zeta_3 - \frac{21037}{54} \right) - 2C_F T_F n_f \left(32\zeta_5 + \frac{16}{27}\pi^4 + \frac{7888}{27}\zeta_3 \right. \\
 & \left. - \frac{110059}{243} \right) + \frac{32}{81} (T_F n_f)^2 \left(\frac{\pi^4}{5} - 20\zeta_3 - \frac{1304}{27} \right) \Big] \Big\} + \dots , \tag{14.5}
 \end{aligned}$$

A. Grozin

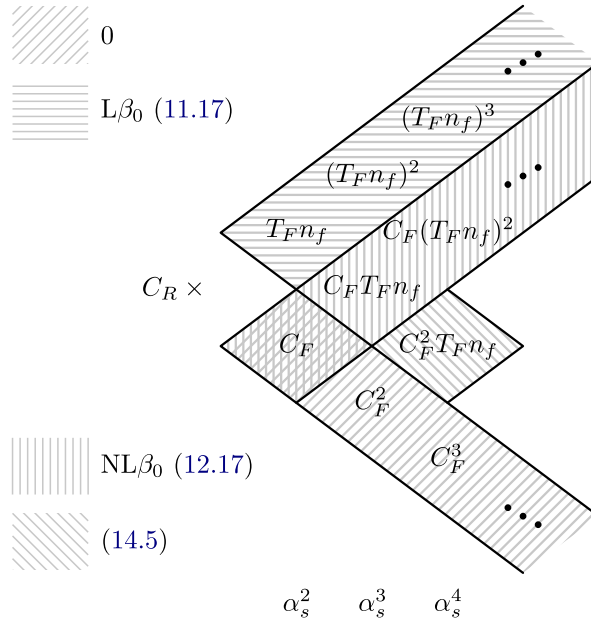


Fig. 8. Abelian color structures for $C(\alpha_s)$.

where dots mean other color structures. The corresponding parts of (9.9), (11.17) and (12.17) are reproduced; all $C_R C_F^{L-1} \alpha_s^L$ -terms vanish (Sec. 13); the $C_R C_F^2 T_F n_f \alpha_s^5$ result is new.

Let's summarize what's known about the conformal anomaly $C(\alpha_s)$. The Abelian structures $C_R C_F^{L-n-1} (T_F n_f)^n \alpha_s^L$ ($L \geq 2$) are shown in Fig. 8. All contributions with $n = 0$ vanish (Sec. 13; they are shown in the corresponding shading in the figure). The contributions $C_R (T_F n_f)^{L-1} \alpha_s^L$ ($L \geq 2$) are the leading large- β_0 ones (Sec. 11); several of them are presented in (11.17), but a practically infinite number of them are easily available. The contributions $C_R C_F (T_F n_f)^{L-2} \alpha_s^L$ ($L \geq 2$) are next-to-leading large- β_0 ones (Sec. 12). The first of them ($L = 2$) also belongs to the first family, and hence vanishes. The contributions with $L \leq 7$ are presented in (12.17); several more can be obtained using known algorithms, but the calculational complexity grows fast with L . The $C_R C_F^2 T_F n_f \alpha_s^4$ result is obtained here. No further $C_R C_F^{L-n-1} (T_F n_f)^n \alpha_s^L$ -terms can be obtained without calculating $\Pi(k^2)$ beyond the four-loop results¹²², and this is a highly nontrivial task. The non-Abelian terms $C_R C_A \alpha_s^2$ and $C_R C_A T_F n_l \alpha_s^3$ are also known (9.9).

15. Conclusion

At four loops, the HQET field anomalous dimension, as well as the small-angle expansion and the large-angle asymptotics of the cusp anomalous dimension,

is completely known. The full-angle dependence is known for all color structures except $C_R C_A^2 T_F n_f$, $C_R C_A^3$ and d_{RA} . The highest weight terms in the QCD results for the Bremsstrahlung function (the φ^2 -term of the small-angle expansion) and for the light-like cusp anomalous dimension (the large- φ asymptotics) coincide with the corresponding results in $\mathcal{N} = 4$ SYM — the principle of maximum transcendentality.

All α_s^4/ε -terms in the on-shell renormalization constant of the massive quark field in QCD are known analytically. The results for the color structures $C_F C_A^3$ and d_{FA} are new.

At five loops, the Abelian color structures $C_R(T_F n_f)^4$, $C_R C_F(T_F n_f)^3$, $C_R C_F^2(T_F n_f)^2$, $C_R C_F^3 T_F n_f$ and $C_R \bar{d}_{FF} n_f^2$ in the HQET field anomalous dimension and the cusp anomalous dimension are known. The results for $C_R C_F^2(T_F n_f)^2$ and $C_R \bar{d}_{FF} n_f^2$ are new. The structures $C_R(T_F n_f)^{L-1} \alpha_s^L$ are known to all loop orders L ; $C_R C_F(T_F n_f)^{L-2} \alpha_s^L$ are presented explicitly up to $L = 8$ loops, and more terms can be obtained using known algorithms. All Abelian results for $\Gamma(\varphi)$ at five and more loops, obtained in Secs. 11–14, have the one-loop φ -dependence $\varphi \coth \varphi - 1$, and hence they trivially give contributions to the light-like cusp anomalous dimension $K(\alpha_s)$.

The conjecture about the cusp anomalous dimension proposed in Ref. 39 works up to three loops and for some color structures at four loops, but breaks for some other four-loop structures (its formulation at $L \geq 4$ is not quite unambiguous). The reason why it works in some highly nontrivial cases is still unknown (all known results for $L \geq 5$ have one-loop angle dependence, and the conjecture holds for them by construction, so they add no new information).

The cusp anomalous dimension with Euclidean angle close to π is related to the static potential. This relation follows from conformal symmetry, and is strictly valid for $\mathcal{N} = 4$ SYM. In QCD, its breaking is given by the conformal anomaly $\Delta(\alpha_s)$. It is conjectured (though not proven) that $\Delta(\alpha_s) = \beta(\alpha_s) C(\alpha_s)$. The coefficient function $C(\alpha_s)$ is known at three loops, most four-loop color structures are also known. The structures $C_R(T_F n_f)^{L-1} \alpha_s^L$ are known to all loop orders L , and $C_R C_F(T_F n_f)^{L-2} \alpha_s^L$ up to $L = 7$ (this expansion can be extended). The structures $C_R C_F^{L-2} T_F n_f \alpha_s^L$ vanish for all L .

New results for the four-loop contributions $C_R C_F^2(T_F n_f)^2 \alpha_s^5$ and $C_R \bar{d}_{FF} n_f^2 \alpha_s^5$ [see (14.1)] to the quark–antiquark static potential $V(\mathbf{q})$ are presented. The last one cancels in $\Delta(\alpha_s)$ [thus giving one more confirmation of its factorization into $\beta(\alpha_s) C(\alpha_s)$]; the first one produced the new $C_R C_F^2 T_F n_f \alpha_s^4$ -term in $C(\alpha_s)$.

There is an additional problem here: the coefficient of $C_R C_A^3 \alpha_s^4$ has a logarithmic singularity at $\delta \rightarrow 0$, and the definition of $\Delta(\alpha_s)$ breaks down. It is supposed that resummation of leading powers of this logarithm will lead to a finite result, probably containing $\log \alpha_s$, but the details are not clear. If this is so, the cusp anomalous dimension will contain a logarithmic dependence on α_s , which is very unusual for anomalous dimensions in quantum field theory. This question needs further clarification.

A. Grozin

Acknowledgments

I am grateful to D. J. Broadhurst, R. Brüser, K. G. Chetyrkin, J. M. Henn, G. P. Korchemsky, A. V. Kotikov, R. N. Lee, P. Marquard, A. F. Pikelner, A. V. Smirnov, V. A. Smirnov, M. Stahlhofen and M. Steinhauser for collaboration on various projects related to this review, and to A. L. Kataev and V. S. Molokoedov for discussing Ref. 104. All Feynman diagrams in this paper have been produced using `feyn.gle`.¹²³ The work has been supported by the Russian Science Foundation under the Grant 20-12-00205.

References

1. I. O. Cherednikov, T. Mertens and F. Van der Veken, *Wilson Lines in Quantum Field Theory, De Gruyter Studies in Mathematical Physics*, Vol. **24** (De Gruyter, 2020).
2. A. M. Polyakov, *Nucl. Phys. B* **164**, 171 (1980), [https://doi.org/10.1016/0550-3213\(80\)90507-6](https://doi.org/10.1016/0550-3213(80)90507-6).
3. V. S. Dotsenko and S. N. Vergeles, *Nucl. Phys. B* **169**, 527 (1980), [https://doi.org/10.1016/0550-3213\(80\)90103-0](https://doi.org/10.1016/0550-3213(80)90103-0).
4. R. A. Brandt, F. Neri and M.-a. Sato, *Phys. Rev. D* **24**, 879 (1981), <https://doi.org/10.1103/PhysRevD.24.879>.
5. H. Dorn, *Fortsch. Phys.* **34**, 11 (1986), <https://doi.org/10.1002/prop.19860340104>.
6. G. P. Korchemsky and A. V. Radyushkin, *Phys. Lett. B* **171**, 459 (1986), [https://doi.org/10.1016/0370-2693\(86\)91439-5](https://doi.org/10.1016/0370-2693(86)91439-5).
7. G. P. Korchemsky and A. V. Radyushkin, *Sov. J. Nucl. Phys.* **44**, 877 (1986) [*Yad. Fiz.* **44**, 1351 (1986)].
8. G. P. Korchemsky and A. V. Radyushkin, *Sov. J. Nucl. Phys.* **45**, 127 (1987) [*Yad. Fiz.* **45**, 198 (1987)].
9. G. P. Korchemsky and A. V. Radyushkin, *Sov. J. Nucl. Phys.* **45**, 910 (1987) [*Yad. Fiz.* **45**, 1466 (1987)].
10. T. Becher and M. Neubert, *Phys. Rev. D* **79**, 125004 (2009), arXiv:0904.1021 [hep-ph], <http://doi.org/10.1103/PhysRevD.79.125004> [*Erratum: Phys. Rev. D* **80**, 109901 (2009)].
11. N. Agarwal, L. Magnea, C. Signorile-Signorile and A. Tripathi, *Phys. Rep.* **994**, 1 (2023), arXiv:2112.07099 [hep-ph], <https://doi.org/10.1016/j.physrep.2022.10.001>.
12. M. Neubert, *Phys. Rep.* **245**, 259 (1994), arXiv:hep-ph/9306320, [https://doi.org/10.1016/0370-1573\(94\)90091-4](https://doi.org/10.1016/0370-1573(94)90091-4).
13. A. V. Manohar and M. B. Wise, *Heavy Quark Physics, Cambridge Monographs on Particle Physics, Nuclear Physics and Cosmology*, Vol. **10** (Cambridge University Press, Cambridge, 2000).
14. A. G. Grozin, *Heavy Quark Effective Theory, Springer Tracts in Modern Physics*, Vol. **201** (Springer, Berlin, 2004).
15. H. Georgi and M. B. Wise, *Phys. Lett. B* **243**, 279 (1990), [https://doi.org/10.1016/0370-2693\(90\)90851-V](https://doi.org/10.1016/0370-2693(90)90851-V).
16. A. F. Falk, H. Georgi, B. Grinstein and M. B. Wise, *Nucl. Phys. B* **343**, 1 (1990), [https://doi.org/10.1016/0550-3213\(90\)90591-Z](https://doi.org/10.1016/0550-3213(90)90591-Z).
17. D. Correa, J. Henn, J. Maldacena and A. Sever, *J. High Energy Phys.* **6**, 48 (2012), arXiv:1202.4455 [hep-th], [https://doi.org/10.1007/JHEP06\(2012\)048](https://doi.org/10.1007/JHEP06(2012)048).
18. G. P. Korchemsky and A. V. Radyushkin, *Nucl. Phys. B* **283**, 342 (1987), [https://doi.org/10.1016/0550-3213\(87\)90277-X](https://doi.org/10.1016/0550-3213(87)90277-X).

19. I. A. Korchemskaya and G. P. Korchemsky, *Phys. Lett. B* **287**, 169 (1992), [https://doi.org/10.1016/0370-2693\(92\)91895-G](https://doi.org/10.1016/0370-2693(92)91895-G).
20. G. P. Korchemsky, *Mod. Phys. Lett. A* **4**, 1257 (1989), <https://doi.org/10.1142/S0217732389001453>.
21. G. P. Korchemsky and G. Marchesini, *Nucl. Phys. B* **406**, 225 (1993), arXiv:hep-ph/9210281, [https://doi.org/10.1016/0550-3213\(93\)90167-N](https://doi.org/10.1016/0550-3213(93)90167-N).
22. J.-L. Gervais and A. Neveu, *Nucl. Phys. B* **163**, 189 (1980), [https://doi.org/10.1016/0550-3213\(80\)90397-1](https://doi.org/10.1016/0550-3213(80)90397-1).
23. I. Y. Arefeva, *Phys. Lett. B* **93**, 347 (1980), [https://doi.org/10.1016/0370-2693\(80\)90529-8](https://doi.org/10.1016/0370-2693(80)90529-8).
24. D. R. Yennie, S. C. Frautschi and H. Suura, *Ann. Phys.* **13**, 379 (1961), [https://doi.org/10.1016/0003-4916\(61\)90151-8](https://doi.org/10.1016/0003-4916(61)90151-8).
25. J. G. M. Gatheral, *Phys. Lett. B* **133**, 90 (1983), [https://doi.org/10.1016/0370-2693\(83\)90112-0](https://doi.org/10.1016/0370-2693(83)90112-0).
26. J. Frenkel and J. C. Taylor, *Nucl. Phys. B* **246**, 231 (1984), [https://doi.org/10.1016/0550-3213\(84\)90294-3](https://doi.org/10.1016/0550-3213(84)90294-3).
27. L. D. Landau and E. M. Lifshitz, *The Classical Theory of Fields*, 4th edn. (Butterworth-Heinemann, 1980) [see particularly the problem after Sec. 69].
28. J. D. Jackson, *Classical Electrodynamics*, 3 (Wiley, 1999) [see particularly Sec. 15.6].
29. S. Aoyama, *Nucl. Phys. B* **194**, 513 (1982), [https://doi.org/10.1016/0550-3213\(82\)90023-2](https://doi.org/10.1016/0550-3213(82)90023-2).
30. D. Knauss and K. Scharnhorst, *Ann. Phys.* **41**, 331 (1984), <https://doi.org/10.1002/andp.19844960413>.
31. D. J. Broadhurst, N. Gray and K. Schilcher, *Z. Phys. C* **52**, 111 (1991), <https://doi.org/10.1007/BF01412333>.
32. X.-D. Ji and M. J. Musolf, *Phys. Lett. B* **257**, 409 (1991), [https://doi.org/10.1016/0370-2693\(91\)91916-J](https://doi.org/10.1016/0370-2693(91)91916-J).
33. D. J. Broadhurst and A. G. Grozin, *Phys. Lett. B* **267**, 105 (1991), arXiv:hep-ph/9908362, [https://doi.org/10.1016/0370-2693\(91\)90532-U](https://doi.org/10.1016/0370-2693(91)90532-U).
34. K. Melnikov and T. van Ritbergen, *Nucl. Phys. B* **591**, 515 (2000), arXiv:hep-ph/0005131, [https://doi.org/10.1016/S0550-3213\(00\)00526-5](https://doi.org/10.1016/S0550-3213(00)00526-5).
35. K. G. Chetyrkin and A. G. Grozin, *Nucl. Phys. B* **666**, 289 (2003), arXiv:hep-ph/0303113, [https://doi.org/10.1016/S0550-3213\(03\)00490-5](https://doi.org/10.1016/S0550-3213(03)00490-5).
36. W. Kilian, P. Manakos and T. Mannel, *Phys. Rev. D* **48**, 1321 (1993), <https://doi.org/10.1103/PhysRevD.48.1321>.
37. N. Kidonakis, *Phys. Rev. Lett.* **102**, 232003 (2009), arXiv:0903.2561 [hep-ph], <https://doi.org/10.1103/PhysRevLett.102.232003>.
38. A. Grozin, J. M. Henn, G. P. Korchemsky and P. Marquard, *Phys. Rev. Lett.* **114**, 62006 (2015), arXiv:1409.0023 [hep-ph], <https://doi.org/10.1103/PhysRevLett.114.062006>.
39. A. G. Grozin, J. M. Henn, G. P. Korchemsky and P. Marquard, *J. High Energy Phys.* **1**, 140 (2016), arXiv:1510.07803 [hep-ph], [https://doi.org/10.1007/JHEP01\(2016\)140](https://doi.org/10.1007/JHEP01(2016)140).
40. S. Moch, J. A. M. Vermaasen and A. Vogt, *Nucl. Phys. B* **688**, 101 (2004), arXiv:hep-ph/0403192, <https://doi.org/10.1016/j.nuclphysb.2004.03.030>.
41. J. Blümlein, P. Marquard, C. Schneider and K. Schönwald, *Nucl. Phys. B* **971**, 115542 (2021), arXiv:2107.06267 [hep-ph], <https://doi.org/10.1016/j.nuclphysb.2021.115542>.
42. S. Moch, J. A. M. Vermaasen and A. Vogt, *J. High Energy Phys.* **8**, 49 (2005), arXiv:hep-ph/0507039, <https://doi.org/10.1088/1126-6708/2005/08/049>.
43. S. Moch, J. A. M. Vermaasen and A. Vogt, *Phys. Lett. B* **625**, 245 (2005), arXiv:hep-ph/0508055, <https://doi.org/10.1016/j.physletb.2005.08.067>.

A. Grozin

44. D. J. Broadhurst and A. G. Grozin, *Phys. Rev. D* **52**, 4082 (1995), arXiv:hep-ph/9410240, <https://doi.org/10.1103/PhysRevD.52.4082>.
45. J. A. Gracey, *Phys. Lett. B* **322**, 141 (1994), arXiv:hep-ph/9401214, [https://doi.org/10.1016/0370-2693\(94\)90502-9](https://doi.org/10.1016/0370-2693(94)90502-9).
46. M. Beneke and V. M. Braun, *Nucl. Phys. B* **454**, 253 (1995), arXiv:hep-ph/9506452, [https://doi.org/10.1016/0550-3213\(95\)00439-Y](https://doi.org/10.1016/0550-3213(95)00439-Y).
47. A. Grozin, Leading and next to leading large n_f terms in the cusp anomalous dimension and the quark-antiquark potential, in *Proc. Loops and Legs in Quantum Field Theory*, Vol. **260** (2016), arXiv:1605.03886 [hep-ph], <https://doi.org/10.22323/1.260.0053>.
48. B. Ruijl, T. Ueda, J. A. M. Vermaasen, J. Davies and A. Vogt, First Forcer results on deep-inelastic scattering and related quantities, in *Proc. 13th DESY Workshop on Elementary Particle Physics: Loops and Legs in Quantum Field Theory* (2016), arXiv:1605.08408 [hep-ph], <https://doi.org/10.22323/1.260.0071>.
49. P. Marquard, A. V. Smirnov, V. A. Smirnov and M. Steinhauser, *Phys. Rev. D* **97**, 54032 (2018), arXiv:1801.08292 [hep-ph], <https://doi.org/10.1103/PhysRevD.97.054032>.
50. R. Brüser, A. G. Grozin, J. M. Henn and M. Stahlhofen, *J. High Energy Phys.* **5**, 186 (2019), arXiv:1902.05076 [hep-ph], [https://doi.org/10.1007/JHEP05\(2019\)186](https://doi.org/10.1007/JHEP05(2019)186).
51. J. M. Henn, A. V. Smirnov, V. A. Smirnov and M. Steinhauser, *J. High Energy Phys.* **5**, 66 (2016), arXiv:1604.03126 [hep-ph], [https://doi.org/10.1007/JHEP05\(2016\)066](https://doi.org/10.1007/JHEP05(2016)066).
52. J. Davies, A. Vogt, B. Ruijl, T. Ueda and J. A. M. Vermaasen, *Nucl. Phys. B* **915**, 335 (2017), arXiv:1610.07477 [hep-ph], <https://doi.org/10.1016/j.nuclphysb.2016.12.012>.
53. A. Grozin, *J. High Energy Phys.* **6**, 73 (2018), arXiv:1805.05050 [hep-ph], doi:10.1007/JHEP06(2018)073, 10.1007/JHEP01(2019)134 [*Addendum: J. High Energy Phys.* **1**, 134 (2019)].
54. J. M. Henn, G. P. Korchemsky and B. Mistlberger, *J. High Energy Phys.* **4**, 18 (2020), arXiv:1911.10174 [hep-th], [https://doi.org/10.1007/JHEP04\(2020\)018](https://doi.org/10.1007/JHEP04(2020)018).
55. A. von Manteuffel, E. Panzer and R. M. Schabinger, *Phys. Rev. Lett.* **124**, 162001 (2020), arXiv:2002.04617 [hep-ph], <https://doi.org/10.1103/PhysRevLett.124.162001>.
56. A. G. Grozin, J. M. Henn and M. Stahlhofen, *J. High Energy Phys.* **10**, 52 (2017), arXiv:1708.01221 [hep-ph], [https://doi.org/10.1007/JHEP10\(2017\)052](https://doi.org/10.1007/JHEP10(2017)052).
57. R. Brüser, C. Dlapa, J. M. Henn and K. Yan, *Phys. Rev. Lett.* **126**, 21601 (2021), arXiv:2007.04851 [hep-th], <https://doi.org/10.1103/PhysRevLett.126.021601>.
58. R. N. Lee, A. V. Smirnov, V. A. Smirnov and M. Steinhauser, *J. High Energy Phys.* **2**, 172 (2019), arXiv:1901.02898 [hep-ph], [https://doi.org/10.1007/JHEP02\(2019\)172](https://doi.org/10.1007/JHEP02(2019)172).
59. J. M. Henn, T. Peraro, M. Stahlhofen and P. Wasser, *Phys. Rev. Lett.* **122**, 201602 (2019), arXiv:1901.03693 [hep-ph], <https://doi.org/10.1103/PhysRevLett.122.201602>.
60. J. M. Henn, R. N. Lee, A. V. Smirnov, V. A. Smirnov and M. Steinhauser, *J. High Energy Phys.* **3**, 139 (2017), arXiv:1612.04389 [hep-ph], [https://doi.org/10.1007/JHEP03\(2017\)139](https://doi.org/10.1007/JHEP03(2017)139).
61. S. Moch, B. Ruijl, T. Ueda, J. A. M. Vermaasen and A. Vogt, *J. High Energy Phys.* **10**, 41 (2017), arXiv:1707.08315 [hep-ph], [https://doi.org/10.1007/JHEP10\(2017\)041](https://doi.org/10.1007/JHEP10(2017)041).
62. A. G. Grozin, R. N. Lee and A. F. Pikelner, *J. High Energy Phys.* **11**, 94 (2022), arXiv:2208.09277 [hep-ph], [https://doi.org/10.1007/JHEP11\(2022\)094](https://doi.org/10.1007/JHEP11(2022)094).
63. N. Kidonakis, *Phys. Rev. D* **107**, 54006 (2023), arXiv:2301.05972 [hep-ph], <https://doi.org/10.1103/PhysRevD.107.054006>.
64. N. Kidonakis, *Int. J. Mod. Phys. A* **31**, 1650076 (2016), arXiv:1601.01666 [hep-ph], <https://doi.org/10.1142/S0217751X16500767>.
65. A. G. Grozin, *J. High Energy Phys.* **3**, 13 (2000), arXiv:hep-ph/0002266, <https://doi.org/10.1088/1126-6708/2000/03/013>.

66. A. G. Grozin, *Int. J. Mod. Phys. A* **19**, 473 (2004), arXiv:hep-ph/0307297, <https://doi.org/10.1142/S0217751X04016775>.
67. M. Beneke and V. M. Braun, *Nucl. Phys. B* **426**, 301 (1994), arXiv:hep-ph/9402364, [https://doi.org/10.1016/0550-3213\(94\)90314-X](https://doi.org/10.1016/0550-3213(94)90314-X).
68. A. Czarnecki and K. Melnikov, *Phys. Rev. D* **66**, 11502 (2002), arXiv:hep-ph/0110028, <https://doi.org/10.1103/PhysRevD.66.011502>.
69. A. G. Grozin, Higher radiative corrections in HQET, in *Proc. Helmholtz International Summer School on Heavy Quark Physics*, eds. A. Ali and M. Ivanov (Verlag Deutsches Elektronen-Synchrotron, 2008), pp. 55–88. arXiv:0809.4540 [hep-ph], <http://www.library.desy.de/preparch/desy/proc/proc09-07.pdf>.
70. R. N. Lee and A. F. Pikelner, *J. High Energy Phys.* **2**, 97 (2023), arXiv:2211.03668 [hep-ph], [https://doi.org/10.1007/JHEP02\(2023\)097](https://doi.org/10.1007/JHEP02(2023)097).
71. R. N. Lee, *Nucl. Phys. B* **830**, 474 (2010), arXiv:0911.0252 [hep-ph], <https://doi.org/10.1016/j.nuclphysb.2009.12.025>.
72. T. Luthe, A. Maier, P. Marquard and Y. Schröder, *J. High Energy Phys.* **10**, 166 (2017), arXiv:1709.07718 [hep-ph], [https://doi.org/10.1007/JHEP10\(2017\)166](https://doi.org/10.1007/JHEP10(2017)166).
73. K. G. Chetyrkin, G. Falcioni, F. Herzog and J. A. M. Vermaseren, *J. High Energy Phys.* **10**, 179 (2017), arXiv:1709.08541 [hep-ph], [https://doi.org/10.1009/JHEP10\(2017\)179](https://doi.org/10.1009/JHEP10(2017)179) [*Addendum: J. High Energy Phys.* **12**, 6 (2017)].
74. A. G. Grozin, *Phys. Lett. B* **692**, 161 (2010), arXiv:1004.2662 [hep-ph], <https://doi.org/10.1016/j.physletb.2010.07.032>.
75. T. van Ritbergen, J. A. M. Vermaseren and S. A. Larin, *Phys. Lett. B* **400**, 379 (1997), arXiv:hep-ph/9701390, [https://doi.org/10.1016/S0370-2693\(97\)00370-5](https://doi.org/10.1016/S0370-2693(97)00370-5).
76. M. Czakon, *Nucl. Phys. B* **710**, 485 (2005), arXiv:hep-ph/0411261, <https://doi.org/10.1016/j.nuclphysb.2005.01.012>.
77. A. G. Grozin, P. Marquard, A. V. Smirnov, V. A. Smirnov and M. Steinhauser, *Phys. Rev. D* **102**, 54008 (2020), arXiv:2005.14047 [hep-ph], <https://doi.org/10.1103/PhysRevD.102.054008>.
78. E. Bagan and P. Gosdzinsky, *Phys. Lett. B* **305**, 157 (1993), [https://doi.org/10.1016/0370-2693\(93\)91121-3](https://doi.org/10.1016/0370-2693(93)91121-3).
79. J. M. Henn and T. Huber, *J. High Energy Phys.* **9**, 147 (2013), arXiv:1304.6418 [hep-th], [https://doi.org/10.1007/JHEP09\(2013\)147](https://doi.org/10.1007/JHEP09(2013)147).
80. B. Fiol, J. Martínez-Montoya and A. Rios Fukelman, *J. High Energy Phys.* **5**, 202 (2019), arXiv:1812.06890 [hep-th], [https://doi.org/10.1007/JHEP05\(2019\)202](https://doi.org/10.1007/JHEP05(2019)202).
81. A. V. Kotikov and L. N. Lipatov, *Nucl. Phys. B* **661**, 19 (2003), arXiv:hep-ph/0208220, [https://doi.org/10.1016/S0550-3213\(03\)00264-5](https://doi.org/10.1016/S0550-3213(03)00264-5) [*Erratum: Nucl. Phys. B* **685**, 405 (2004)].
82. A. V. Kotikov, L. N. Lipatov, A. I. Onishchenko and V. N. Velizhanin, *Phys. Lett. B* **595**, 521 (2004), arXiv:hep-th/0404092, <https://doi.org/10.1016/j.physletb.2004.05.078> [*Erratum: Phys. Lett. B* **632**, 754 (2006)].
83. N. Beisert, B. Eden and M. Staudacher, *J. Stat. Mech.* **701**, P01021 (2007), arXiv:hep-th/0610251, <https://doi.org/10.1088/1742-5468/2007/01/P01021>.
84. Z. Bern, M. Czakon, L. J. Dixon, D. A. Kosower and V. A. Smirnov, *Phys. Rev. D* **75**, 85010 (2007), arXiv:hep-th/0610248, <https://doi.org/10.1103/PhysRevD.75.085010>.
85. F. Cachazo, M. Spradlin and A. Volovich, *Phys. Rev. D* **75**, 105011 (2007), arXiv:hep-th/0612309, <https://doi.org/10.1103/PhysRevD.75.105011>.
86. T. Huber, A. von Manteuffel, E. Panzer, R. M. Schabinger and G. Yang, *Phys. Lett. B* **807**, 135543 (2020), arXiv:1912.13459 [hep-th], <https://doi.org/10.1016/j.physletb.2020.135543>.

A. Grozin

87. E. Remiddi and J. A. M. Vermaasen, *Int. J. Mod. Phys. A* **15**, 725 (2000), arXiv:hep-ph/9905237, <https://doi.org/10.1142/S0217751X00000367>.
88. D. Maître, *Comput. Phys. Commun.* **174**, 222 (2006), arXiv:hep-ph/0507152, <https://doi.org/10.1016/j.cpc.2005.10.008>.
89. D. Maître, *Comput. Phys. Commun.* **183**, 846 (2012), arXiv:hep-ph/0703052, <https://doi.org/10.1016/j.cpc.2011.11.015>.
90. H. Frellesvig, arXiv:1806.02883 [hep-th].
91. J. Vollinga and S. Weinzierl, *Comput. Phys. Commun.* **167**, 177 (2005), arXiv:hep-ph/0410259, <https://doi.org/10.1016/j.cpc.2004.12.009>.
92. C. W. Bauer, A. Frink and R. Kreckel, *J. Symb. Comput.* **33**, 1 (2002), arXiv:cs/0004015 [cs.SC], <https://doi.org/10.1006/jsco.2001.0494>.
93. T. Gehrmann and E. Remiddi, *Comput. Phys. Commun.* **141**, 296 (2001), arXiv:hep-ph/0107173, [https://doi.org/10.1016/S0010-4655\(01\)00411-8](https://doi.org/10.1016/S0010-4655(01)00411-8).
94. S. Buehler and C. Duhr, *Comput. Phys. Commun.* **185**, 2703 (2014), arXiv:1106.5739 [hep-ph], <https://doi.org/10.1016/j.cpc.2014.05.022>.
95. J. Ablinger, J. Blümlein, M. Round and C. Schneider, *Comput. Phys. Commun.* **240**, 189 (2019), arXiv:1809.07084 [hep-ph], <https://doi.org/10.1016/j.cpc.2019.02.005>.
96. W. Kilian, T. Mannel and T. Ohl, *Phys. Lett. B* **304**, 311 (1993), arXiv:hep-ph/9303224, [https://doi.org/10.1016/0370-2693\(93\)90301-W](https://doi.org/10.1016/0370-2693(93)90301-W).
97. M. Prausa and M. Steinhauser, *Phys. Rev. D* **88**, 25029 (2013), arXiv:1306.5566 [hep-th], <https://doi.org/10.1103/PhysRevD.88.025029>.
98. D. J. Broadhurst and A. L. Kataev, *Phys. Lett. B* **315**, 179 (1993), arXiv:hep-ph/9308274, [https://doi.org/10.1016/0370-2693\(93\)90177-J](https://doi.org/10.1016/0370-2693(93)90177-J).
99. R. J. Crewther, *Phys. Lett. B* **397**, 137 (1997), arXiv:hep-ph/9701321, [https://doi.org/10.1016/S0370-2693\(97\)00157-3](https://doi.org/10.1016/S0370-2693(97)00157-3).
100. V. M. Braun, G. P. Korchemsky and D. Müller, *Prog. Part. Nucl. Phys.* **51**, 311 (2003), arXiv:hep-ph/0306057, [https://doi.org/10.1016/S0146-6410\(03\)90004-4](https://doi.org/10.1016/S0146-6410(03)90004-4).
101. A. V. Smirnov, V. A. Smirnov and M. Steinhauser, *Phys. Rev. Lett.* **104**, 112002 (2010), arXiv:0911.4742 [hep-ph], <https://doi.org/10.1103/PhysRevLett.104.112002>.
102. C. Anzai, Y. Kiyo and Y. Sumino, *Phys. Rev. Lett.* **104**, 112003 (2010), arXiv:0911.4335 [hep-ph], <https://doi.org/10.1103/PhysRevLett.104.112003>.
103. R. N. Lee, A. V. Smirnov, V. A. Smirnov and M. Steinhauser, *Phys. Rev. D* **94**, 54029 (2016), arXiv:1608.02603 [hep-ph], <https://doi.org/10.1103/PhysRevD.94.054029>.
104. A. L. Kataev and V. S. Molokoedov, arXiv:2211.10242 [hep-ph].
105. R. Brüser, A. G. Grozin, J. M. Henn and M. Stahlhofen, Four-loop results for the cusp anomalous dimension, in *Proc. Loops and Legs in Quantum Field Theory* (2018), arXiv:1807.05145 [hep-ph], <https://doi.org/10.22323/1.303.0018>.
106. N. Brambilla, A. Pineda, J. Soto and A. Vairo, *Phys. Rev. D* **60**, 91502 (1999), arXiv:hep-ph/9903355, <https://doi.org/10.1103/PhysRevD.60.091502>.
107. N. Brambilla, A. Pineda, J. Soto and A. Vairo, *Nucl. Phys. B* **566**, 275 (2000), arXiv:hep-ph/9907240, [https://doi.org/10.1016/S0550-3213\(99\)00693-8](https://doi.org/10.1016/S0550-3213(99)00693-8).
108. A. G. Grozin and A. V. Kotikov, arXiv:1106.3912 [hep-ph].
109. A. I. Davydychev and M. Y. Kalmykov, *Nucl. Phys. B* **605**, 266 (2001), arXiv:hep-th/0012189, [https://doi.org/10.1016/S0550-3213\(01\)00095-5](https://doi.org/10.1016/S0550-3213(01)00095-5).
110. A. I. Davydychev and M. Y. Kalmykov, *Nucl. Phys. B* **699**, 3 (2004), arXiv:hep-th/0303162, <https://doi.org/10.1016/j.nuclphysb.2004.08.020>.
111. A. G. Grozin, *Eur. Phys. J. C* **77**, 453 (2017), arXiv:1704.07968 [hep-ph], <https://doi.org/10.1140/epjc/s10052-017-5021-4>.
112. K. S. Kölbig, *SIAM J. Math. Anal.* **17**, 1232 (1986), <https://doi.org/10.1137/0517086>.

113. A. Palanques-Mestre and P. Pascual, *Commun. Math. Phys.* **95**, 277 (1984), <https://doi.org/10.1007/BF01212398>.
114. D. J. Broadhurst, *Z. Phys. C* **58**, 339 (1993), <https://doi.org/10.1007/BF01560355>.
115. A. V. Kotikov, *Phys. Lett. B* **375**, 240 (1996), arXiv:hep-ph/9512270, [https://doi.org/10.1016/0370-2693\(96\)00226-2](https://doi.org/10.1016/0370-2693(96)00226-2).
116. D. J. Broadhurst, J. A. Gracey and D. Kreimer, *Z. Phys. C* **75**, 559 (1997), arXiv:hep-th/9607174, <https://doi.org/10.1007/s002880050500>.
117. A. G. Grozin, *Int. J. Mod. Phys. A* **27**, 1230018 (2012), arXiv:1206.2572 [hep-ph], <https://doi.org/10.1142/S0217751X12300189>.
118. P. A. Baikov, K. G. Chetyrkin, J. H. Kühn and J. Rittinger, *J. High Energy Phys.* **7**, 17 (2012), arXiv:1206.1284 [hep-ph], [https://doi.org/10.1007/JHEP07\(2012\)017](https://doi.org/10.1007/JHEP07(2012)017).
119. Y. Schröder, *Phys. Lett. B* **447**, 321 (1999), arXiv:hep-ph/9812205, [https://doi.org/10.1016/S0370-2693\(99\)00010-6](https://doi.org/10.1016/S0370-2693(99)00010-6).
120. A. V. Smirnov, V. A. Smirnov and M. Steinhauser, *Phys. Lett. B* **668**, 293 (2008), arXiv:0809.1927 [hep-ph], <https://doi.org/10.1016/j.physletb.2008.08.070>.
121. S. G. Gorishnii, A. L. Kataev, S. A. Larin and L. R. Surguladze, *Phys. Lett. B* **256**, 81 (1991), [https://doi.org/10.1016/0370-2693\(91\)90222-C](https://doi.org/10.1016/0370-2693(91)90222-C).
122. B. Ruijl, T. Ueda, J. A. M. Vermaasen and A. Vogt, *J. High Energy Phys.* **6**, 40 (2017), arXiv:1703.08532 [hep-ph], [https://doi.org/10.1007/JHEP06\(2017\)040](https://doi.org/10.1007/JHEP06(2017)040).
123. A. Grozin, *Comput. Phys. Commun.* **283**, 108590 (2023), arXiv:2207.01351 [hep-ph], <https://doi.org/10.1016/j.cpc.2022.108590>.